FLOOD INUNDATION ASSESSMENT OF DATA-SCARCE GHED REGION AT THE DELTA OF OZAT RIVER, GUJARAT

A Thesis submitted to Gujarat Technological University

for the Award of

Doctor of Philosophy

In

Civil Engineering

by

Nevil Kishorkumar Trambadia

189999912039

Under supervision of

Dr. Vinodkumar M. Patel

GUJARAT TECHNOLOGICAL UNIVERSITY

AHMEDABAD

October - 2023

FLOOD INUNDATION ASSESSMENT OF DATA-SCARCE GHED REGION AT THE DELTA OF OZAT RIVER, GUJARAT

A Thesis submitted to Gujarat Technological University

for the Award of

Doctor of Philosophy

In

Civil Engineering

by

Nevil Kishorkumar Trambadia

189999912039

Under supervision of

Dr. Vinodkumar M. Patel

GUJARAT TECHNOLOGICAL UNIVERSITY

AHMEDABAD

October – 2023

DECLARATION

I declare that the thesis entitled **Flood Inundation Assessment of Data-Scarce Ghed Region at The Delta of Ozat River, Gujarat** submitted by me for the degree of Doctor of Philosophy is the record of research work carried out by me during the period from December 2018 to December 2022 under the supervision of **Dr. Vinodkumar M. Patel and Dr. Manoj J. Gundalia** and this has not formed the basis for the award of any degree, diploma, associateship, fellowship, titles in this or any other University or other institution of higher learning.

I further declare that the material obtained from other sources has been duly acknowledged in the thesis. I shall be solely responsible for any plagiarism or other irregularities, if noticed in the thesis.

Signature of the Research Scholar:  Date: 30 / 10 /2023

Name of Research Scholar: **Nevil Kishorkumar Trambadia**

Place: **Ahmedabad**

CERTIFICATE

I certify that the Work incorporated in the thesis **Flood Inundation Assessment of Data-Scarce Ghed Region at The Delta of Ozat River, Gujarat** submitted by **Mr. Nevil Kishorkumar Trambadia** was carried out by the candidate under my supervision/guidance. To the best of my knowledge: (i) the candidate has not submitted the same research work to any other institution for any degree/diploma, Associateship, Fellowship or other similar titles (ii) the thesis submitted is a record of original research work done by the Research Scholar during the period of study under my supervision, and (iii) the thesis represents independent research work on the part of the Research Scholar.

Signature of Supervisor:  Date: 30/10/2023

Name of Supervisor: **Dr. Vinodkumar M. Patel**

Signature of Co-Supervisor:  Date: 30/10/2023

Name of Co- Supervisor: **Dr. Manoj J. Gundalia**

Place: **Ahmedabad**

Course-work Completion Certificate

This is to certify that **Mr. Nevil Kishorkumar Trambadia** enrolment no. is **189999912039** enrolled for PhD program in the Civil Engineering branch of Gujarat Technological University, Ahmedabad.

(Please tick the relevant option(s))

☐ He has been exempted from the course-work (successfully completed during M.Phil Course)

☐ He has been exempted from Research Methodology Course only (successfully completed during M.Phil Course)

☑ He has successfully completed the PhD course work for the partial requirement for the award of PhD Degree. His/ Her performance in the course work is as follows-

Grade Obtained in Research Methodology [PHD22-01]	Grade Obtained in Research and Publication Ethics [PHD22-02]	Grade Obtained in Self-Study Course/ Contact Program
BB	**-----NA---**	**BB**

Supervisor's Sign

Dr. Vinodkumar M. Patel

Originality Report Certificate

It is certified that PhD Thesis titled **Flood Inundation Assessment of Data-Scarce Ghed Region at The Delta of Ozat River, Gujarat** by **Mr. Nevil Kishorkumar Trambadia** has been examined by us. We undertake the following:

a) Thesis has significant new work / knowledge as compared already published or are under consideration to be published elsewhere. No sentence, equation, diagram, table, paragraph or section has been copied verbatim from previous Work unless it is placed under quotation marks and duly referenced.

b) The Work presented is original and own Work of the author (i.e., there is no plagiarism). No ideas, processes, results or words of others have been presented as Author own Work.

c) There is no fabrication of data or results which have been compiled / analysed.

d) There is no falsification by manipulating research materials, equipment or processes, or changing or omitting data or results such that the research is not accurately represented in the research record.

e) The thesis has been checked using **Urkund (powered by Turnitin) (copy of originality report attached)** and found within limits as per GTU Plagiarism Policy and instructions issued from time to time (i.e., permitted similarity index <=10%).

Signature of the Research Scholar:  Date: 30/10/2023

Name of Research Scholar: **Mr. Nevil Kishorkumar Trambadia**

Signature of Supervisor:  Date: 30/10/2023

Name of Supervisor: **Dr. Vinodkumar M. Patel**

Place: **Ahmedabad**

Document Information

Analyzed document	Thesis_NKTrambadia_189999912039.docx (D163288379)
Submitted	2023-04-06 08:14:00
Submitted by	Nevil Trambadia
Submitter email	patel.nil26@gmail.com
Similarity	1%
Analysis address	patel.nil26.gtuni@analysis.urkund.com

Sources included in the report

W	URL: https://doi.org/10.3390/rs13183778 Fetched: 2023-04-06 08:14:00	9
W	URL: https://doi.org/10.1007/s40808-022-01426-2 Fetched: 2023-04-06 08:14:00	9

Ph.D. Thesis Non-Exclusive License to GUJARAT TECHNOLOGICAL UNIVERSITY

In consideration of being a Research Scholar at Gujarat Technological University, and in the interests of the facilitation of research at the University and elsewhere, I, **Mr. Nevil Kishorkumar Trambadia** having **189999912039** hereby grant a non- exclusive, royalty free and perpetual license to the University on the following terms:

a. GTU is permitted to archive, reproduce and distribute my thesis, in whole or in part, and/or my abstract, in whole or in part (referred to collectively as the "Work") anywhere in the world, for non-commercial purposes, in all forms of media;
b. GTU is permitted to authorize, sub-lease, sub-contract or procure any of the acts mentioned in paragraph (a);
c. GTU is authorized to submit the Work at any National / International Library, under the authority of their "Thesis Non-Exclusive License";
d. The Universal Copyright Notice (©) shall appear on all copies made under the authority of this license;
e. I undertake to submit my thesis, through my university, to any Library and Archives. Any abstract submitted with the thesis will be considered to form part of the thesis.
f. I represent that my thesis is my original Work, does not infringe any rights of others, including privacy rights, and that I have the right to make the grant conferred by this non-exclusive license.
g. If third party copyrighted material was included in my thesis for which, under the terms of the Copyright Act, written permission from the copyright owners is required, I have obtained such permission from the copyright owners to do the acts mentioned in paragraph (a) above for the full term of copyright protection.
h. I understand that the responsibility for the matter as mentioned in the paragraph (g) rests with the authors / me solely. In no case shall GTU have any liability for any acts / omissions / errors / copyright infringement from the publication of the said thesis or otherwise.
i. I retain copyright ownership and moral rights in my thesis, and may deal with the copyright in my thesis, in any way consistent with rights granted by me to my university in this non-exclusive license.

j. GTU logo shall not be used /printed in the book (in any manner whatsoever) being published or any promotional or marketing materials or any such similar documents.

k. The following statement shall be included appropriately and displayed prominently in the book or any material being published anywhere: "The content of the published work is part of the thesis submitted in partial fulfilment for the award of the degree of Ph.D. in Civil Engineering of the Gujarat Technological University".

l. I further promise to inform any person to whom I may hereafter assign or license my copyright in my thesis of the rights granted by me to my university in this nonexclusive license. I shall keep GTU indemnified from any and all claims from the Publisher(s) or any third parties at all times resulting or arising from the publishing or use or intended use of the book / such similar document or its contents.

m. I am aware of and agree to accept the conditions and regulations of Ph.D. including all policy matters related to authorship and plagiarism.

Date: 30/10/2023

Place: Ahmedabad

Signature of the Research Scholar

Recommendation of the Supervisor: **RECOMMENDED**

Recommendation of the Co-Supervisor (if any): **RECOMMENDED**

Signature of Supervisor

Signature of Co-Supervisor

Thesis Approval Form

The viva-voce of the PhD Thesis submitted by **Shri Nevil Kishorkumar Trambadia (189999912039)** entitled **Flood Inundation Assessment of Data-Scarce Ghed Region at The Delta of Ozat River, Gujarat** was conducted on Monday (30th October, 2023) at Gujarat Technological University.

(Please tick any one of the following options)

☑ The performance of the candidate was satisfactory. We recommend that he be awarded the PhD degree.

☐ Any further modifications in research work recommended by the panel after 3 months from the date of first viva-voce upon request of the Supervisor or request of Independent Research Scholar after which viva-voce can be re-conducted by the same panel again.

(Briefly specify the modifications suggested by the panel)

☐ The performance of the candidate was unsatisfactory. We recommend that he/she should not be awarded the PhD degree.

(The panel must give justifications for rejecting the research work)

Name and Signature of Supervisor

Dr. Vinodkumar M. Patel

1) (External Examiner 1) Dr. Ravish Chandra

2) (External Examiner 2) Dr. Deepak Singh

ABSTRACT

Flood disaster is one of the primary concerns for developing country worldwide. Flood inundation assessment is vital for evaluating the soggy effect on various land cover classes. Many hydraulic models are available for this kind of analysis, and in recent days, machine learning techniques are more popular because of fast results. Ozat river basin is located in the deep western part of Gujarat. The river begins from the forest near the Gir region and flows to the Ghed region, following the river mouths. Actual inundation has appeared in the Ghed region near the delta of the river basin because of the higher elevated coastal line. The origin of the river lies in the Junagadh district and delta region, where the adverse effect is laid in the Porbandar district. Ozat river highest order reach bifurcates into two other reaches from Tikar village. River mouths are located near Pata village and Navi Bandar for both reaches. This research aims to calibrate sensitive parameters, Manning value by a 1D hydrodynamic model for all three reaches, and flood inundation assessment in 2D hydrodynamic modeling to generate various flood hazard maps. HEC-RAS software (developed by US army cops) is used for research by 1D and 2D hydrodynamic models. In this regard, digital elevation models; SRTM and ALOS, were utilized for 1D modeling to analyze the reliability of DEM for further analysis with a 2D model. Two parameters are in focus; water surface elevation changes and cross-section inundation. For 2D modeling, various hazard maps like depth, velocity, inundation boundary, water arrival, and percentage time inundation maps are helpful for around the edge analysis. Beyond this research, spatiotemporal analysis of Ghed region in flood inundation visualization was also employed using google earth engine cloud computing. Satellite images of sentinel are used for this analysis from 2017 to 2021. The Ozat River basin is data-scarce because after the inflow point of the model, few places are available for data record and tidal water elevation data is absent. All three kinds of analysis show the multiple criteria related to flood disaster maps. The 1D model indicates that the value 0.03 is best suited manning value for Ozat River basin; analysis has been made for DEMs SRTM and ALOS. Regression analysis using root mean square error (RMSE) and co-efficient of determination (R^2) is used for water surface elevation and cross-section inundation studies. In this context, RMSE values for water surface elevation change, giving the value of 1.31 and 0.34 for ALOS and SRTM, respectively. A cross-section inundation study indicates the R^2 values of 0.59 and 0.81 for ALOS and SRTM. From the comparative analysis, the higher value of R^2 and lower value of RMSE depicts the SRTM as superior to ALOS. Further research is carried out for a

2D hydrodynamic model using SRTM DEM. Land Use Land Cover map is generated in the google earth engine (GEE) from the archived storage of Landsat 8 to illustrate the vulnerability of different land cover classes. The 2-dimensional hydrodynamic model reveals many outcomes in terms of hydraulic parameters. The validation of a 2D model is carried out using observed water depth at four places of study area with the help of regression analysis. The hazardous maps assist the researchers about future events. An arrival time map is helpful as an early warning system for the local community. A depth map indicates the water gets steady over many days even after the simulation ends. Velocity in the area of interest lies between 0.1 to 0.33, which is not a significant concern. The outcomes from the google earth engine satellite mapping depict that more than 170 km^2 area gets inundated frequently. This analysis was carried out for five years as images were available on a cloud platform. Fundamental research is boosting the capability of decision-makers to work with data-scarce conditions in the semi-arid region.

Acknowledgement

I am incredibly grateful to everyone who has contributed to completing this PhD thesis on flood mapping of Ghed region.

First and foremost, I would like to express my deepest gratitude to my supervisors, Dr. Vinodkumar M. Patel and Dr. Manoj J. Gundalia, for their invaluable guidance, support, and encouragement throughout my research journey. their insightful comments and constructive criticisms have been instrumental in shaping the direction and quality of this Work.

I would also like to thank the members of my doctoral progress committee, Dr. Dhruvesh P. Patel and Dr. Yogeshkumar S. Patel, for their time, expertise, and feedback on my research. Their thoughtful comments and suggestions have greatly improved the quality of this Work.

I would like to thank the Junagadh district irrigation department, flood cell and maintenance department for constant support during the field visits and data regarding water surface elevation and river discharge. The community alive on the side of the river valley is also appreciated for the supportive discussion about past flood levels and contingencies faced during the peak flow moments.

I am writing to sincerely acknowledge the Hydrologic Engineering Center, US army corps engineers' team, for giving the valuable open-source software HEC-RAS. Your software has been invaluable in conducting my research and analysing the data collected. I am also thankful to the google workspace team for allowing working with the cloud platform of the google earth engine for generation of the flood mapping algorithm.

Lastly, I would like to thank my family for their unconditional love, support, and encouragement throughout my academic pursuits. Their unwavering belief in me has been a constant source of inspiration and motivation.

Thank you for your invaluable contributions to my PhD research on flood mapping of ghed regions and the decision support system framework.

Nevil Kishorkumar Trambadia

Table of Contents

List of Abbreviations

DEM	Digital Elevation Model
SRTM	Shuttle Radar Topography Mission
ALOS	Advanced Land Observing Satellite
1D	One Dimensional
2D	Two Dimensional
HEC-RAS	Hydrologic Engineering Center's River Analysis System
RMSE	Root Mean Squared Error
GEE	Google Earth Engine
FHM	Flood Hazard Mapping
GIS	Geographical Information System
SWAT	Soil and Water Assessment Tool
SWMM	Storm Water Management Model
ESRI	Environment System Research Institute
IRS	Indian Remote Sensing
IMD	Indian Meteorological Department
TRMM	Tropical Rainfall Measurement Model
SOI	Survey of India
USGS	United States Geological Survey
JAXA	Japan Aerospace Exploration Agency
NASA	National Aeronautics and Space Administration
DRIP	Dam Rehabilitation and Improvement Project
LULC	Land Use Land Cover
JASON	JavaScript Object Notation
CART	Classification and Regression Tree
NDVI	Normalized Difference Vegetation Index
NDWI	Normalized Difference Water Index
SAR	Synthetic Aperture Radar
API	Application Programming Interface
WSE	Water Surface Elevation
CS	Cross Section
UAV	Unmanned Aerial Vehicle

List of Figures

List of Tables

Chapter 1. Introduction

1.1 Background

A flood is the surplus flow that overruns the conveying or holding medium when its capacity is surpassed. Flooding is divided into two types: pluvial flooding, which occurs when rain causes excessive runoff, resulting in a rapid rise in water level, and fluvial flooding, which occurs when the level of water in a stream or river rises, causing an overflow into the surrounding environment and coastal regions. Excessive rainfall or snowmelt may have caused the rise in water level. Snowmelt floods can produce multiple flood occurrences, resulting in the loss of life and property. Flooding caused by snowmelt plays an integral part in studying hydrological processes in cold locations, which is vital for reducing flood disaster risk.

Floods are categorized as fluvial (river), groundwater, pluvial, and surge (coastal) floods based on numerous variables such as velocity, location, and causes. When the river's discharge exceeds its usual water carrying capacity, water spills over one or both banks, resulting in a flood. This form of flooding may cause waterlogging in cities located along river banks. Pluvial flooding is caused by poor or insufficient urban drainage concerning the accompanying rainfall in a city. In such circumstances of pluvial flooding, the area's present drainage system cannot handle high-intensity torrential rain, resulting in waterlogging. Where the water table is higher, and the water is inundated on the surface, groundwater flooding occurs. Enormous tidal waves cause surges or Coastal flooding, affecting places along the coast. Because it is surrounded by the Arabian Sea, Indian Ocean, and the Bay of Bengal, India is one of the most flood-prone countries. According to the Geological Survey of India, India's most extensive flood-prone zones cover over 12.5 percent of the country. According to the National Flood Commission, almost 40 million hectares of land in India are at risk of flooding. River floods are India's most common and destructive natural hazards, causing considerable damage to infrastructure, agriculture, transportation, community health, livestock, and human life. Gujarat has had numerous devastating floods. Before reaching the ocean, almost all of Gujarat's major rivers go across a long expanse of flat land. The lower river basins' flat plains are prone to flooding every year.

Almost every year, floods wreak significant harm to human lives and property. Since the Government of India adopted the National Flood Policy in 1954, it has become clear that absolute flood protection through structural means is not achievable and that the best solution is a combination of structural and non-structural measures. As a result, non-structural methods

such as flood forecasting and warning have been emphasized as the essential means of reducing flood damage potential.

Flood hazard mapping (FHM) FHM is essential for flood risk analysis because it efficiently estimates flood characteristics such as velocity, depth, and frequency (Mudashiru et al., 2021). Flood hazard maps are helpful for flood management practices because they effectively represent flood hazards' spatial extent and distribution (Khattak et al., 2016). Over the years and recently, there has been much effort to understand, predict, analyze, and quantify floods and their global impact. Historical data and FHM are essential in determining flood hazard potential areas, hazard intensity, flood depth, and spatial damage extent. There are three major approaches to creating a flood hazard map: physically-based, empirical, and physical modeling (Namara et al., 2021). Even though physically-based models have primarily replaced physical modeling, some researchers continue to simulate past and future flood event scenarios using real-life experiments (Saidani & Shibani, 2014). Experimentation is required to validate the model's prediction performance using the physical modeling method. Alternatively, numerical models are applicable if they simulate or represent the physical/real processes of a flow/flood occurrence (Gabriel et al., 2020). Physically-based models are helpful in flood prediction and early warning systems, but they require a large amount of input data in the form of hydrological parameters, river network geometry, topographic data, and sometimes remote sensing data processing in GIS (Ji et al., 2015). Physically-based models have errors and associated uncertainties ((Duan et al., 2016) and have limitations in replicating the actual physical process of complex flows. The numerical models, also known as hydrodynamic models, rely on numerical solutions to solve flow equations in one, two, and three dimensions. Several physically based and empirical models capable of predicting floods may require data from remote sensing. Physical experimentation allows the physical models to analyze past flood hazard extent and predict future flood hazard extent. The empirical models can be used in conjunction with various statistical and data-driven approaches. The statistical and data-driven approaches rely on hydrological, topographic, Digital Elevation Model (DEM), and geomorphology data, sometimes obtained through remote sensing and processed in GIS(Huo et al., 2016).

1.2 Flood hydrodynamic modeling

Hydrological simulation has been around since the 1850s. Modeling has advanced rapidly, owing primarily to simple access to nearly limitless software capability (Singh et al., 2021). The flood modeling simplifies the actual event. For example, a flood model of a given river

basin mimics natural flood events utilizing accurate input data, hydraulic parameters, and boundary conditions of a specific area. Based on the input data, a flood model of a specific river basin can be created that has a varying impact on performance. The flood risk activities or hydraulic qualities can thus be determined and calculated over time.(Soncini et al., 2009) hydrodynamic modeling as "the art and science of applying conservation equations for momentum, continuity, and transport to depict developing velocity, density, and scalar fields. Hydrodynamic modeling provides immediate insight into spatial and temporal changes in physical processes observed but less visible in field data (Jena et al., 2016).

Hydrodynamic models are mathematical models that attempt to mimic the fluid movement and characterize water movement through the resolution of formulas created by physics rules. Hydrodynamic models are especially beneficial for flood danger mapping, particularly when numerical modeling, physical modeling, or historical data mapping with prior extreme flood events are used. Because of its efficacy in simulating real-world events with fewer data and lower cost than physical models, numerical modeling is preferred for researchers and hydrologists to develop flood risk maps. In comparison, physical modeling can be used as a supplement and support tool in flood hazard mapping for extensive areas with severe social and economic harm. Using historical data mapping appears valuable for calibrating various parameters employed by numerical algorithms (Boori et al., 2016). Based on the spatial representation of the flood plain stream, the simulations are classified as 1D, 2D, and 3D (Ghimire et al., 2022).

Hydrodynamic modeling is a practical approach in recent times that plays a significant part in flood risk assessment due to its capacity to simulate real-time flood events. Its outputs can be efficiently employed for emergency flood management, such as adaptive traffic control, evacuation, and infrastructure development (Shekhar et al., 2021).

(Devia et al., 2015) Investigated various hydrological models, such as variable infiltration capacity model (VIC), MIKESHE, TOPMODEL, and soil and water assessment tool (SWAT) model, and classified them as lumped and distributed models based on a function of space and time, deterministic and stochastic models based on output values produced for single set input, static and dynamic models based on the time factor, and event-based and continuous models They went on to talk about empirical, conceptual, and physically-based models. Researchers such as (Kumar et al., 2017) have discussed the use of various 1D and 2D hydrodynamic models such as HEC-RAS, HEC-HMS, MIKE-11, MIKE-21, LISSFLOOD-FP, and

DAMBRK, FLDWAV, TELEMAC-2D, FLO-2D, SMPDBK, and suggested HEC-RAS as a more capable tool to produce more reliable results in a dam break.

1.3 Hypothesis/ Problem definition

Ghed is located in the deep western part of Gujarat state near the delta of the Ozat River basin. Before reaching the Arabian sea, the Ozat River is scattered in the cup-shaped Ghed region. In the preliminary investigation of this research, two major reasons have been identified; the width of Ozat River gradually decreases towards the sea, and before the 50 km of River mouth the width of the river is sufficient as more than 210 m. However, before the 25 km from the river mouth, it's become 10 m and more minor. The river L-profile depicts the elevation difference between river bed and banks are much more significant in the deep upstream face and reducing towards the river mouth. Here, authors mentioned the three tributaries, because in this research single Ozat River main reach bifurcates into two another reaches.

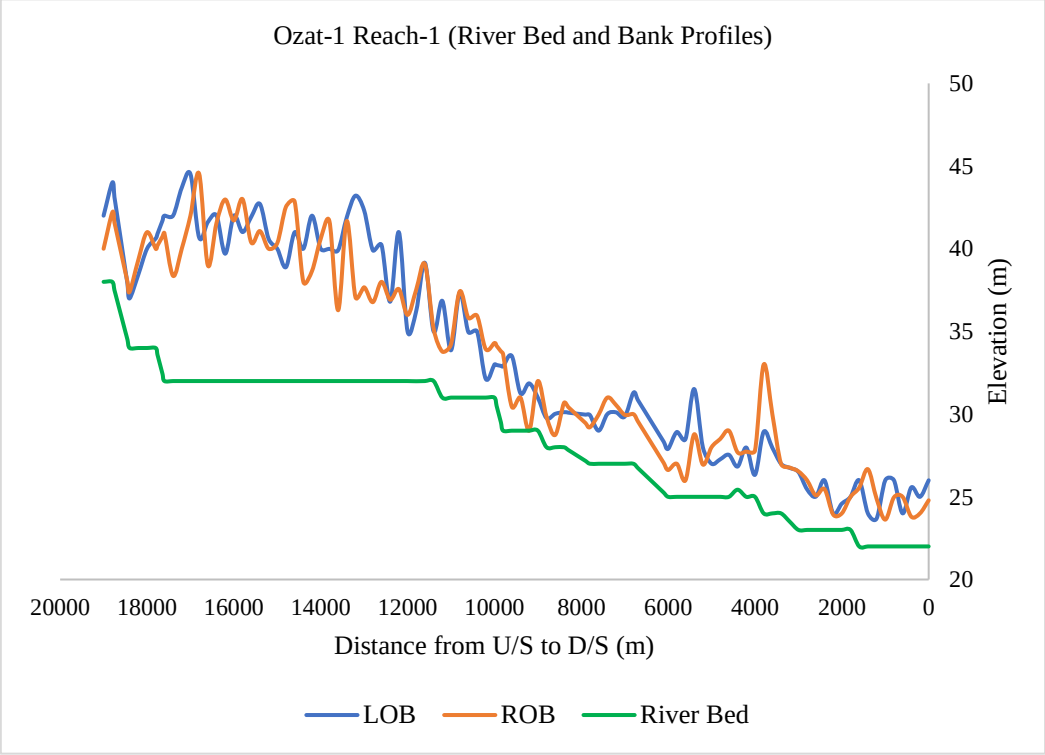

(a)

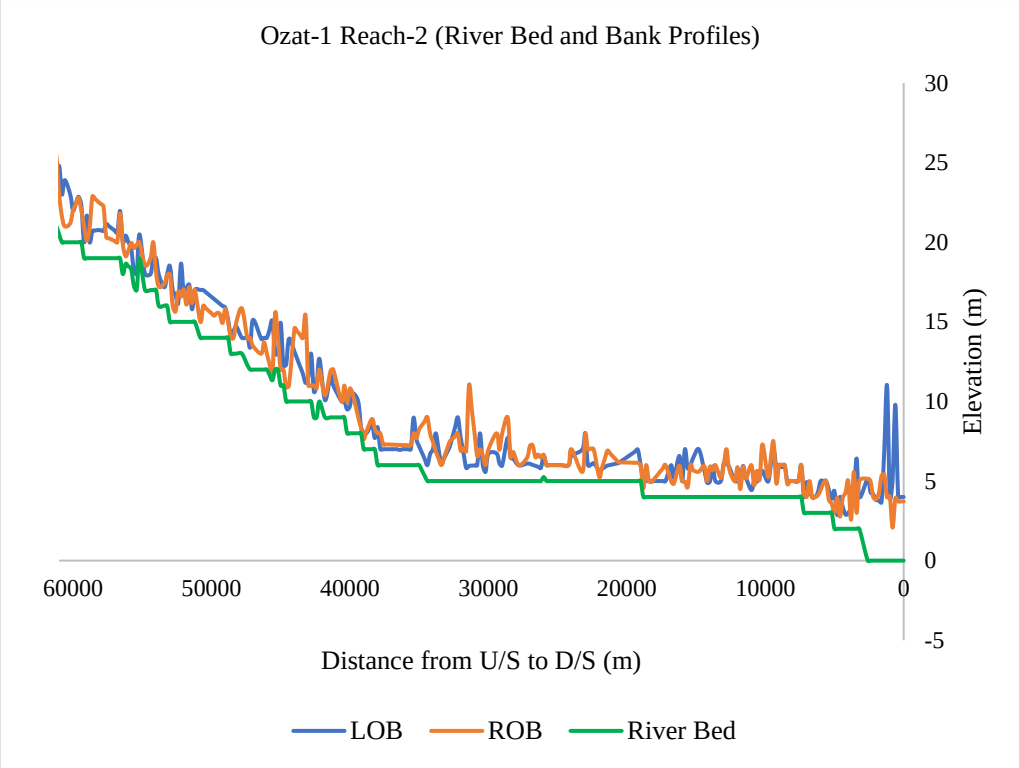

(b)

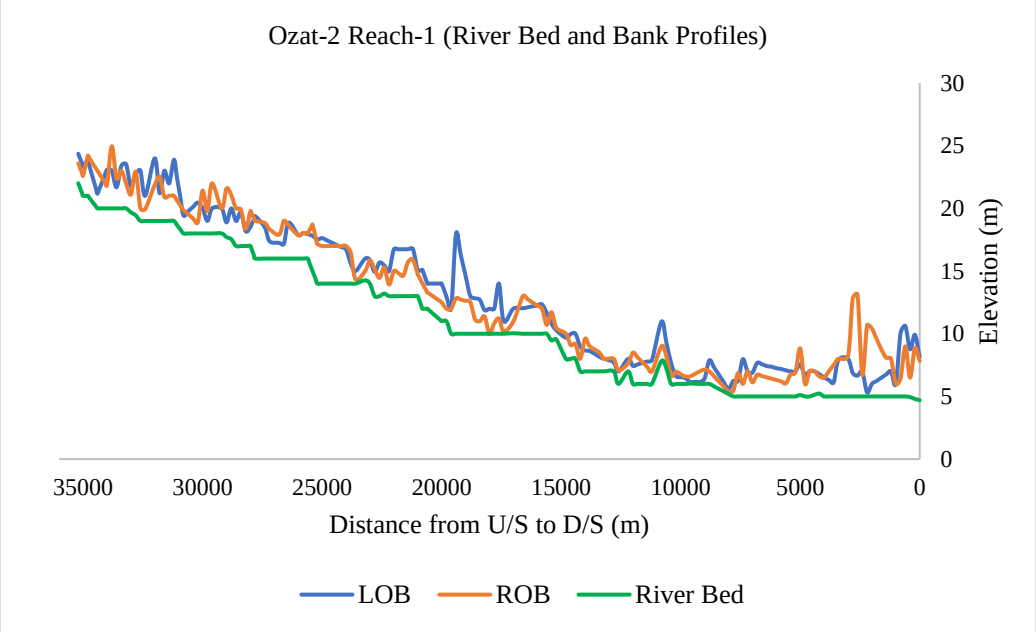

(c)

Figure 1.1 (a),(b) and (c) Ozat River banks and bed L-Profiles for all three reaches

Another reason for inundation is higher elevated coastal zone and deeper inland areas. The area of Ghed region is more than 180 km^2, which falls the majority under the cropland class on the LULC map. All built-up areas are located on the periphery of the Ghed region and connectivity

becomes overwhelmed in an inundated scene. An inundated zone is situated just before the river mouth, though the Ozat River must cross this area to reach the river mouth and meet the Arabian sea. In this regard, the water level of the Ozat River has to reach sufficient height to meet the sea level; in this achievement of level, more area gets inundated due to low laying terrain. Field visits and satellite images reveal the water gets steady for many months, even after the monsoon season. In this research, the 1D model was executed to calibrate manning's roughness value and check the river stage analysis. The 2D model was executed for deep analysis of velocity, water depth, arrival time, and inundation boundary maps.

1.4 Research objectives

1. To develop a 1D unsteady hydrodynamic model of Ozat river to predict stages at various locations along the study area.
2. To develop a 2D hydrodynamic model of Ozat river for inundation mapping.
3. To calibrate manning's roughness coefficient for study reach of Ozat river.
4. To develop flood inundation and hazard maps for Ghed region.
5. To identify suitable measures for frequently submerged areas and develop an integrated flood mitigation plan.

1.5 Scope of study

1. Prepare an emergency action plan for the Submergence of Ghed region before the final event.
2. A flood inundation map is helpful for local government authorities, engineers, and researchers to plan the vulnerable area of Ghed region and the new development of the surrounding culture.
3. Establish new hydraulic structures on the Ozat River downstream basin for better water management.
4. It is beneficial for infrastructure development near the delta of Ozat river basin and the development of Ghed region.
5. This research helps to design the sustainable inter-road connectivity of the study area.
6. Decision-makers will become aware of the safe grade elevation of the lower basin and can also make the early warning system before the event.

1.6 Thesis outline

The thesis of this research contains a total of 8 chapters. Initially, the introduction includes the details of the flood scenario, a background of research, problem statements, research objectives

and the scope of the study. Moreover, the literature part expresses the research journey of past work examination in different ways like GIS and digital mapping work, hydrodynamic modeling via HEC-RAS and Spatio-temporal analysis of flood scene in google earth engine. The 3rd chapter study area reveals detailed things with interactive maps of regions, the river reaches, ground condition images by field visits and modeling setup parameters. Next, the 4th chapter of the thesis contains the specific methodology of 1D and 2D hydrodynamic modeling. This chapter also includes the flood map algorithm preparation in the google earth engine. The 5th chapter expresses that the result comes from the 1D and 2D hydrodynamic models like manning roughness value calibration and validation; from the 2D model, the all-result maps like depth, velocity, percent time inundation and arrival time maps are analyzed. The 6th chapter includes the discussion of the research; the many limitations faced during the various modelling stages. The 7th chapter consists of the conclusion that comes from the multiple result maps and river stage analysis of hydrodynamic models and also expresses the research on critical places of the study area, especially in the Ghed region. The 8th chapter of the thesis includes the recommendation made in the form of various suggestions and also prepares the integrated flood mitigation plan with visualization.

Chapter 2. Literature Review

The research journey of literature review for the Ozat river basin is carried out in two ways; hydraulic analysis using HEC-RAS and satellite mapping using GEE. Behind the research, evaluation of case studies plays an essential role in forming appropriate methodology. Initially, the hydraulic models are developed after 1991 and over the years, the latest available models like HEC-RAS, MIKE, tuflow, flow master, SWMM (stormwater management model), WSPRO, and HydroCAD. Selecting an appropriate one is also a concern for researchers' community for precision analysis. However, in recent days, satellite mapping has been popular for wetlands through the machine learning algorithms using the google earth engine, but hydraulic mapping is not possible in this way.

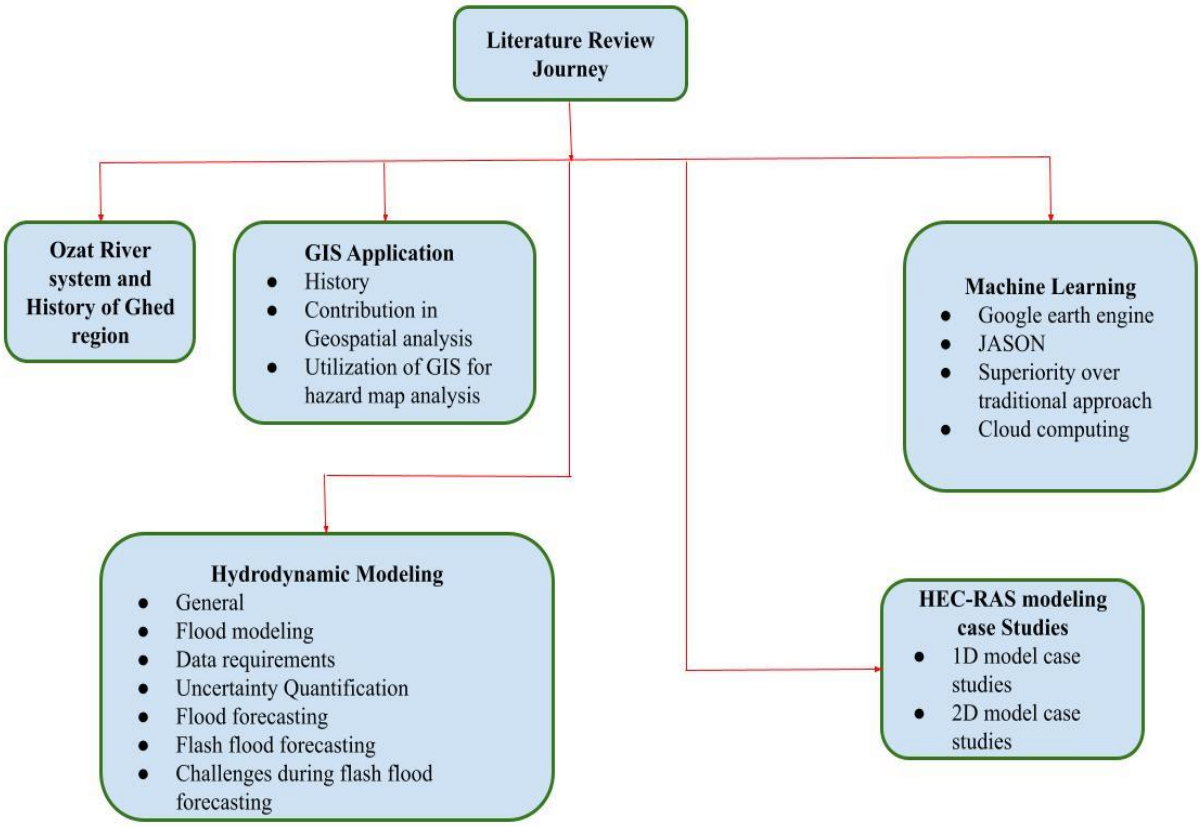

Figure 2.1 Flow chart of literature review

2.1 Ozat River system and History of Ghed region

Ozat River originates from the Bhesan taluka (Gir forest area) of Junagadh district and passes through the visavadar, Junagadh, Vanthli, Manavadar, Keshod, and Porbandar taluka. Many major, minor, and check dams are constructed on the highest order tributary of the Ozat River. After 63 kilometers from the origin point, the river reached Shapur weir. Here is the inflow point of the hydrodynamic model. Shapur weir can store 70.91 million cubic feet of water to

irrigate the 6 villages of 1500 hector land. Vanthli Ozat weir was constructed 5 kilometers away from the Shapur weir and 68 kilometers away from the origin point. After this place, river shows a continuous decreasing mode of width and depth. Near the vanthli weir, one religious place is also located on the left bank. This place is vital for flood inundation analysis because the Uben River also meets in the main reach of Ozat River. After the vanthli weir, the river passes through the Piplana village, whereas the check dam is constructed for local irrigation utilization. Finally, the river reaches Tikar village, where the main river reach splits into two other tributaries; one passes through the Bamnasa, Balagam, Sandha, Samarada and River mouth near Pata village. Another branch of the river reaches Ambaliya, Matiyana, Koylana, Osa, and Padardi and finally reaches the Ghed region, which is the area of interest in this research.

Ghed region is located near the deep western part of Gujarat, whereas the much less industrial and economic zone appears. The Ghed word originated from “Ghado”, in the Gujarati language, the Ghado means pot of water. The people of this area mostly depend upon the farming occupation and prefers the same kind of crop sue to wetlands. The wetland or flood inundated area frequently spreads and covers more than in the past. It has been noted that the depressed part of Ghed region is lower elevated than the estuary zone. Many villagers of this study area get overwhelmed due to water submergence, and it gets steady for more months following the monsoon season. In this condition, the topsoil of cropland is washed out, and farmers have no option to amend this change, which adversely affects the crop pattern selection. The shape of Ozat River basin catchment area is fan-type; the hydrological conditions and other parameters indicate that the fan shape catchment depicts flash floods.

Moreover, in this basin, the inundation of the Ozat River basin's delta area appears like very little time is available for early warning due to flash floods. This effect suffered the life of local people, transportation, and medical supply during peak flow conditions. In the place where water gets steady for more days, resulting from inundation, the water met to groundwater. As stated earlier, the submergence area is a delta of the river basin and very close to the seacoast line. This inundated water meets the salty groundwater table. In this context, the dry saline soil appears in the summer season. The solution to this complication is much needed as earlier of this unseen part of Gujarat.

2.2 GIS Application

GIS software generates the catchment characteristics like size, shape, stream order, stream network, and other hydrological parameters. Many researchers related to this field are available, like morphometry analysis, sedimentation, and flood disasters. The study related to natural resources is difficult to exhibit in computer programs because the actual ground condition varies from region to region. To eliminate this adversity, flood inundation mapping plays an important role. These models are helpful for the mitigation of disasters and future town planning scenarios. Flood mitigation and risk assessment planning are vital for the sewer network, a healthy aquatic ecosystem, and other emergency operations related to human life. After the invention of GIS in 1963, the era of digital land mapping started, and researchers came forward in this way. Initially, GIS development aimed to investigate drainage, climate, and soil characteristics. The GIS became commercial from 1975 to 1990 by leading company ESRI (Environmental System Research Institute). Nowadays, GIS is the most powerful software for delineating drainage features, streamline analysis, and flood detection through satellite images and interpretation. In this research, the stream network delineation, terrain file generation from the digital elevation model (DEM), and layout mapping of the study area have been carried out from ArcGIS. Drainage path analysis, highest order tributary, and catchment area calculation employed in ArcGIS. The land cover class and area determination of each class have been calculated through GIS. After the simulations of flood effects on various land covers, GIS was utilized to determine the inundation effect of each land cover separately for Ozat River basin case study.

2.3 Hydrodynamic flood modeling: state of the art

2.3.1 General

Flood modeling is a critical initial step in understanding and managing floods at all spatial scales, from a vast river's basin to densely populated urban regions and individual properties and infrastructure. Flood modeling has advanced rapidly following recent developments in modeling approaches and powerful computational tools and data products. Despite this advancement, precise flood assessment and forecasting and the risk associated with them remain elusive due to uncertainty at each stage of the modeling process. This work examines flood modeling with a particular focus on India. Indian researchers have made significant contributions to hydrologic science and flood modeling.

After storms and earthquakes, floods are the most common and severe natural danger. Flooding is a big worry in India, as it is worldwide. As a result, the Indian research community has

worked hard to develop models and approaches for understanding floods at various spatial scales. In recent years, the community has made significant contributions to flood estimation, multivariate hydrologic modeling, uncertainty quantification, climate change implications, and flood hazard and risk assessment. Several academics have researched large river basins such as the Mahanadi, Ganga, Godavari, and Krishna basins to better understand the nature of river floods. Flood modeling, encompassing hydrologic challenges, data requirements, and uncertainty quantification, is presented first, followed by climate change impact assessment modeling. This topic is flood forecasting, with a focus on flash flood forecasting. Presented research examines cropland flooding, which is known to be growing in frequency and spatial extent across the country.

2.3.2 Flood modeling approach

Flood modeling and the creation of flood inundation maps are critical for determining the potential impacts of floods of a specific scale and initiating efforts on the ground to reduce the damage. Flood features, such as the amplitude, duration, and spatial distribution of floods, are determined by hydrodynamic modeling. During the last decade, advances in hydrodynamic modeling have resulted in significant increases in the capacity to simulate flooding events. Models are categorized based on how catchment processes are represented (deterministic or stochastic) and how the catchment is spatially discretized (lumped or distributed). The continuity, momentum, and data-driven techniques have been used to build routing models that estimate flood wave propagation along a river channel. Flood frequency analysis studies are commonly used to understand long-term variations in flood magnitudes and frequencies using statistical models covering several elements of floods, including flood hydrology, climate change impacts assessment, remote sensing and GIS for flood modeling, and case studies.

Several hydrological modeling tools such as HEC-HMS, SWAT, MIKE, VIC, and SWMM are utilized to model flows in river basins. It's worth noting that most hydrologic models do an excellent work of reproducing ordinary circumstances but fall short of simulating extremes. The models perform poorly in catchments with major structural interventions such as dams unless the flows are normalized. For example, (Hurkmans, 2009) used a VIC model to simulate hydrological variables over the Krishna River Basin and found that while the VIC model can handle large-scale variability, it overestimates streamflow in the downstream portion because of the effect of storage structures is not taken into account in their model. One research indicated that the VIC model replicates the Upper Ganga Basin (UGB) and examines streamflow patterns and runoff magnitude. Hydrodynamic models designed explicitly for flood

flow simulations, on the other hand, might be more appropriate. (Hurkmans, 2009) utilized a one-dimensional hydrodynamic model to model discharges in the Mahanadi River watershed during the monsoon season of 2004 (June-September). They created the model by combining data from various sources, such as revising SRTM DEM cross-sections with measured river cross-sections, accessible river discharge, and water-level data at several gauging locations.

Hydrologic models, designed to simulate stream flows, are frequently used in flood modeling studies, concluding that the models can reproduce flood flows with acceptable accuracy. Hydrologic models are being driven by state-of-the-art numerical weather prediction (NWP) models and better rainfall data products to improve their usage for modeling floods at river basin scales. (Shah & Mishra, 2016) assessed the performance of the VIC model using several rainfall data sets to simulate daily discharges in the Mahanadi River basin, concluding that bias in real-time precipitation products affects the initial condition and precipitation forcing which affects flood peak timing and magnitudes. On the other hand, statistical goodness-of-fit measurements quantify model efficiency to overcome this constraint. Even using such metrics does not guarantee an objective assessment of model performance, which depends on the model application's unique goals for a given catchment and observed data. Additionally, each group working on a basin creates its model, resulting in an overabundance of such tools for each major basin. Many scholars, for example, model the Mahanadi basin ((Mondal & Mujumdar, 2012); (Saha et al., 2010); (Ganguli et al., 2020); (Parhi, 2013); (Pinos & Timbe, 2019); (Rangari et al., 2019); (Petteri Alho, 2008)). How much modeling is enough for a river basin was debated by (Johnston & Smakhtin, 2014). Their research looked at hydrological modeling in four significant basins: the Nile, Mekong, Ganges, and Indus, and came up with four recommendations for improving efficiency and reducing duplication in hydrological modeling. To allow more coordinated approaches and benefit from past modeling experiences, the input data, model details, and outcomes should all be published on a common platform. To eliminate redundancy of effort and increase collaboration among researchers, an appropriate agency should be formed for each significant basin to take responsibility for coordination and data exchange. New ways of data collecting (remote sensing, crowdsourcing, and community-based observations) and data assimilation from many sources are required.

2.3.3 Data Requirements

The quantity and quality of data supplied to any model during the calibration and validation stages determines its efficiency and utility. Flood modeling for river basins requires three types of data: (i) topographic data for the basin, channel, and/or river, (ii) hydrometeorological data

such as precipitation, temperature, solar radiation, land use-land cover, and subsurface hydraulic properties, and (iii) time series of flow rates and stage data to provide model input and output boundary conditions for model calibration and validation. Developments in the field of remote sensing enabled the acquisition of some of this data. Remote sensing from satellites and planes allows for the collection of spatially scattered data across wide areas and eliminates the need for expensive ground surveys. Ground measurements, on the other hand, complement satellite data and are important for validating satellite products. More and more geo-spatial datasets linked to hydrology, such as topography, soil, and land use, have become available through numerous open sources as a result of developments in satellite remote sensing in recent decades.(Thameemul Hajaj et al., 2019) used a distributed modeling approach using space inputs to construct a flood forecast model for the Godavari Basin. They used the land use/land cover grid produced from the Indian Remote Sensing Satellite (IRS-P6) AWiFS sensor data (56 m resolution), the Shuttled Radar Topographic Mission (SRTM) Digital Elevation Model (DEM), and the soil textural grid to calculate the topographic and hydraulic parameters. With hydrometeorological field data, the model is calibrated and validated. With real-time 3-hour interval hydrometeorological and daily evapotranspiration data from the 2010 floods, the model accurately estimated peak flood discharge and lag time.(Siswanto & Francés, 2019) examined the progress made in hydrological modeling in India over the last five years and explored the data requirements for hydrological modeling. Despite a variety of open sources for relevant data, there is still a dearth of excellent quality and quantity of data at the essential spatial and temporal scales, mainly when extremes are being modeled, resulting in ambiguous model outputs. Due to limited ground measurements and resource constraints, the modeler must frequently extrapolate information from the available observations in space and time. Furthermore, errors in climate models, which are used to predict the expected hydrological impact of future system responses (such as climate and land management change), add to the forecasts' uncertainty. Quantifying and communicating such uncertainties is critical for policymaking.

2.3.4 Uncertainty Quantification

Uncertainties exist in any modeling process and can come from various places, ranging from model formulation to data quality and quantity. Uncertainties cannot be avoided, but their magnitude and causes should be understood to comprehend their impact on modeling (Dotto et al., 2012). According to (Mitchell et al., 2009), numerous sources of uncertainty in the modeling process interact non-linearly. However, not all uncertainty sources can be assessed

with sufficient precision, and the proportion of uncertainty sources disregarded in environmental (including hydrological) modeling research may be considerable((Walker et al., 2003); (Doherty & Welter, 2010). Wherever possible, uncertainties should be quantified and propagated to risk decisions.

Quantifying uncertainty in precipitation data is especially important for determining the hazards and resilience of the hydrologic system. Because of its considerable unpredictability in geography and time, precipitation is one of the hydrologic variables with tremendous potential for introducing uncertainty. Although the Indian Meteorological Department (IMD) maintains an extensive network of rain gauges, (Mondal & Mujumdar, 2012) found that there are still data-poor locations. To bridge this gap, a few studies have looked into collecting rainfall data from satellites like the Tropical Rainfall Measurement Mission (TRMM) (Indu & Nagesh Kumar, 2014). There have also been attempts to incorporate satellite data with forecasting systems to improve the models' performance in predicting floods((Mosavi et al., 2018);(Seal, 2012). However, there are significant uncertainties connected with precipitation, and there are still gaps in the literature in terms of precisely measuring the uncertainties. Statistical methods (assimilating data from diverse sources) and Bayesian techniques can quantify uncertainty, particularly in high rainfall that causes flooding (Chandra et al., 2015). There are various uncertainties in the other inputs to a hydrologic model and the variability in precipitation. The uncertainty in the modeled water levels is influenced by upstream discharge and the roughness relationship for the main channel. The most significant sources of uncertainty in model outcomes are floodplain bathymetry, weir formulation, and discretization of floodplain topography (Warmink et al., 2011). Using a soil and water assessment method, (Yaduvanshi et al., 2018) investigated the runoff response during extreme rain events in the Subarnarekha River Basin in India (SWAT). They investigated basin characteristics' sensitivity to increase the model's flood runoff simulation efficiency.

2.4 Flood Forecasting

Over the previous three decades, weather forecasting has significantly improved. Weather forecasting has improved due to developments in monitoring, remote sensing, data collecting, and models, as well as advances in monitoring, remote sensing, data collection, and models. Depending on the regional scale of interest and the availability of trustworthy weather forecasts, flood forecasting systems can be constructed over many temporal periods, ranging from hours today to months. Different flood-forecasting approaches are employed in India

depending on the availability of data (both hydrological and meteorological), basin features, computing capacity, forecast lead time, and the reason for which the forecast is used.

2.5 Flash flood forecasting

Flash floods are defined by their fast occurrence and limited ability to issue warnings. They are frequently accompanied by other natural dangers (such as landslides and mudflows), resulting in damage to structures and enterprises, the collapse of hydraulic infrastructure, and, in severe cases, death. Flash floods on the Mandakini River killed thousands of people and livestock in Kedarnath, Uttarakhand, in 2013 and 2015. Though the occurrences were brief compared to earlier flood disasters in the country, they caused significant property and life loss since landslides and debris flows accompanied them. Due to the flash floods, the riverbanks of the Kedarnath valley were entirely eroded, according to post-disaster satellite photographs. As a result, it's critical to pinpoint potential flash flooding hotspots and sensitive areas. (Durga Rao et al., 2014) determined that, in addition to the breach of Chorabari Lake and the deposition of debris/sediments in the valley, extreme erosion occurred in the upstream area of Kedarnath. They used space-based inputs in a hydrological and hydraulic simulation study of the Mandakini River to determine the causes and impacts of flash floods. The combined effect of lake breach and high-intensity rainfall flood was explored utilizing CARTO DEM of 10 m posting in flood inundation simulations. The lag-time of the peak flood was determined to be less in the upstream catchment area due to the steep slopes, and the Kedarnath valley was wiped away without warning. According to the report, the calamity was caused by an integrated effect of high rainfall intensity, unexpected breach of Chorabari Lake, and highly steep topography. Mandal and Chakrabarty (2016) used HEC-RAS and HEC-HMS to create a simulation model of surface runoff in the upper Teesta basin, incorporating meteorological and morphological data in a geo-spatial setting. (Chawla et al., 2018) used a WRF model to study the impact of several processes on extreme rainfall simulation using a specific event that occurred over the Ganga Basin in India during June 15–18, 2013. They improved the model's performance by using detailed land surface models (LSMs) and investigated the effects of model grid spacing using two sets of downscaling ratios. They concluded that a higher downscaling ratio creates more variability and, as a result, significant inaccuracies in simulations. In recent years, there has been an increased focus in India on improving flash flood alerts. Climate change predictions show an increase in extreme precipitation events, potentially leading to more catastrophic flash flooding.

Furthermore, due to rising urbanization, more places will be vulnerable to flash flooding (Elhag & Abdurahman, 2020). Flash flood forecasting with high spatial resolution and significant lead-time is required to manage the threats posed by flash floods. Improvements in observing capabilities, modeling methodologies, and decision support systems have contributed to advancements in flash flood forecasting (Wu et al., 2020). Satellite and radar observations and associated systems for using these data have seen significant advancements. On the other hand, India needs more attention in the domain of radar hydrology, which is now lacking. Advanced methodologies have been developed to estimate very high resolution (spatial and temporal) real-time rainfall estimates from weather radar data blended with gauged rainfall. Also recently produced are several satellite-based precipitation products with high temporal and spatial precision (near real-time). New strategies for combining numerous data sources to make rainfall forecasts with longer lead times have been developed. To provide rainfall forecasts, these systems incorporate satellite-based rainfall, radar rainfall, gauged rainfall, and Numerical Weather Prediction (NWP) model outputs ((Xie et al., 1996); (Huffman, 1997); (Amorati et al., 2000); (Sinclair & Pegram, 2005); (Teng et al., 2017)). These approaches' applications to Indian conditions are still being researched and demonstrated.

2.6 Challenges during flash flood forecasting

Many problems face developing a completely working end-to-end forecasting system, from data observations to public evacuation. Because the time lag between a rainfall event and a flash flood is small, the anticipated lead time is crucial in such a system. Predictions must be generated with sufficient advance time; hence, obtaining credible precipitation forecasts with sufficient lead time is critical. Precipitation forecasting systems must be enhanced with science and computer facilities developments, a better understanding of meteorological and climatological processes, and better observation networks. Complicated phenomena trigger flash floods, and high-quality observable data, such as land use, soil characteristics, soil moisture, morphology, and upstream circumstances, are needed to understand the complex natural hydrological processes. Hydrologic/hydraulic models can be utilized for flash flood forecasting with the availability of trustworthy data, and prediction uncertainty estimates improve the credibility of a forecast system. However, in flash flood forecasting and warning, developing approaches that include uncertainties in decision-making is a huge problem. More research is needed to produce dynamically varying probabilistic risks employed in decision-making. Even if the warnings are accurate and timely, disseminating the alerts to the general population to take appropriate action is a key difficulty when using a credible forecast. Though

advances in communication technologies have made public transmission of flood warnings possible, there is often a knowledge gap between what the public understands and what the authorities communicate. As a result, increasing public awareness and information about flash floods is critical. As a result, the research community must collaborate with stakeholders such as the government and the general public to guarantee that the knowledge and technology created by them are put to the best possible use for social benefit.

2.7 HEC-RAS modeling Case studies

The River Analysis System (HEC-RAS) of the United States Army Corps of Engineers is a developed software system that includes a graphical user interface (GUI), independent hydraulic analysis components, data storage and administration capabilities, visuals, and reporting capabilities. Hydraulic Engineering Center (HEC), a branch of the Institute for Water Resources (IWR), US Army Corps of Engineers, developed the software. HEC-II was the first version of HEC-II.

HEC-RAS is an open-source tool for performing one-dimensional, two-dimensional and coupled one-dimensional and two-dimensional hydraulic simulations for a whole network of channels. RAS was first launched in July 1995, and many improvements and updates have been made since then, with the most recent version 5.0.7 being released in 2021. The current version of HEC-RAS supports the calculation of constant and unchanging water flow profiles, integrated 1D and 2D hydrodynamics, sediment movement / mobile beds measurement, water temperature analysis, water quality analysis, and spatial modelling of numerous measured parameters. The key advantages are the standard geometrical software representation and common geometrical and hydraulic computing procedures. Geometric data is essential for the creation of any hydrodynamic model. To execute 1D and 2D flow simulations, HEC-RAS requires exact channel geometry in cross-section data or a digital elevation model. To simulate water flows, researchers are now utilizing hydraulic models and GIS. DWOPER, FLDWAV, MIKE-11, ISIS, SOBEK, CCHE2D, TUFLOW, Infoworks-2D, RiverFLO-2D, and other widely used software programs are used to simulate 1D and 2D flow in rivers.

Many academics have successfully created a one-dimensional HEC-RAS model for streams worldwide. Numerous researches depict the application of HEC-RAS in the two-dimensional model to understand flood depth in various scenarios better. Here are presented some case studies which are related to this concern.

2.7.1 1D model case studies

(Azouagh et al., 2018) used the HEC RAS and HEC Geo RAS tools included in the Arc GIS program to create floodplain maps for a 30 km stretch of the torrential Martial River in Morocco. Because the job required higher precision and DEMs of 30 m, 12 m, and 10 m resolution didn't meet the study's requirements, a combination of 2 m resolution aerial images and DEM was used to construct geometry data in the form of a 146 cross-section using the HEC Geo RAS tool. The highest discharge for each station was evaluated for model simulation using discharge data from the previous record of three sites from 1970 to 2013. The 1D HEC RAS model was simulated for return periods of 10 years, 20 years, and 50 years for three flood zones. The model's output allows for the identification of flood zones and other hydraulic factors such as water levels and velocity. The authors found that the results are compatible with the area's morphology and that the HEC RAS program, combined with aerial pictures and detailed information on river morphology, helps identify flood risk areas for flood management and mapping.

(Masood & Takeuchi, 2012)

Using SRTM DEM of 90 m grid and previous flood records from 1972 to 2004, (Masood & Takeuchi, 2012) created a 1D hydrodynamic model for a 37 sq.km area of mid-eastern Dhaka. According to the author, DEM can only mimic channels with widths higher than twice its resolution. As a result, using the obtained 90 m resolution SRTM DEM, it was impossible to solve the Balu River in a study region with an average width of 100 m. Using the bilinear interpolation method, the authors re-sampled a DEM with a resolution of 90 m to 30 m. The original DEM was blended with the updated DEM of 30 m resolution, which was changed according to the actual river cross-section and raised elevation. Using the Gumbel distribution, the authors computed the maximum water level for a 100-year return period and applied it as an upstream and downstream border condition. The findings of the RAS simulation were used to calculate the risk zone, which is a product of inundation depth and flood vulnerability of persons and property. This research demonstrates how HEC RAS and DEM data may be appropriately combined to prepare flood risk management information.

(Thameemul Hajaj et al., 2019) developed a flood forecasting model for the Subernarekha river with a length of 154 km for forecasting flood levels by combining HEC-RAS and GIS for producing geometric data and mapping inundation and damaged regions. Using 10 m grid DEM generated from Cartoset 1 stereo data obtained from the National Remote Sensing

Centre, the authors created 239 cross-sections of the River (NRSC). By choosing 233 random spot elevation locations, the elevation data of Cartoset 1 DEM with a resolution of 10 m was compared and validated with topo-sheet data and determined to be rationally fit. Upstream and downstream boundary conditions were determined using stage hydrographs in Jamshedpur and Bhosraghat. The model was calibrated with stage hydrographs from 1985 and 1988, and the best appropriate manning's roughness coefficients of 0.11 for banks and 0.047 for channels. Statistical performance indices such as the Nash-Sutcliffe Coefficient, index of agreement, and percentage of deviation in peak were utilized to validate discharge and water level from 16th June to 22nd September 1997 using the calibrated hydrodynamic model. The authors determined that a hydrodynamic model created for the Subarnarekha river using a 10 m grid Cartoset 1 DEM can accurately predict floods for various return times. They were using physically surveyed geometry data and flood data from 1998, 2003, and 2006.

(Timbadiya et al., 2011) constructed a 1 D unsteady HEC-RAS model for the Lower Tapi River. For the 103.5 km length of the lower Tapi river, river geometry was represented by 135 cross-sections, and Manning's roughness coefficient was taken as a single value of 0.035. The authors chose the flow hydrograph at Ukai Dam as the upstream border and the stage hydrograph at Hope Bridge in Surat as the downstream boundary. The model was run for 10 minutes of the calculation time step for the extreme flood years of 1998, 2003, and 2006, and stage hydrographs at Kakrapar weir and Ghala station were investigated. The statistical metrics of percentage error, root mean square error, mean absolute difference, and mean difference were calculated and inspected while comparing observed and simulated stage hydrographs at two gauging stations. The author determined that the HEC-RAS simulated stage hydrographs and actual stage hydrographs were nearly identical.

(Nandalal, 2009) constructed the HEC-RAS model for the 79 km length of the Kalu River in Sri Lanka, from Ratanpura to Kalutara, to determine water levels across the river. The river was represented in the form of 86 surveyed cross-sections using 1:10,000 topo-sheets, which provided the necessary geometric data for developing a model. The model was initially trained using five distinct steady flow profiles, and the model calculated water levels at three gauging stations, namely Ratanpura, Ellagawaa, and Ptupaula, which were compared to observed water levels. The author then used Manning's n calibrated from steady flow simulation to simulate the HEC-RAS model under unsteady conditions for the reported flood event of May 17th to 20th, 2003, demonstrating good agreement between observed and simulated water levels. The unstable model was simulated for fifty different flood events to demonstrate a probability

relationship between upstream and downstream flood levels. The generated model also includes three-dimensional images of waterlogged sites along the river and the extent of inundation on both banks. The author concluded that the proposed model can calculate water levels downstream based on upstream water levels and that these results can be utilized to inform people about water flow in downstream regions based on upstream populations' experiences.

2.7.2 2D model case studies

(Arash & Yasi, 2023) Digital elevation models (DEMs) are a crucial input to hydraulic models to simulate flood danger maps. Higher levels of uncertainty are present in coarser resolution DEMs, particularly when recording river-bed bathymetry. The main goal of the current study was to evaluate the potential use of openly downloadable DEMs and the 1D and 2D HEC-RAS modelling techniques for flood mapping in four different types of river morphology. Three remote sensing-based DEMs (i.e., ALOS, SRTM, and ASTER) were evaluated using the DEM produced through a direct river survey (referred to as the "Surveyed DEM"). The outcomes showed that ALOS is more precise. The number and arrangement of representative sections were optimized to correct the DEMs. There were 144 tests performed in all. According to the findings, the ALOS flood-mapping index F increased from 86% to 91%. In straight reaches, the flood mapping using a 1D model was adequate (F-index 84%). To achieve an F-index of up to 81% in rivers that meander through the floodplain, a 2D model was required. In the case of wide-braided rivers, the responses of both 1D and 2D models were essentially equal.

(Pathan et al., 2022) identified in the semi-arid Navsari district region, the mesh grid stability of geometrical analysis has been optimized with a trial and error. The maximum water depth maps are compared with the modeled data in the calibration of suitable mesh. This study examines the impact of floods under various data produced throughout the model's simulation. As a result, this Big Data platform has proven to be a reliable method for flood assessment, serving as the foundation for building a solid HEC-RAS 2D model for the model's validation utilizing Big Data from previous flood events. Navsari City's flood incident on August 4, 2004, was reproduced using a variety of mesh grids. The model's findings showed that although there were no appreciable variations in the depth and scope of the inundation, there were considerable variations in the length of the simulation.

(Asitatikie et al., 2022) This study uses 2D hydrodynamic models for unsteady flow and GIS to prepare floodwater depth, flood velocity, and water surface elevation profiles. The analysis

of flood frequencies is used to forecast peak flow. A significant region of 52.5134 km^2, 52.4756 km^2, and 52.4403 km^2 was submerged by water up to 1 m for a 10-, 100-, and 1000-year return period, respectively. In all flood episodes, a sizable area was submerged at a velocity of up to 0.15 m/s, corresponding to 53.207, 52.656, and 52.064 km^2 for flood events of 10, 100, and 1000 years, respectively.

(Chowdhury et al., 2020) constructed a combined 1D and 2D hydrodynamic model for the Jamuna River Basin utilizing HEC RAS and GIS to develop flood inundation maps. For building a 1D HEC-RAS model of the river ignoring the surrounding floodplain, geometry was prepared in HEC GeoRAS using a 10 m grid re-sampled DEM. The adjacent floodplain on the left and right banks of the river was turned into a 2D mesh of 300 m x 300 m cell size after importing 1D geometry into HEC-RAS. The model simulation has fixed the calibrated manning's value of 0.032 for the main channel and 0.035 for the floodplain. From 2004 to 2008, the validated HEC-RAS model was used to generate multiple water surface profiles for varying flow conditions throughout 5 years. The simulation results were utilized to create flow inundation maps with the help of GIS. The inundation area was in close accord with the MODIS data map. The work demonstrated a systematic method for flood inundation maps utilizing a connected 1D and 2D model with HEC-RAS and GIS. The author also confirmed the compatibility of HEC-RAS, Arc GIS, and HEC GeoRAS to create a connected 1D/2D model.

(Quirogaa et al., 2016) constructed a 2D HEC-RAS model for Bolivian Amazonia based on geometric data generated using a 90 m grid SRTM DEM and flood data from 2nd February to 2nd March 2014. At the upstream and downstream extremes of the Mamore River, the flow hydrograph and normal depth have been used as upstream and downstream boundaries, respectively. The author ensured the model's stability using a 15-second time step determined using the Courant-Friedrichs-Lewy condition. The study shows that the model effectively generates flood levels and that the data supplied by satellite photos matches the model well. On the other hand, the simulated model provides additional data such as water depth, velocity, duration, and inundation border, which aids in analysing prospective flood management approaches.

(Rind et al., 2018) used HEC-RAS 2D, Arc GIS, and HEC GeoRAS tools to create a two-dimensional hydrodynamic model for the lower Indus river from Kotri Barrage to the Arabian Sea for the flood year 2010. The study's main goal was to draw flood inundation maps and identify flood-vulnerable locations in case of future flooding. The researchers employed the

free ALOS World 3D digital surface model with a resolution of 30 m to generate detailed bathymetry of river sections with GIS, and model simulation was done in HEC-RAS. The study uses Land Use Land Cover, identified by the Landsat 8 Archive and later confirmed by FAO and SUPARCO using Atlas.

The major goal was to differentiate between distinct land use features of classes in the research area and assign different manning's n values to each class based on these categories. According to the United States Geological Survey, the roughness value of alluvial and non-alluvial streams has been assigned to each group (USGS). The calibrated model from 2010 was then validated for the 2015 flood event using Manning's roughness. Regarding geographic match, % match, and measure of fit, "F" technique, the flood inundation simulation results were compared to MODIS data. This analysis addresses the design of an adaptive flood system that may be used on local and regional sizes to establish and implement an effective flood management plan. The authors indicate that the proposed template can be improved by using higher-resolution topographical data and that the findings might theoretically be utilized for hazard assessment, flood insurance, future flood forecasting, and land use planning.

(Shustikova et al., 2019) compared the performance of HEC-RAS 1D, HEC-RAS 2D, LISFLOOD-FP sub-grid, and LISFLOOD-FP diffusive models in model structure and relative sensitivity to surface roughness categorization for the same input data and boundary condition to perform unsteady flow analysis for four past flood events in the United States. The application of these models to four different areas with varying river geometry and roughness categorization demonstrates that the geometry of the 1D or 2D models has no effect on the performance of the river's sinuosity, length, or wavelength for a given set of roughness. A 1D model's quality is somewhat comparable to that of the 2D models used in the analysis, with the 2D models yielding slightly superior results. The study finds that low channel roughness influences the quality of 2D models, which improves as channel roughness rises, allowing more water to enter the floodplain, whereas increased floodplain roughness influences the quality of 1D models favorably. The researchers examined uniform and distributed roughness classification in the floodplain, concluding that uniform surface categorization produces better results than distributed roughness categorization.

(Patel et al., 2017) used GIS and HEC-RAS software to create a coupled 1D/2D hydrodynamic model for the Tapi river and Surat city. Researchers used 299 cross-sections at an average spacing of 150 m to 200 m for 1D modeling of the Tapi River and geometric data from SRTM

DEM of 30 m and 90 m resolutions for 2D modeling of the Tapi River. The researchers recreated the flood of 2006 and generated the results in flood depth, water surface level, flow velocity, arrival time, distance, and flooding in seven locations. The model is run in two scenarios, one without bank protection and the other with bank protection, to determine the future risk of flooding. The simulated findings are compared to the regional flood level map and observed depth. The new version 5.0.1 of HEC-RAS for flood analysis in a 1D/2D set was analyzed in this study, and it was concluded that it is an appropriate way for decision-makers to consider the likelihood of flood rate, size, arrival time, depression, and length in advance, in a specific location in the flood plain. It also assists decision-makers in making the best choices possible based on simulated results to minimize the loss of people and infrastructure.

The goal of (Yadavrao Nandurkar et al., 2017) was to build urban flash flood modeling by combining remote sensing data with the HEC-RAS hydrodynamic model. QGIS software is used to create all of the required map layers. Rainfall data for the Pune district has been collected since 1998, and average daily rainfall has been determined for the past 20 years based on data of significant rainfall. Cross-section data for the Mula and Mutha Rivers was estimated using a 1 m interval contour map, and for a segment of the Mutha River that passes through a city area where a contour map is not available, a regular interval of 1 m in a triangle form was assumed. The city of Pune's geometric data was extracted using a 30 m resolution SRTM DEM. The researchers used recent Landsat data to determine the impervious surface. The metropolitan area was divided into different vegetation, impervious surface, and soil classes, with appropriate Manning's roughness values. The researchers used the HEC-RAS model to calculate flood flow depths at several locations throughout the city. The authors stated that HEC-RAS is particularly effective in predicting water depths due to heavy rains in metropolitan areas and that the full model simulation is data-intensive, requiring a thorough topography model to build precise geometry. The authors also advise expanding this study by adding more information from physical surveys, RS, and GIS to provide vulnerability assessments and mitigation plans.

2.8 Application of google earth engine in flood modeling

Since 2014, the google earth engine has been the most popular platform for geospatial analysis. Many researchers worked on flood mapping and its effect on various land cover conditions. Here, I represented the case studies related to the google earth engine to simulate the flood scenarios with specific time instances. Many studies also depicted the capability of GEE in the various field of land observation like NDVI, NDWI, and crop monitoring systems.

(Chung et al., 2015) prepared the article regarding flood prevention and early warning system using the google earth engine for typhoon Forrest. This article examines the efforts and lessons learned in developing the Google Earth Engine-powered Flood Prevention and Emergency Response System (FPERS), focusing on its applicability at the three stages of floods. In the post-flood stage, FPERS uses Formosat-2 optical imaging to detect and monitor barrier lakes, synthetic aperture radar images to create an inundation map, and high-spatial-resolution pictures obtained by unmanned aerial vehicles to assess damage to river courses and structures. FPERS integrates a massive quantity of geographic data at the pre-flood stage, divided into four categories: typhoon forecast and archive, disaster prevention and warning, disaster occurrences and analysis, and primary data and layers. Three tactics are employed during the flood stage to ease access to real-time data: displaying vital information, generating a sound recommendation, and aiding decision-making. From 2013 to 2016, the example of Typhoon Soudelor in August 2015 was used to show how FPERS enhanced flood prevention and emergency response operations. The ability to transition between several topographic models and the flexibility of organizing and finding data through a geospatial database are also discussed, with recommendations for future work.

(Singha et al., 2020) evaluated the flood effect on the paddy rice field using sentinel 1 images in the GEE. Flooding is the most significant cause of natural disaster-related deaths worldwide, particularly in Bangladesh, where overflowing rivers flood roughly one-third of the country every year during the monsoon season, wreaking havoc on paddy rice agriculture and food security. However, there are few research on the pattern of floods in Bangladesh and their influence on agriculture. Using all accessible Sentinel-1 Synthetic Aperture Radar (SAR) pictures and the Google Earth Engine (GEE) platform, They looked at the spatiotemporal pattern of floods across the country from 2014 to 2018. They identified them by combining flood-affected paddy rice fields with remote sensing-based paddy rice planting areas. According to our findings, flooding is expected in northern Bangladesh and along the three major rivers, the Ganges, Brahmaputra, and Meghna. Flood-affected paddy rice regions accounted for 1.61–18.17 percent of total paddy rice area between 2014 and 2018. Using satellites to detect floods and flood-affected paddy rice fields improves our understanding of the annual dynamics of flooding in Bangladesh, which is critical for developing adaptation and mitigation strategies in areas where severe annual floods threaten human lives, property, and agricultural production.

(Tamiminia et al., 2020) wrote the systematic review for applications of the GEE in various fields of earth observation study. Google Earth Engine (GEE) is a geospatial processing engine for large-scale environmental monitoring and analysis in the cloud. The development of GEE has sparked a lot of interest and involvement in remote sensing and geospatial data science. The GEE platform is free to use and gives users access to (1) petabytes of publicly available remote sensing imagery and other ready-to-use products via an explorer web app; (2) high-speed parallel processing and machine learning algorithms using Google's computational infrastructure; and (3) a library of Application Programming Interfaces (APIs) with development environments that support popular coding languages like JavaScript and Python. These essential capabilities allow users to search, analyze, and visualize extensive geospatial data in powerful ways without supercomputers or specific coding knowledge.

Although GEE has been operational for a decade, its impact on remote sensing and geospatial science has not been thoroughly investigated. As a result, a systematic review of GEE is required, offering readers a "broad picture" of the current state and general trends in GEE. A meta-analysis of current peer-reviewed GEE studies was conducted, focusing on numerous features such as data, sensor type, study region, spatial resolution, application, strategy, and analytical methodologies. Between 2010 and October 2019, 349 peer-reviewed publications published in 146 journals were examined. Publications and geographical distribution patterns revealed various environmental analysis applications at both regional and global scales. In 90% of the research, remote sensing datasets were used, whereas 10% of the articles used ready-to-use products for analysis. Optical satellite imagery with a medium spatial resolution has been extensively used, particularly Landsat data with a 40-year archive. The most often utilised methods for satellite imagery processing were linear regression and random forest. The normalised difference vegetation index (NDVI) was employed in 27% of research for vegetation, crop, land cover mapping, and drought monitoring using ready-to-use products. The findings of this study show that GEE has made and continues to make significant progress on global difficulties concerning geo-big data processes.

(Inman & Lyons, 2020) have analyzed the large inundated area using Landsat images in the GEE platform. Accurate inundation maps are essential for managing and maintaining flooded wetlands and rivers. Using Landsat imagery and Google Earth Engine, they automate a method (thresholding of the short-wave infrared band) for determining peak inundation in the Okavango Delta, northern Botswana. Because of the spectrum overlap between inundated areas covered with aquatic vegetation and dryland vegetation classes on satellite data makes

inundation classification in the Okavango Delta complicated, and classifications have primarily been implemented on broad spatial resolution imagery. They show the Okavango Delta's most extended time series of inundation maps for the peak flood season at a high spatial resolution (30 m) (1990–2019). They used image-based and in-situ data accuracy tests to confirm the maps, with overall accuracy ranging from 91.5 percent to 98.1 percent. Landsat imagery produced consistently lower estimates of inundation extent (on average, 692 km2) than previous studies that used Moderate Resolution Imaging Spectroradiometer (MODIS) and National Oceanic and Atmospheric Administration Advanced Very-High-Resolution Radiometer (NOAA AVHRR) imagery. This is likely due to the increased number of mixed pixels that occur when using broad spatial resolution imagery, leading to overestimating inundation size. They make the inundation maps and Google Earth Engine code available to the public. This classification method can most likely be used to map inundation in other areas.

(DeVries et al., 2020) The Copernicus program of the European Space Agency (ESA) has decided to make data from its Sentinel-1 SAR satellites available to the general public for the first time. This development, combined with the rise of cloud computing platforms like the Google Earth Engine (GEE), offers the disaster response community a huge window of opportunity. The community needs quick access to data ready for analysis to inform effective flood disaster response interventions and management plans. Here, the algorithm quickly maps surface inundation during flood events using historical Landsat, additional auxiliary data sources, and all accessible Sentinel-1 SAR pictures. Our system uses multi-temporal SAR statistics to detect unexpected floods quickly. Additionally, historical Landsat-based surface water class probabilities are used to identify unexpected floods from perennial or seasonal surface water.

(Zhao et al., 2021) denotes the trends and progress in google earth engine and google earth over the years. Because of global environmental changes and the development of Earth observation equipment, Earth system research has changed swiftly. As a result, new technologies for monitoring, measuring, analysing, evaluating, and modelling Earth observation data are necessary. Google Earth (GE) was published as a "geobrowser" in 2005, and Google Earth Engine (GEE) was released in 2010 as a cloud computing platform with significant computational capabilities. These two tools or platforms in diverse applications have multiplied, notably in the remote sensing community. In this research, they used scientometric analysis (i.e., utilising CiteSpace) and meta-analysis to examine the applications and trends in the use of GE and GEE by examining peer-reviewed papers in the Web of Science

(WoS) core collection up to January 2021. The following is what they discovered: (1) From two publications in 2006 to 530 in 2020, the number of papers describing the use of GE or GEE has expanded dramatically. The number of GEE articles grew significantly higher than the number of GE articles. (2) The remote sensing community made considerable use of GE and GEE as transdisciplinary tools. GE papers appeared in a more excellent range of publications than GEE articles and covered many academic disciplines (e.g., biology, education, disease and health, economics, and information science). (3) The use of similar terminology by GE and GEE (e.g.,"land cover,""water,""model,""vegetation," and "forest") suggests that their application is critical in particular research fields. The key distinction was that publications about GE focused on its application as a visual display platform, whereas papers about GEE focused more on big data and time-series analysis. (4) Most GE and GEE applications were carried out in countries including the United States, China, and the United Kingdom. (5) GEE is a valuable tool for analysis, whereas GE is useful for visualisation. Finally, this work discusses the strengths and limits of GE and GEE and proposals for additional enhancements from an Earth system science perspective.

(Pandey et al., 2022) The Ganga-Brahmaputra basin is extremely vulnerable to the effects of climate change and frequently floods, which has a negative impact on vast agricultural areas and poses a serious risk to the populace. The recent flood crisis in the Ganga-Brahmaputra basin, which mostly hit the Indian states of Bihar, West Bengal, and Assam as well as the nearby nation of Bangladesh during the months of July, August, and September 2020, is the subject of the current study. The Google Earth Engine (GEE) platform was used to determine the flood extent using Sentinel-1A Synthetic Aperture Radar (SAR) data. Bangladesh was expected to have 25,889.1 km^2 of the combined area flooded from July to September, followed by Bihar (20,837 km^2), West Bengal (17,307.1 km^2), and Assam (13,460.1 km^2). The damaged agricultural area and settlement that was impacted by the flood were extracted from the Copernicus Global Land Cover dataset. Floods have had a negative influence on communities and agricultural grounds, affecting 5.66-9.15% and 23.68-28.47% of these areas, respectively.

2.9 Research gap

This research focuses on inundation mapping Ghed regions using hydrodynamic models and satellite image analysis techniques, especially for data constraint regions. Past research indicates that the validation of hydrodynamic models is rare in areas where the observed data set is limited. Moreover, satellite techniques are widely used for flood inundation mapping and early warning. However, the previous study indicates the rare use of satellite images for

hydrodynamic model validation with the inundation boundary of the post-flood image. In addition, the study region has cup shape geometry, and the velocity of a flood is not a primary concern, but the flood depth and arrival time are significant for hydrodynamic modelling; this kind of region geometry rarely appears in the literature study. This research emphasizes dealing with the data-constrained region, especially for the study area with a large ponded depressed river delta. In the analysis of flood mapping, a large data set is required for hydraulic modelling, mainly where the river water is scattered towards the open ground. In this condition, It is necessary to measure the water depth in the dispersed region periodically. However, this kind of data set in this research is limited but efficiently utilized for model validation.

Chapter 3. Study area and data used

3.1 General

Ozat river originates from the hilly area of Gir forest; most of the river runs through the Junagadh district, where the delta region and river mouth lie in the Porbandar district. The Ozat is one of the ancient river of the region where Junagadh city mostly depends on the Ozat water. Mostly the people asides from the river valley depend on agriculture, but nowadays government has also planned a recreational area near vanthli village. It has also utilized this water source for drinking purposes. The Ozat River is the lifeline for a community of more than ten lacs.

3.2 Hydrological aspect of Ozat river basin

Ozat River basin has a vital hydrological viewpoint in regards to water utilization. The total length of the river is 145 kilometers from Gir forest to the river mouth near Navi Bandar. It has been identified that the initial portion of the river has sufficient width and depth, whereas the part 70 kilometers before the river mouth has insufficient depth and width compared to upstream. The delta region is flat and even dipped than the river mouth, which plays a significant role in inundation. Many adjoining tributaries make the Ozat river more full and give water to storage areas. The popatadi and ambajal are right bank reaches, whereas Uben and utavadi are left bank reaches of Ozat River. On the highest order reach of Ozat River has two major dams, Ozat-1 dam is also known as dhrafad irrigation project, and Ozat-2 dam is also known as badalpur dam. Dharafad dam, constructed in 1986, is a type of gravity dam with a catchment area of 169 km^2. It is 20 kilometers away from the origin point of the river having total storage capacity of 339.73 million cubic feet. The 2112 hectares of agricultural land of 7 villages benefited from irrigation and drinking water supply.

The badalpur dam was constructed in 1995, having a catchment area of 475 km^2. It is the largest dam built on the main tributary of the Ozat River. The dam site is 39 kilometers away from the origin point of the river, having a storage capacity of 1278.40 million cubic feet. A total of 13082 hector land of 43 villages benefited from this irrigation scheme of the Junagadh district. Afterward, the Anandpur major weir was established in the downstream region of badalpur dam. Its significance is to supply the irrigation water to the surrounding village and provide the drinking water to the Junagadh municipal corporation area. After this location and 63 kilometers from the origin point of this river, Shapur weir has a total storage capacity of 70.91 cubic million feet. It provides the irrigation water to 1500 hector of 6 villages. Here, the facility is made for direct and indirect irrigation water supply.

After this location, the Ozat River passes through the flat terrain towards the delts region. The 82 kilometers of the stretch after the shapur weir is considered for this research because no major hydraulic structure influences the main river reach of the Ozat River. After the 19 kilometers from the shapur weir, the downstream location shows the bifurcation of the river main reach near Tikar village. From this location, two reaches run towards the river mouth; one is straight towards the sea face and meets the Arabian sea near pata village. Another bifurcated reach, heading towards the Ghed region, having more than 200 km^2 area, and meet the Arabian after crossing the cup shape Ghed area. As discussed earlier, the coastal line between two river mouths is slightly higher elevated than inland. The total river basin has a 3185 km^2 catchment area up river mouth near Navi Bandar.

3.3 River system under study

Junagadh district falls under the coordinates of 21.3321° N to 70.3361° E, whereas the study area of this research falls under the 21°N to 21°45’ N and 69°45’ E to 70°45’ E. Most of the Ozat River lies in the Junagadh district; despite the downstream portion, the delta region and cup shape Ghed region falls under the Porbandar district. The primary study of this research is to identify the inundation assessment of Ghed region, and it’s assessment. The total length of Ozat River is 145 kilometers, but in this research, the portion of the river considered for analysis is only 82 kilometers after the Shapur weir. This location is selected like minimum hydraulic structures need to be considered for hydraulic modeling. Here, Fig. 3 depicts the location sketch of the entire study area region. The bifurcated reaches from tikar village have 62.6 kilometers for tributary towards Ghed region and meeting the Arabian sea near Navi Bandar. Another tributary runs straight towards the sea and meets the Arabian sea near Pata village, having a length of 36.6 kilometers. The total three reaches are considered for the hydrodynamic analysis and examined for comparative study.

From a hydrodynamic modeling point of view, it needs to assign the upstream and downstream boundary conditions, and all other needs to simulate the model in 1D conditions like cross section width, spacing, and interpolation. For a 2D model, input parameters like upstream and downstream boundary conditions are needed for modeling. In the Fig. 4, a schematic view of the model setup has been developed for a better understanding of pre modeling stage. In this view, the different setup points are far from each other, and in this section, all are well described. The model inflow point is 63.3 kilometers from the beginning of Ozat River. Afterwards, the vanthli bridge site is considered for water stage elevation comparison with

observed and simulated discharge for calibration of manning roughness value. This location is far away as 5.1

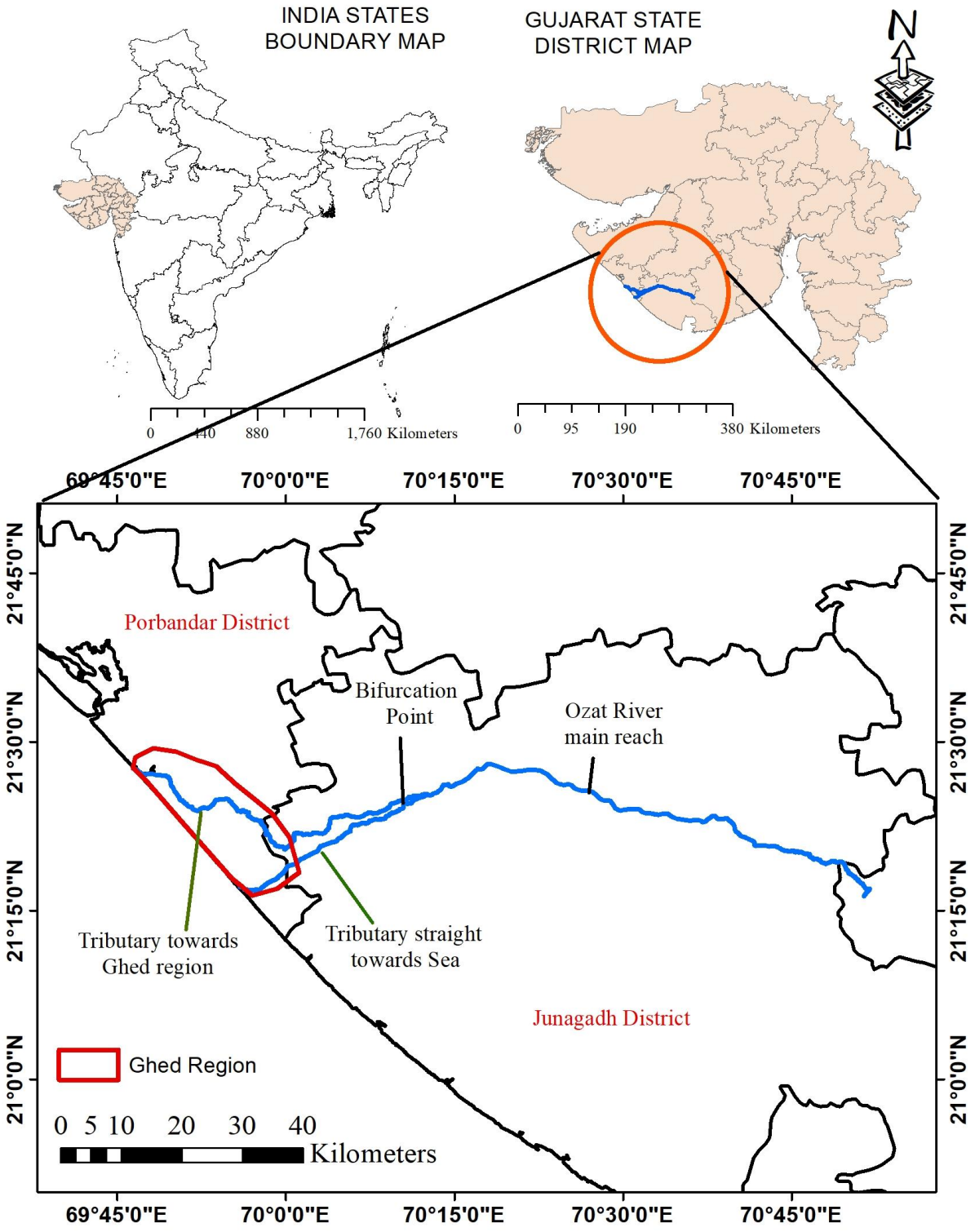

Figure 3.1 Location sketch of study area with river reaches

kilometers from the inflow point. In the schematic view, after the vanthli bridge site, the main river reach (Ozat-1 Reach-1) is bifurcated from the Tikar village. This location is 19.1 kilometers far from the inflow point of the model. After the bifurcation, the model is set up like water surface elevation needs to be compared on bifurcated tributaries. In this context, the tributary towards the Ghed region (Ozat-1 Reach-2) is calibrated near Indrana village. This location is far as 33.9 kilometers from the inflow point.

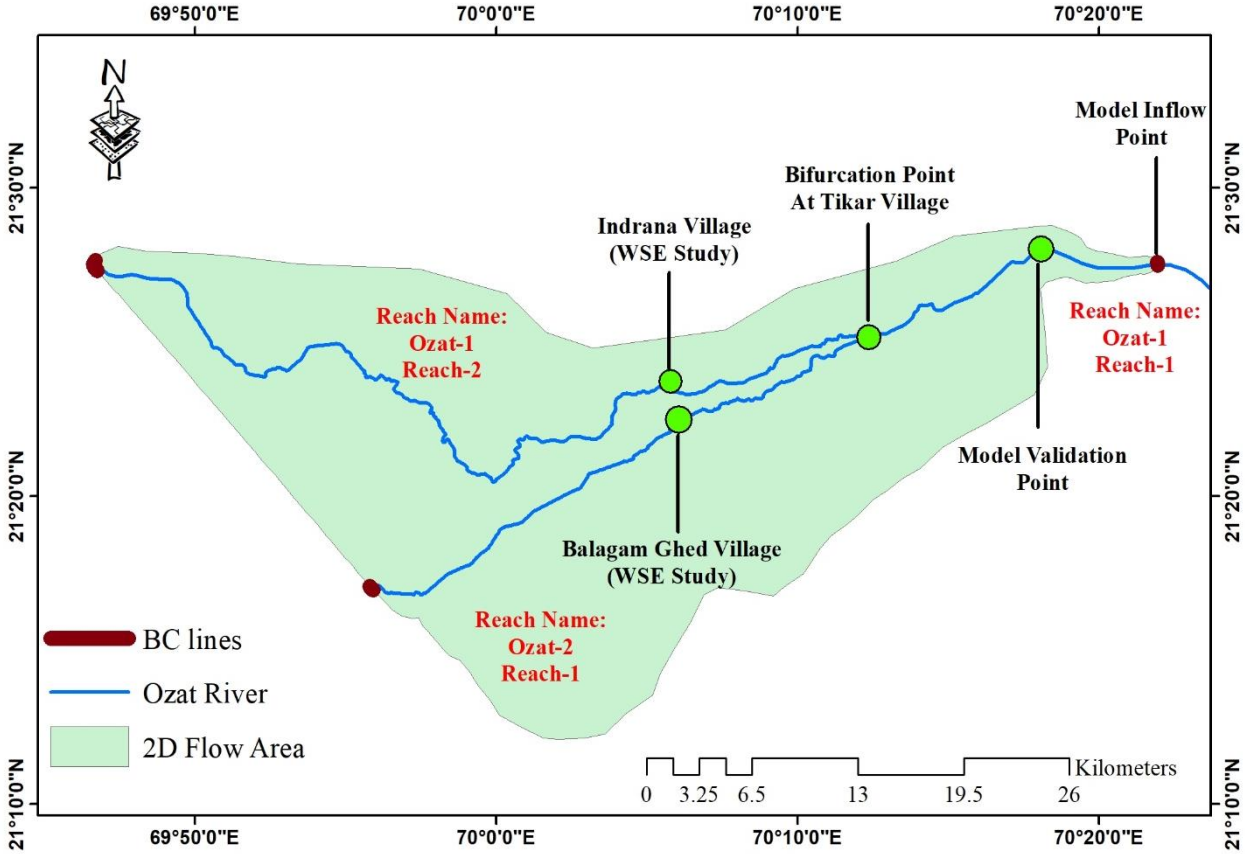

Figure 3.2 Schematic view of various key features with locations

Another bifurcated reach, heading straight towards the sea (Ozat-2 Reach-1) is calibrated near the Balagam ghed village. This location is far as 34.4 kilometers from the model inflow point. These locations (vanthli bridge, Indrana village and Balagam Ghed village) are considered to calibrate Manning roughness value with the water surface elevation study. After stations on bifurcated reaches, the tributaries heading towards the river mouths, the reach Ozat-1 Reach-2 meet the Arabian sea near Navi Bandar; this location is as far as 80.7 kilometers from the model inflow point. Another reach, Ozat-2 Reach-1 is heading straight towards the sea face and meet the Arabian sea near Pata village; this location is far as 55.7 kilometers from the model inflow place.

In the 2D model parameter setup, the upstream boundary condition is set near the shapur weir, and downstream boundary conditions are set at two places of both river mouths. One d/s boundary is near Navi Bandar for tributary Ozat-1 Reach-2, and another d/s boundary is set near Pata village for reach Ozat-2 Reach-1. Selecting a 2D flow area is a critical stage for pre-model setup. The spreading water area is identified from the field study and traced to finalize the 2D flow area boundary. The total 2D flow area is 870.70 km^2; details of villages and more locations about the inside of a 2D flow area will be discussed in further sections.

3.3.1 First Segment (Origin to bifurcation point)

The study area's first segment is Ozat River's main tributary from shapur weir to the bifurcation point near tikar village. Generally, the field visit is divided into three segments to understand the study area better. This visit is chosen for a dry period in winter to assess the maximum region. The Ghed region has been visited numerous times during the research. Initially, the study area of this research started from the shapur weir despite the Ozat River origin point is far as 63.3 kilometers from this place on the upstream side.

Sr No.	Name of Village	Aside from river bank	Distance from inflow point	Horizontal distance from river valley
1.	Vanthli	Right	4.4	1.86
2.	Kanja	Left	8.1	1.48
3.	Navda	Right	11.4	1.73
4.	Pipalana	Right	14.6	0
5.	Akha	left	17	0.709
6.	Tikar	Right	19.1	0

Table 3.1 Details of villages aside from Ozat-1 Reach-1

At the shapur weir (model inflow point), the Ozat River has a width of more than 200 m and a depth of 5 to 8 m near this weir. Further, moving toward the bifurcation point vanthli bridge is

5.1 kilometers far from the shapur weir. This location is considered for the water surface elevation comparison for better achievement of manning roughness value. After the vanthli bridge site, the bifurcation point is 14 kilometers away at Tikar village. Between the shapur weir inflow point of the model and the bifurcation point near tikar village, many villages are located aside from the river valley. The Table 1 details the river station near the village area

from the inflow point, and the horizontal distance between the river valley and the village built-up area for Ozat River reach code Ozat-1 Reach-1.

Sr No.	Name of Village	Aside from river bank	Distance from inflow point	Distance from bifurcation point
1.	Kothadi	right	19.8	2.06
2.	Koyalana	right	22.7	0
3.	Mandodara	right	24	0.879
4.	Matiyana	right	28.8	0
5.	Ambaliya	right	31.3	0
6.	Indrana	right	33.3	0
7.	Padardi	Left	35	0
8.	Osa	right	37	0
9.	Fulrama	right	41	3.17
10.	Bhathrot	right	43	1.49
11.	Ghodadar	Left	47	0.58
12.	Ghed Bagasara	Right	52	0
13.	Amipur	Right	58	1.68

Table 3.2 Details of villages aside from Ozat-1 Reach-2

In Fig. 5, the places are shown, like upstream to downstream river slopes. Fig.5 (a) indicates the inflow place of the model with 230m width between river banks. Fig.5 (b) shows the vanthli bridge site; this place is considered for water surface elevation comparison in the case of 1D model calibration and has sufficient width between banks. Fig.5 (c),(d) indicate the bifurcation point near the tikar village; at this place, the water is passed under the minor road bridge, and the bridges are constructed on both bifurcated reaches.

3.3.2 Second segment (Bifurcation point to river mouth near Navi bandar)

The second segment of the field visit was made between the bifurcation point and the river mouth near Navi Bandar. This segment is more vital than other parts of the study reach. Because the Ghed region has lied this way, cup shape geometry is filled with water in monsoon. A total of 13 villages are located near the valley of Ozat-1 Reach-2. In this visit, a detailed evaluation is made for past flood event analysis like marking of water levels, effect on barren

Land, cropland, and the presence of water after a big event. Out of 13 villages (Table 2), seven villages are located exactly touching the river valley area and are highly affected by the flood events. These villages are koylana, Matiyana, ambaliya, Indrana, padardi, osa and

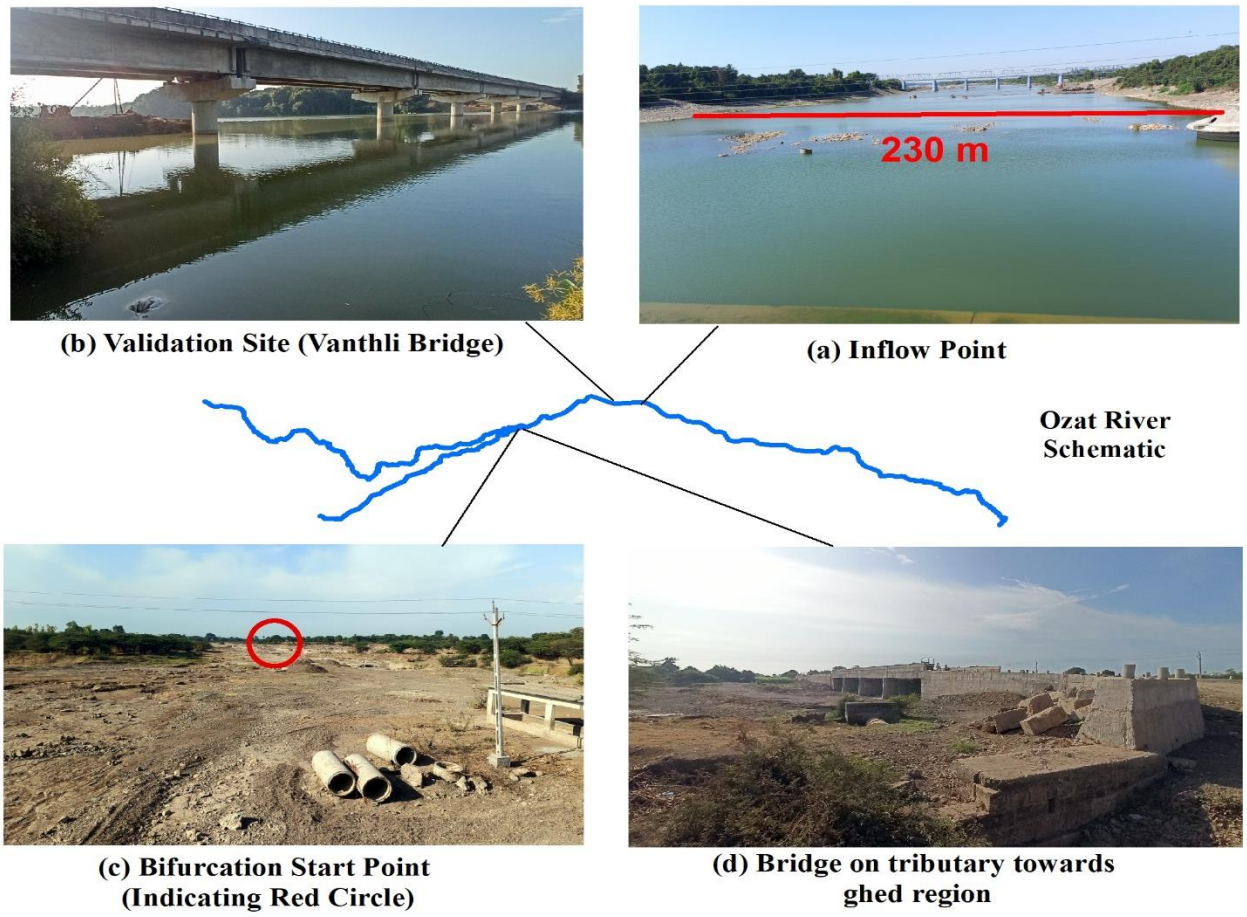

Figure 3.3 Ozat River reach (Ozat-1 Reach-1) from vanthli to tikar village

Ghed bagasara. In this way, the Indrana village is considered for the water surface elevation changes study, for the better gain of manning roughness value through the 1D hydraulic model simulation. Indrana village is far as 33.3 kilometers from the model inflow point. After the Ghed bagsara village, the river reach is passed through a large cup shape area of more than 180 km^2, and water is spread in this region is called Ghed region. The primary aim of this research is to serve this region from the inundation and detailed assessment of hazard maps from the event of 2017. In the section of the Ozat-1 Reach-2 after the ghed bagasara village, the river reach is hardly far as 9 kilometers to arrive at the river mouth. However, after this village, water is spread on a large area of cup shape geometry and needs to achieve sufficient height to reach the river mouth near Navi Bandar. The Table 2 details the village condition aside from this

river valley and the distance between the inflow point and river station near the village area with horizontal distance between the valley and village built-up area for Ozat-1 Reach-2.

Fig. 6 depicts the schematic view of Ozat River with the details of Ozat-1 Reach-2 field images. In this segment of the field study, the various sections of river reach have been evaluated for river depth and width and compared to the upstream section of river. Initially, this river's reach starts from the tikar village and moves through the villages close to the valley. Fig. 6 (a), (b) shows the koylana and Indrana village having river widths of 62 and 45 m, respectively.

Afterward, the Fig. 6 (e), (f) shows the river width situation near ambaliya and Bagasara Ghed village, having a width of 20 and 15m, respectively. The condition of river reach depicts that, moving towards the delta region or river mouth, the river width gradually appears in decreasing mode from 62 m to 15 m. After crossing the bagasara ghed village, river water spread in the large cup area of Ghed region, and as shown in Fig. 6 (c), during the visit time of the dry spell, the site is still inundated after four months of monsoon season. After crossing the ghed region, the river meets the Arabian sea near Navi Bandar.

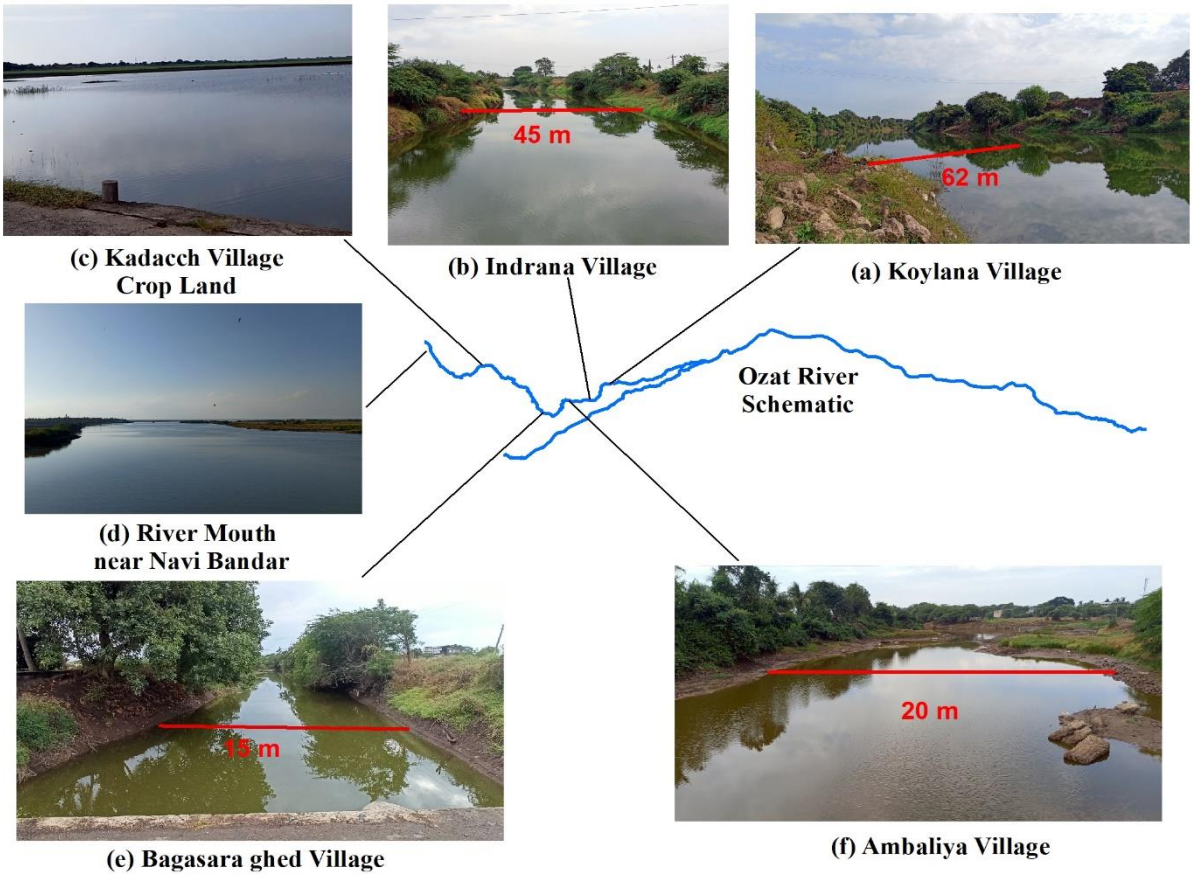

Figure 3.4 Ozat River reach (Ozat-1 Reach-2) from tikar village (bifurcation point) to river mouth near navi bandar

3.3.3 Third segment (Bifurcation point to river mouth near Pata village)

Sr No.	Name of Village	Aside from river bank	Distance from inflow point	Horizontal distance from river valley
1.	Bamnasa Ghed	Left	27.24	0.72
2.	Balagam Ghed	Left	34.4	0
3.	Samarda	Left	47.3	0.81
4.	Sarma	Right	47.3	1

Table 3.3 Details of villages aside from Ozat-2 Reach-1

The third part of the field visit shows the tributary (Ozat-1 Reach-2) condition towards the river mouth near pata village. After the tikar village, the river crosses the bamnasa village and leads toward the balagam village. The field situation depicts that, on this section of river reach, only one village is very close to the river valley, Balagam. Only four villages are situated aside from the river valley; this reach does not affect more than Ozat-1 Reach-2. During the field visit, the Fig. 6 (a), (c), and (d) show that from the upstream to downstream portion, the width of the river gradually decreases toward the river mouth. The Fig.6 indicates the river width near bamansa is 28m, near the balagam ghed village 23m, and at sarama village 15m appeared. On the way to Ozat-2 Reach-1, only village balagam ghed situated very close and highly affected built-up area in past flood events. The Table 3 details the location of the river valley area from the inflow point of a model and other details of the distance between the river valley and the village built-up area.

In Fig. 7, various conditions from upstream sections to river mouth till pata villages are described with images. This portion of the river stretch is vital for field analysis because very few villages are located aside from the river valley, and the affected area is much less except balagam ghed village. Geometrical study of this section of the river depicts that water of this stretch has more velocity to reach the river mouth than Ozat-1 Reach-2. It has a total length of 36.6 kilometers from the bifurcation point. As per the table 3, four villages are located aside from the river valley; out of this, balagam ghed village is considered for water surface change analysis for 1D model calibration concerning optimization of manning roughness value.

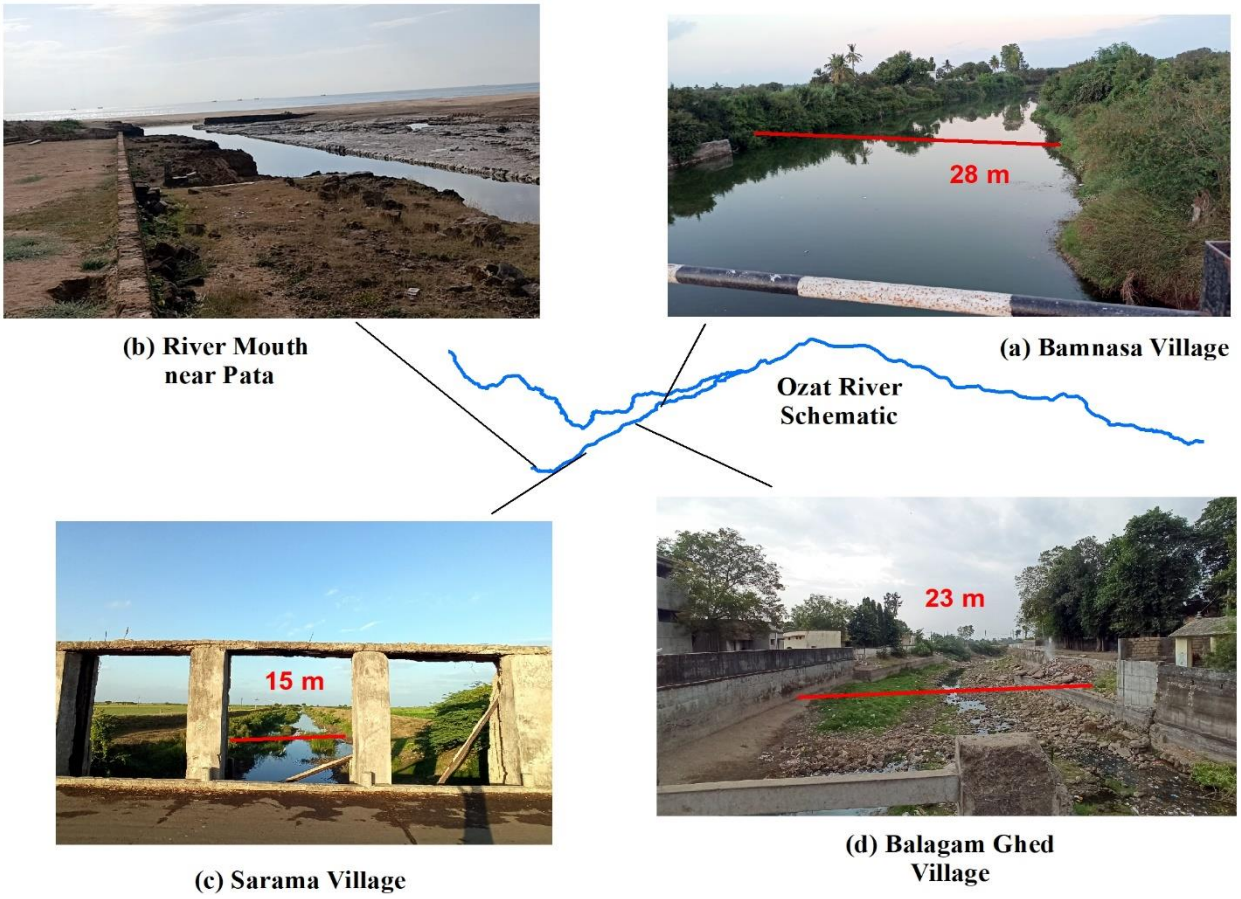

Figure 3.5 Ozat River reach (Ozat-2 Reach-1) from tikar village (bifurcation point) to river mouth near pata village

3.3.4 Between two river mouths (Pata village to Navi Bandar)

The portion of land area between two river mouths (pata village to navi bandar) is an important aspect of inundation. In the list of villages mentioned in the table 4, most villages are situated very close to the coastal highway and have no concern about inundation due to higher elevation. However, there are two villages, kadachh and mandor, which are highly affected in past events because of their location. These two villages are inland from the coastal zone, and the surrounding land is lower than the village's built-up area. If we discuss the periphery of ghed region cup shape geometry polygon, these two villages are situated precisely on the border of this polygon. As per discussion with local people of this region, past flood events created significant devasting and highly affected the local transportation of people during peak flow conditions, and water stays on the road network for more days even after the event.

Sr No.	List of Villages between estuary of Ozat-2 reach-1 and Ozat-1 reach-2
1.	Pata
2.	Mander (Highly affected due to surrounding submergence)
3.	Kadachh (Highly affected due to surrounding submergence)
4.	Chingariya
5.	Gorsar
6.	Mocha
7.	Balej
8.	Untada
9.	Ratiya
10.	Navi Bandar

Table 3.4 List of villages located between two river mouths

3.4 Salient features of Ghed region

Ghed is located in deep western part of Gujarat state. Over many years, this location gets inundated frequently because of it’s cup shape and natural terrain. The name Ghed originates from “Ghado”, and Ghado means a pot of water in Gujarati. This region gets flooded with direct rainfall and river water from the upstream side. In this region, the Ozat River becomes narrow, and many places are identified where people of the surrounding valley encroach on natural hydrology by forcedly straightening the meander section of the river. The area surrounded by the villages like sarama, osa, bagasra ghed, amipur , kadachh and mander create the deep cup shape polygon like a pot of water. The Ozat River needs to cross this polygon to reach the river mouth near Navi Bandar, and this cross of the region causes a significant inundation.

Since the river's carrying capacity is less than the amount of water that can be received in a short period, it floods whenever there are heavy rains in the catchments area. This causes the river's rage to manifest as an inundation of the Ghed region, which it finally reaches before flowing into the Arabian Sea. The amount of water floods the Ghed region with its ferocity. Local transportation being diverted ultimately prevents the area's natural connections from providing connectivity, making it inaccessible to deliver the necessary food and other necessities. A farmer expects assistance from the government or any comparable group when

their land's topsoil has been washed away. The river goes to the sea near Ghed, where it converges with other rivers and rivulets. As a result, the Ghed plains see a massive water buildup that causes a significant portion of the land to become submerged. Due to Ghed's low elevation, water gets held there for days or months at a time, washing out fields from both the flow of the water and its prolonged presence. Communication and transportation are disrupted due to the adverse effects on road and rail systems. Technocrats need to develop a long-term solution as this has become regular. There has to be a quick fix for this issue.

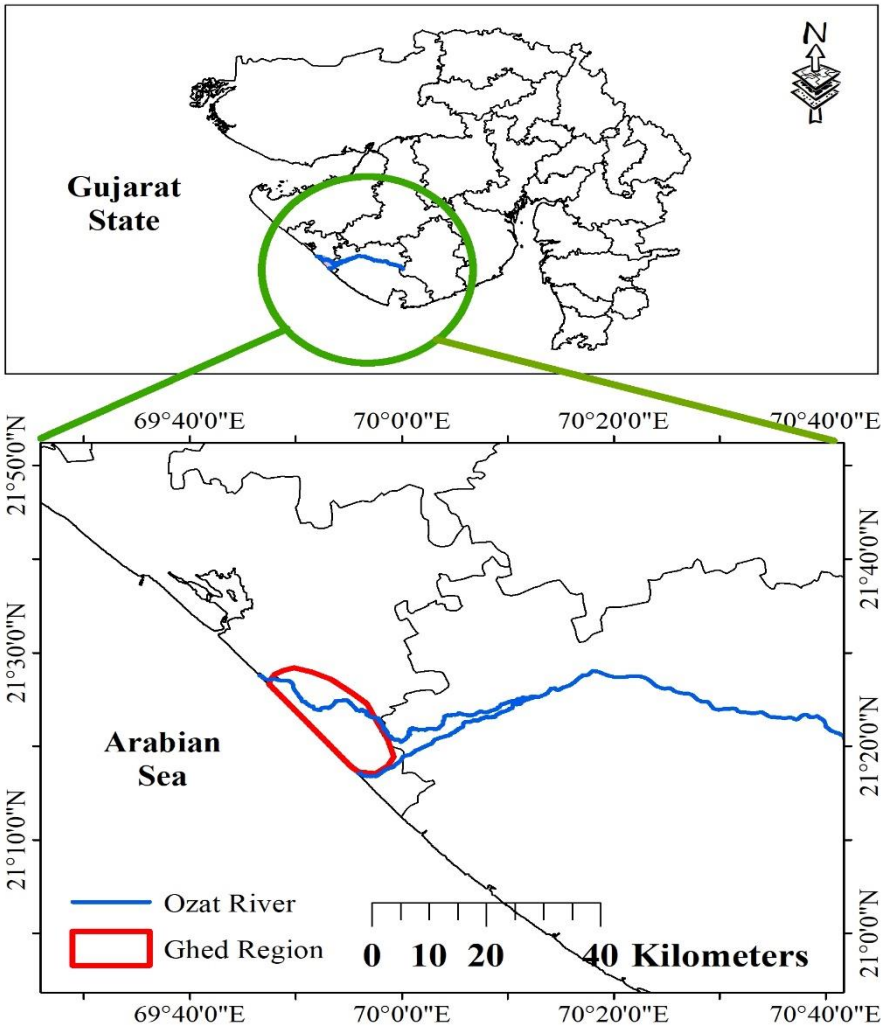

Figure 3.6 Location sketch of ghed

3.5 Data collection

Data collected from the various sources are detailed in this section. Initially, the digital elevation model plays a significant role in any hydraulic modelling, especially flood mapping. The data plays a vital role in validating simulations and all other results. In this research, the Ozat River basin is data-scarce regarding the tidal data unavailable at the river mouths. The

word data scarce has been incorporated into the research title. Initially, the 1D model was developed for river stage analysis. In this case, the digital elevation models (DEMs), SRTM, and ALOS have been compared for the Ozat River study area with calibration of water surface elevation and manning value.

For the hydrodynamic simulations of flood models, many input parameters are required for model performance, and they should be precise for better results. For the 1D model, DEM, cross section (CS) elevation, CS spacing, CS width, discharge data, calibration stations, and boundary conditions are required for modeling. The performance of a 1D model is only to analyze the river stage for a better assessment of a 2D model. For a 2D model, the input parameters like DEM, 2D flow area, cell size, model time step, land use land cover (LULC) map, discharge data, and boundary conditions are required for modeling. As we stated earlier, the Ozat River basin is data-scarce; the most data was collected from the Junagadh district irrigation flood cell and project division. However, the data on tidal waves and water levels at river mouths are not available in the span of the desired model simulation period. The water has been stored in sizeable depressed terrain like a pond. Although the water surface elevation of this pond needs to be required for 2D model validation, this data is not available in this regard, and the model has been calibrated in other ways. Many pieces of literature reveal the methodology for developing hydraulic models for data-scarce basins, especially in semi-arid regions. This is a similar case to that studies, and the study area depicts the river's main reach bifurcates into two other reaches, which needs validation for water distribution. These bifurcated reaches show the water separation, and it was validated in a 1D model with a limited data source. The Table 5 shows input data required for hydrodynamic modeling, source of data, and frequency and data type requirements.

Type of Data	Details	Source of Data	Use in Study
Topographic Maps	1:50000 Scale Maps	Survey of India (SOI 2008)	Trace the actual tributary of the river
Digital Elevation Models	30m SRTM	USGS Earth Explorer (USGS 2011)	Terrain file creation
	30m ALOS	JAXA website (JAXA 2008)	Terrain file creation

Stream Gauge Data (2 hours frequency)	Ozat River, Shapur village	Junagadh, Irrigation Department	Input Parameter
Water surface elevation data	Ozat bridge gauge, vanthli	Junagadh, Irrigation Department	Manning roughness coefficient Validation
Water surface changes	Indrana village and Balagam Ghed village	Junagadh, Irrigation Department	Comparative study
Cross-section inundation validation	Questionnaire survey	Field observation	Comparative study
Landsat 8 OLI	Collection-2 Level-1	Cloud store of Google Earth Engine	Land use/Land cover classification 2D model validation and flood visualization
Sentinel-1	C-band Synthetic Aperture Radar		

Table 3.5 Data type, details, source and help in study

If researchers working in conditions like the study area is far away from the working stations, the digital elevation models must be precise in all aspects. In this case, the purpose of a 1D model is only to predict the river stage up to river mouths and validate with a limited available data source. For the 1D modeling, the DEMs have also been compared in terms of manning values and water surface elevation changes. After revels the best DEM, the 2D hydrodynamic model has been simulated with this DEM. In this regard, the SRTM and ALOS have been compared. The other data is discharge data at specific places; it is vital for validating hydraulic simulations. There are three places where data is available for a specific period. These places are vanthli bridge site, Indrana village (Oat-1 Reach-2) and Balagam ghed village (Ozat-2 Reach-1). These places are considered for the validation purpose of a 1D model and calibration of manning roughness value. The validation is challenging for a 2D model because the water is spread out from the tributaries and scattered over a large cup shape area. In this context, the limited places are observed for past flow events and help validate the approach. The koylana, sarama, bagasara, and kadachh villages are considered for water depth study with observed and simulated water surfaces.

For creating, the cross sections in the geometry of a 1D model, the DEM-generated cross sections have been used instead of field surveyed sections. Field surveys of cross sections are not available for this study region. In the 2D model, the 2D flow area works with cell size and optimization of courant-Friedreich theory for better time step optimization.

As stated earlier, the DEMs play a significant role in hydraulic flood modeling, especially in the case of data-scarce regions. For 1D simulations, SRTM and ALOS are utilized for hydrodynamic assessment of the Ozat River basin. A worldwide initiative called the Shuttle Radar Topography Mission (SRTM) is being led by NASA and the National Imagery and Mapping Agency (NIMA), a US Department of Defense department. The SRTM payload space shuttle Endeavour was launched on February 11th, 2000. SRTM covered 80% of the earth's land surface with its radars, collecting enough data over its ten days to create the most comprehensive near-global high-resolution database of the planet's topography. The absolute accuracy of the SRTM's elevation measurements is predicted to be better than 16 m. Two radar antennae were installed in the SRTM payload to collect topographic (elevation) data. When the Shuttle was in orbit, one antenna extended from the payload bay, and the other was mounted on the end of a 60-m (200-ft) mast. The processing of the SRTM data and its integration with already-existing digital elevation models required several years. Numerous users in over 200 countries have used the SRTM 90 m resolution (3 arc-second) and 30 m resolution (1 arc-second) data sets, the latter of which is only for the United States. This makes it the most widely used Earth science data set produced by the Space Shuttle missions. Fig. 9 shows the view of elevation data via DEM of the Ozat River basin study area, which comes from the 30 m spatial resolution of SRTM DEM.

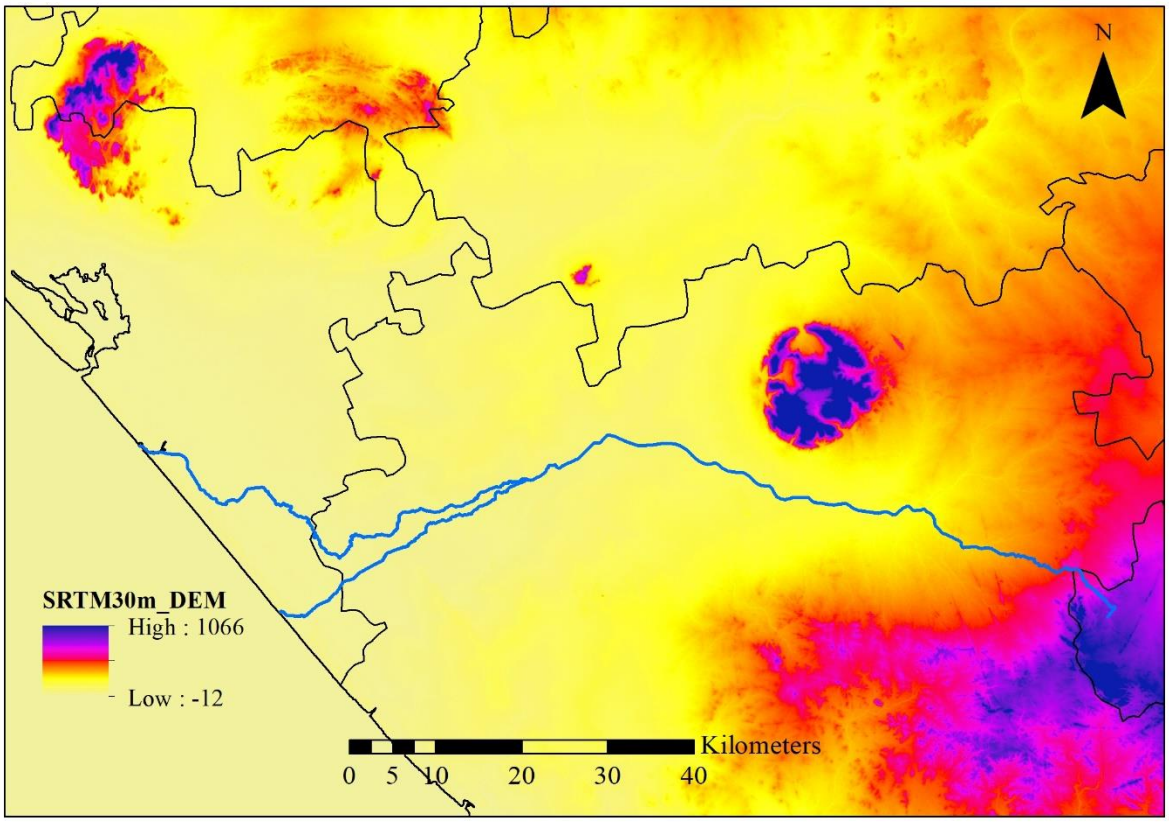

Figure 3.7 View of SRTM DEM 30m resolution of study area with Ozat River

ALOS was launched by the H2-A launcher from Tanegashima Space Center on January 24, 2006, and it was fully operational by the middle of October that same year. ALOS abruptly ceased operations on April 22, 2011. Its failure could have been caused by the power line shorting out of the paddle-driving mechanism. The goal of ALOS was to contribute to the prevention of natural disasters by providing enough data to create base maps at a scale of 1:25,000 over the globe. There were three sensors on ALOS. One was the PALSAR L-band synthetic aperture radar (Phased Array L band Synthetic Aperture Radar). The AVNIR-2 and PRISM optical sensors were also part of ALOS. The successor to AVNIR on ADEOS, AVNIR-2 (Advanced Visible and Near Infrared Radiometer), was a multispectral scanner. With its three telescopes and panchromatic sensor, PRISM could concurrently capture stereo images from the nadir, fore, and aft angles.

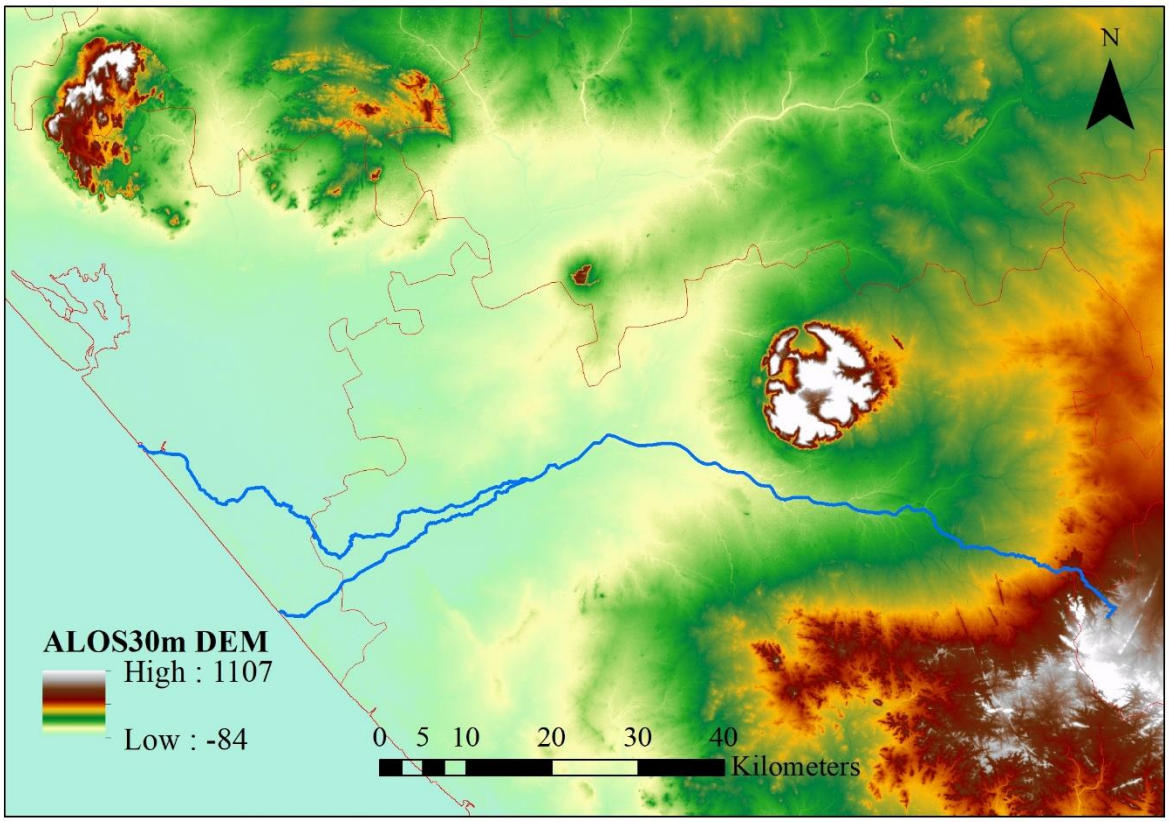

Figure 3.8 View of ALOS DEM 30m resolution of study area with Ozat River

Essential features of ALOS were its ability to send and store a sizable amount of data. It was able to collect and transmit all land-related data on the planet. It was anticipated that the PALSAR's multi-polarization properties would offer valuable data on soil moisture. The Fig. 10 shows the ALOS 30m DEM for the Ozat River basin study area. The fig. shows the raster view with river reaches and the color code of the elevation model. It indicates the same color code after the bifurcation, revealing the delta region's flat terrain.

Land Use Land Cover (LULC) Code	Details	Manning's n
1,2,5	Wasteland (land with scrubs)	0.1
14,16	Agriculture (cropland)	0.035
18	Plantation	0.160
30	River	0.03
31	Canal	0.04

100	Built-up area (rural)	0.1
101,800	Built-up (urban/cities) - medium	0.08
181	Others, Prosopis	0.160
300	Water bodies (pond/lake)	0.04
303	Water body (tank)	0.04
1000	Built-up (urban/cities)- high	0.15

Table 3.6 Allotment of manning roughness values as per DRIP chart for 2D model development

The Table 6 details the various Manning values of different land cover classes. This table exhibits the Dam Rehabilitation and Improvement Project (DRIP). However, many theories revealed the study-related optimization of manning roughness value for river beds. Initially, the manning approach was made for river velocity in various terrain conditions and gave the value of a non-linear constant for predicting velocity in natural streams. Although, in 2012, the government of India formed a body to improve the operation and safety of major dams in the country with the assistance of the world bank. The table 6 fetches from the guidelines of DRIP and is implemented in this research for the allotment of manning regions in the 2D model development phase.

Chapter 4. Methods

Flood inundation study of the Ghed region is challenging due to the limited data set. Another thing is that no past research is available for this study region. The 1D and 2D models are developed for hydraulic modeling to analyze inundation in all aspects. The purpose of a 1D model is only to predict the river stage and check the overbank discharge along the tributaries of the Ozat River. The 1D model also helps delineate the boundary of the 2D flow area and calibrate the manning roughness value for the river valley region. After the completion of a 1D model, the development of a 2D model for water inundation has been executed. In the 2D model, many options are available in the new HEC-RAS v 6.1.

Input parameters are a generation of terrain file, 2D flow area, import of LULC, allotment of manning values, optimization of the time step, and running the program. The 2D model reveals the result of various hazards maps like inundation boundary map, depth map, velocity, arrival time, percent time inundation, and courant number maps. The actual scenario on the ground concerning water depth is validated with observed and simulated elevation during the specific period. As stated earlier, the model was simulated between 14th August and 27th August 2017. Further, a flood algorithm has also been developed using the google earth engine (GEE). It is the latest available technique that works with the machine learning algorithm. In this method, the platform of the earth engine works with previously stored data in cloud storage of google and is accessed via Javascript. This is popular due to its speed and non-requirement of software installation. At last, the result of the GEE flood map overlapped on the depth map generated in the RAS mapper to check the consistency of hydrodynamic modelling.

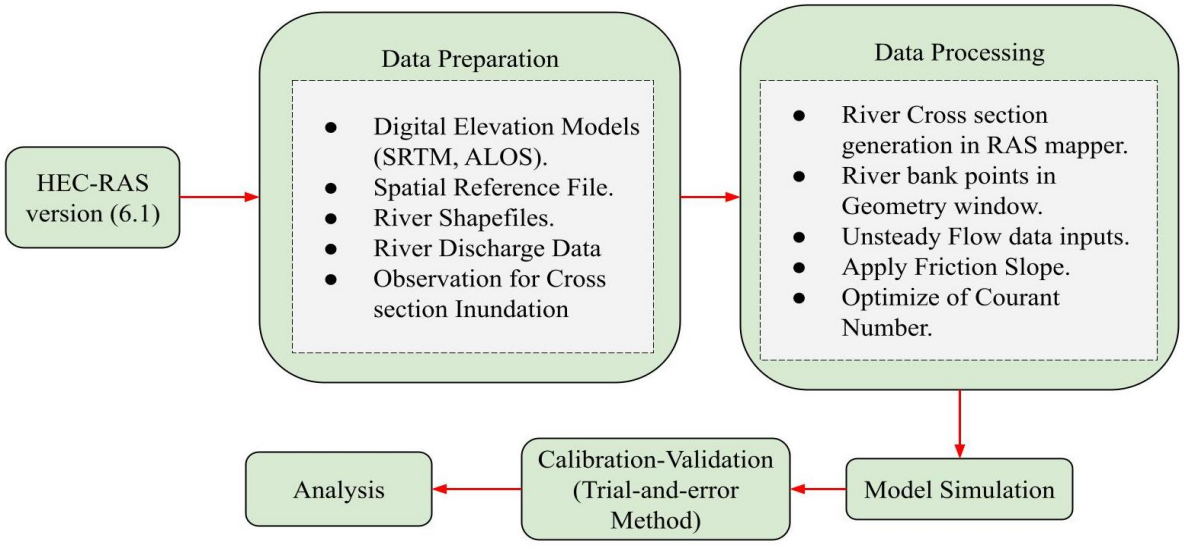

Figure 4.1 Flow chart indicates the process algorithm of a 1D model

4.1 Development of a 1D model

For the development of a 1D model, many input parameters are required for simulations. Fig. 11 depicts the entire process of a 1D model execution with data requirements. The 1D model is developed to calibrate the manning roughness coefficient and river stage analysis of the Ozat River till river mouths near pata and navi bandar villages. The 1D model of the Ozat River basin was executed in two DEMs, SRTM and ALOS. Both DEMs have a spatial resolution of 30m. DEMs play an essential role in hydraulic simulations, primarily when researchers work with unidentified study regions. The work with two DEMs is vital to identify the best one, and further research on a 2D model has been extended with the more appropriate DEM. In the 1D model, calibration of the 1D model is challenging for the basin with limited observed data set available. As mentioned in the title of this research, the Ozat River basin is data-scarce because of the limited data set of flood discharge, and no data is available at the river mouth of tidal waves. The calibration and validation of a 1D model are performed via a comparison of water surface elevation changes and a cross-section inundation study with regression analysis.

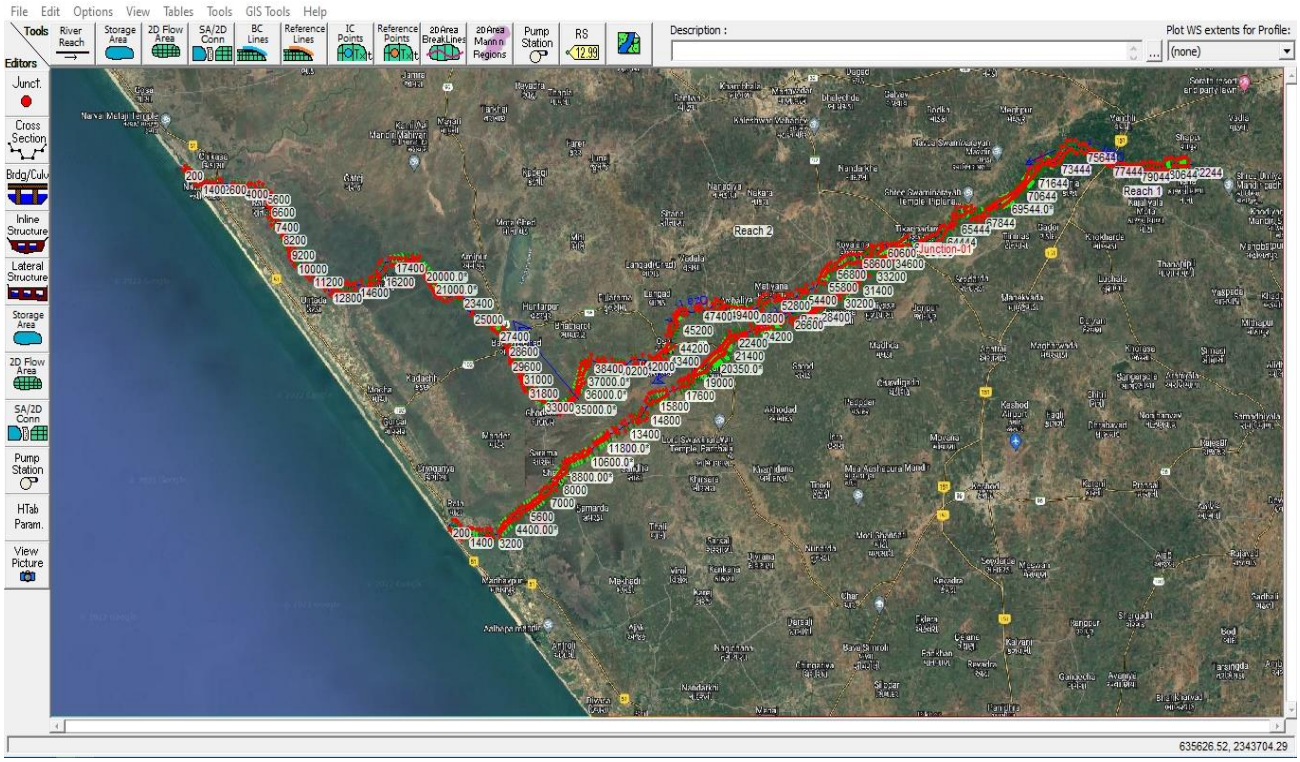

Figure 4.2 Screenshot of geometry window showing river station numbers, bank lines, flow path and cross-sections

In the development stage of a 1D model, initially, the DEM needs to import for the generation of the terrain file; this is essential for the hydraulic model to work with better DEM. After the terrain file generation, the cross-sections must be generated in the RAS mapper. In this

research, the river reaches (one single and two bifurcated reaches) are traced in the google earth pro, and further, it will be imported into ArcGIS for making shape files. The generated shape files of river reaches are directly imported into the RAS mapper. Cross section spacing is 200 meters, and the width of each section is 700 m for better prediction of river stages along the river path. Fig. 12 shows the schematic view of the cross-section setup along all three tributaries. Further work will perform in the geometry window for allotment of manning roughness values. In this context, the manning values are considered as 0.025, 0.030, 0.035 and 0.04. These values are selected from various literature and semi-arid study regions. After the allotment of manning values, a model needs discharge data for all reaches. This research, the 1D model is performed as a flow hydrograph at the upstream boundary condition and normal depth as the downstream boundary condition. However, in this downstream boundary condition, the friction slope is calculated in the geometry window as 0.23 for reach Ozat-1 Reach-2 and 0.31 for reach Ozat-2 Reach-1. This scene shows the cross sections are placed at single and bifurcated reaches till the river mouth. The Fig. 13 depicts the SS of the geometry window showing the cross-sections, flow path lines, bank lines and river stations.

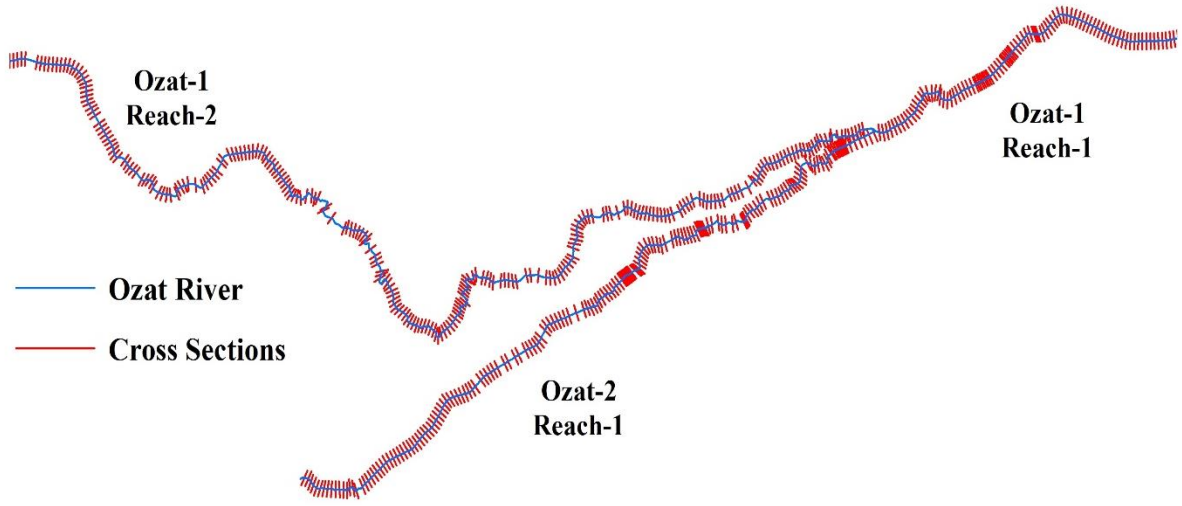

Figure 4.3 Schematic view of cross-section placement of the Ozat River

The length of bifurcated reaches is 62.6 km for Ozat-1 Reach-2 and 36.6 km for Ozat-2 Reach-1. These lengths are measured via the google earth pro version with a spatial resolution of 10m. After allotment of friction slope and model needs to input inflow hydrograph for up-stream boundary condition. As shown in Fig. 13 inflow, the hydrograph depicts six peaks from 14th August to 27th August 2017. This date is considered for simulation because observed data like discharge at other places and water surface elevation changes on bifurcated reaches are

available for this span. The year 2015 considered for the calibration period while 2017 is the validation period for specific days.

HEC-RAS model utilizes the saint venant equation for simulation of open channel flow. In this context, the other data requirements for a model are fetched from the input parameters like DEM, stream flow and friction slopes. The momentum equation is as follows,

$$\frac{1}{A}\frac{\partial Q}{\partial t}+\frac{1}{A}\frac{\partial}{\partial x}\left(\frac{Q^2}{A}\right)+g\frac{\partial y}{\partial x}-g(S_0-S_f)=0 \quad (1)$$

Where Q= discharge through the channel, A= area of cross-section of flow, y = depth of flow, S_0 = channel bottom slope, S_f = Friction slope

After allotment of manning roughness values and up-stream and down-stream boundary conditions, a model needs to input time steps. Fig. 14 shows the four types of time steps required for model execution.

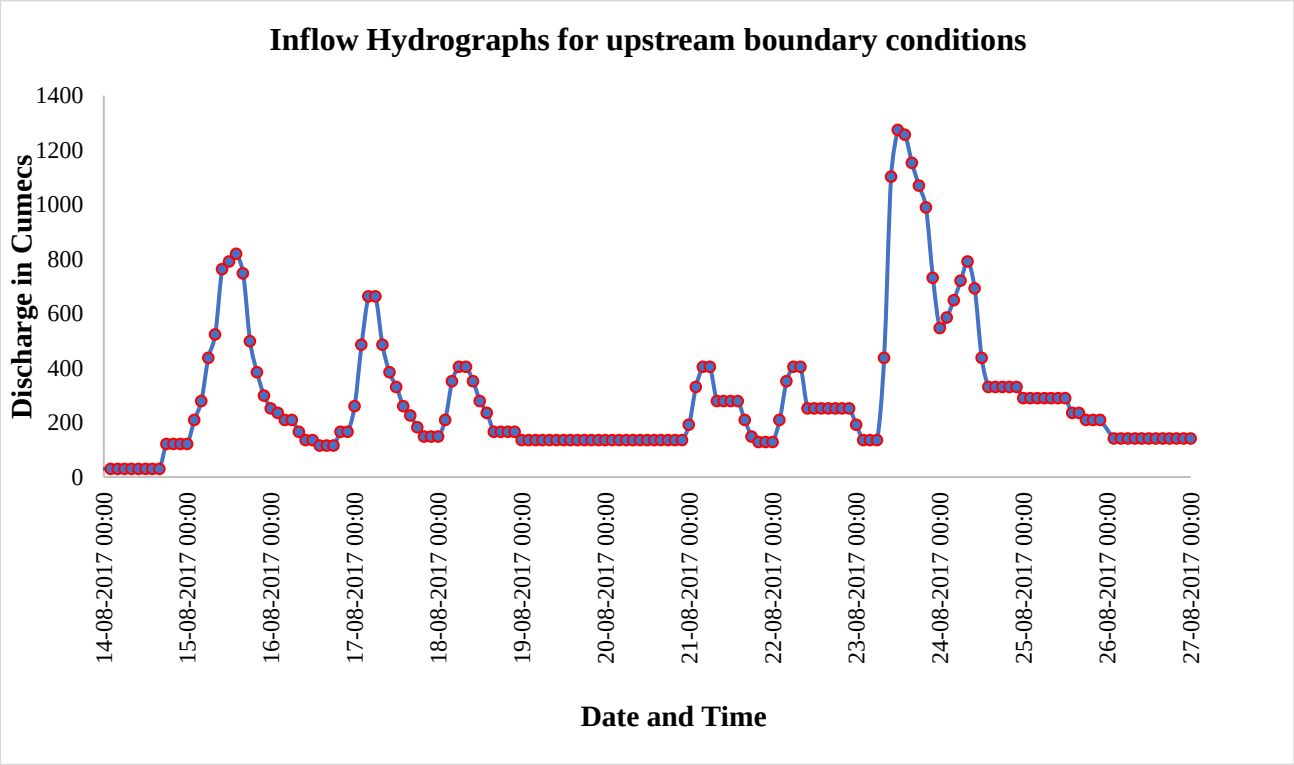

Figure 4.4 Inflow hydrograph showing peaks and 2-hour interval spots

In Fig. 14 show, there are four types of time steps computation interval (1 min), hydrograph output interval (1 hrs), mapping output interval (2 hrs) and detailed output interval (1 day). In the case of detailed output interval, a larger time step is considered because a 1D model is

utilized only for river stage prediction. Although, the large time step will reduce the computation time. In Fig. 15 Computation time, a screenshot appears with the selected time range.

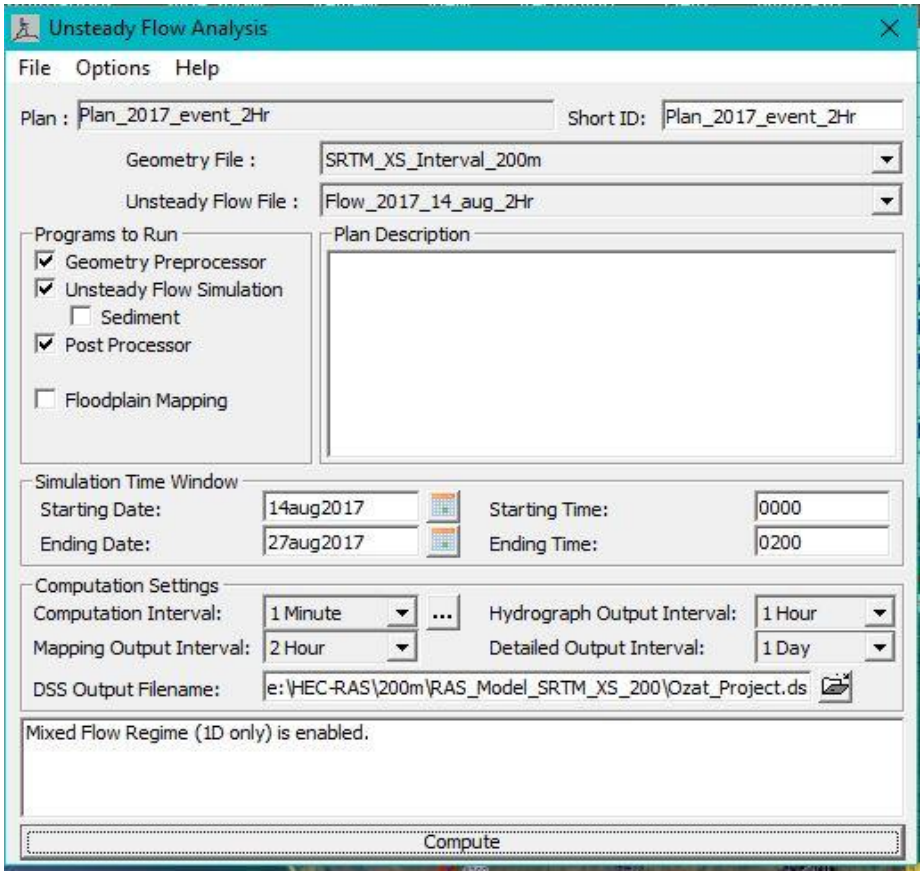

Figure 4.5 Time step setup of 1D model

The actual 1D modelling has been executed on both DEMs, SRTM and ALOS. Both DEMs have variable geometry, and authors need to check the consistency for further analysis of a 2D model. In this regard, the comparison for both DEMs is made concerning water surface elevation changes and cross-section inundation study. Fig. 15 (model setup) indicates the various model setup parameters for modelling performance. For the water surface elevation study on bifurcated reaches, the balagam ghed village and Indrana village were considered for this analysis, for Ozat-1 Reach-1 and Ozat-1 Reach-2, respectively. These places are considered as per the data availability. For the calibration of the manning roughness coefficient, the vanthli bridge water surface indicator is considered; this place is 5 km away from the inflow place. For the comparative analysis of water surface elevations, the data has been compared with simulated and observed and achieved the RMSE value via regression analysis. The cross-sections for both DEMs show different total numbers because some places need to be

interpolated after simulations. The Table 7 shows the number of cross-sections placed on all three reaches.

River Name	DEM	Length of River reach (km)	No. of C/S
Ozat -1 Reach -1 (Single reach)	SRTM	19.1	116
	ALOS		96
Ozat -1 Reach -2 (bifurcated)	SRTM	61.6	268
	ALOS		278
Ozat -2 Reach -1 (bifurcated)	SRTM	36.6	197
	ALOS		158

Table 4.1 Details of Ozat river reach length and number of cross sections along the study area on both DEMs

Many places are needed for interpolation because of different terrain conditions on both DEMs. For this context, the simulations are made by trial-and-error method to minimize the error and optimize the time step by interpolating the required places.

For the comparative study of cross-section inundation, the model results of cross-section inundation compared with the ground condition. Suppose the particular cross-section is inundated in modelling. This place has been observed on the ground whether this place is flooded in this time span or not. The large observed data set has been analyzed with the help of regression analysis and achieved the coefficient of determination value.

4.2 Development of a 2D model

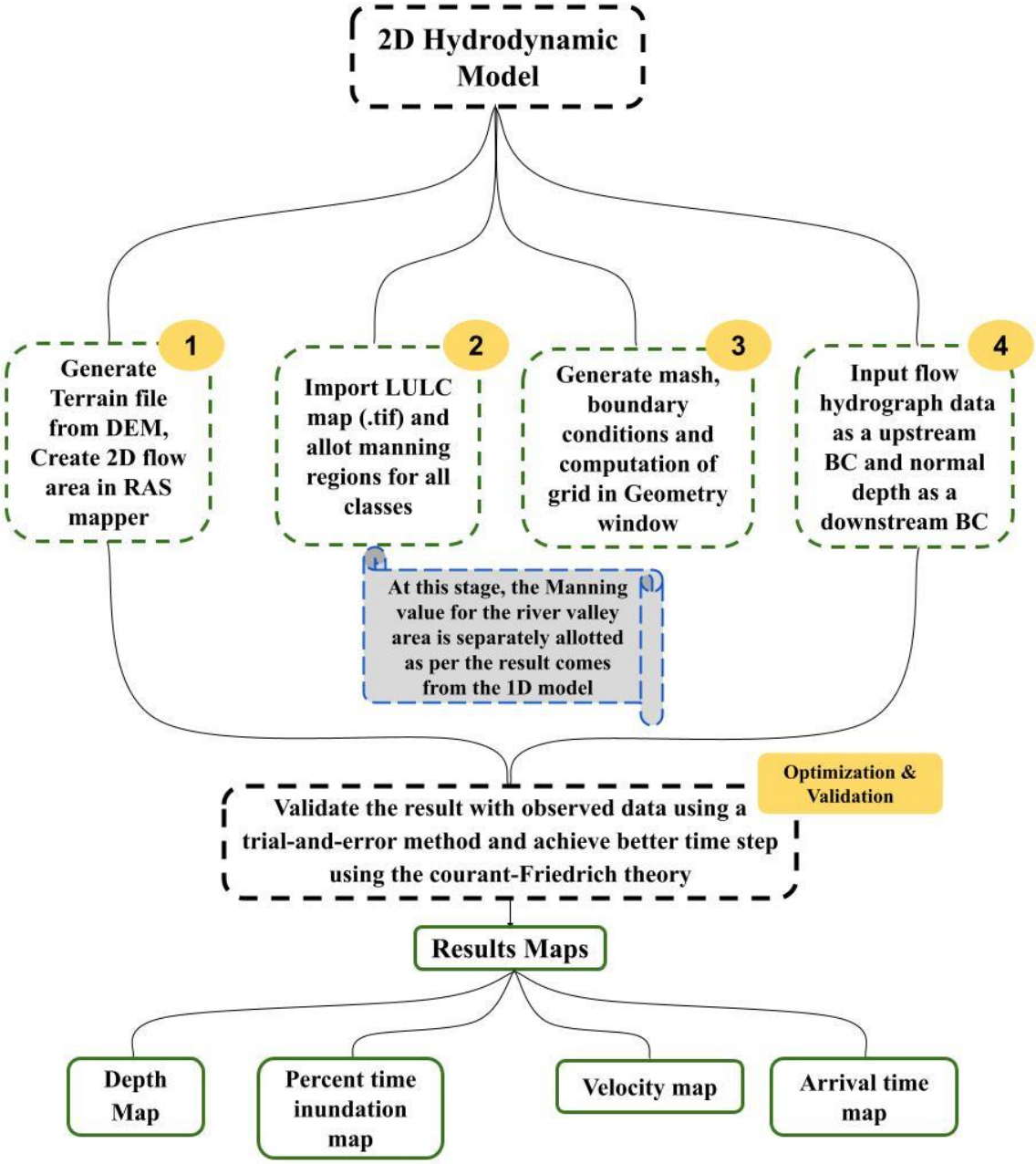

Figure 4.6 2D Model process algorithm

In the 2D model, the process algorithm is shown in Fig. 16 This modeling stage is more vital for hydrodynamic and analytical points of view. In the earlier stages, the river geometry, water level stage analysis, and manning roughness coefficient for the river valley area have been identified for enhancement in a 2D model. In the 1D model, inundation mapping is not possible, and in this research on Ghed region inundation, water is scattered on the large pond and gets

steady over many days even after the monsoon; that's the reason to perform necessarily of a 2D modeling. For the 2D hydrodynamic modeling, DEM is a vital part of the input parameter. The SRTM DEM has been utilized for this study with a spatial resolution of 30 m. HEC-RAS software v 6.1 is used for this analysis to generate various hazards maps and inundation mapping. The hydrodynamic study reveals all aspects of the inundation assessment and hydraulic parameters of unsteady flow. The purpose of the 2D model is the creation of various flood hazard maps like depth maps, inundation boundary maps, arrival time maps, velocity maps, and percent time inundation maps for assessment and early warning system for the local community. The detailed procedure will discuss in this section the performance, steps, and post-processing of a 2D model for the inundation mapping of the Ozat River basin.

The total 2D flow area is 870.11 km^2; the entire region is categorized into five land cover classes: cropland, barren land, built-up area, forest, and permanent water bodies. The purpose of generating the LULC map is to check the inundation effect on each land cover class and suggest suitable measures to eliminate this. The title of this research is framed to mention the word " data-scarce" ghed region; this word needs to incorporate in this statement because tidal wave water elevation data is not available at river mouths near pata village and navi Bandar. For this context, the 2D modeling necessarily simulation with normal depth conditions instead of tidal wave conditions. The model has been simulated as an upstream boundary condition with a flow hydrograph at shapur weir. The steps of a 2D modeling will discuss in further sections. For the validation of the 2D model is performed via a comparison of observed data of water depth and flood map generated in the RAS mapper also compared with the flood map generated in the google earth engine via sentinel-2 images. The post-processing of flood mapping in the cloud platform of the google earth engine will discuss in the next section of this document. For the steps involved in this methodology have been executed as follows. Initially, the digital elevation model (DEM) needs to import into the RAS mapper to create the terrain file. In this case, the SRTM with 30m spatial resolution has been used for this analysis. After generating the terrain file, the model must import the .tif file of the land use land cover map. The HEC-RAS utilizes the saint-venant equation (2,3,4).

$$\frac{\partial \zeta}{\partial f} + \frac{\partial p}{\partial x} + \frac{\partial q}{\partial x} = 0 \qquad 2$$

$$\frac{\partial p}{\partial t} + \frac{\partial}{\partial x}\left(\frac{p^2}{h}\right) + \frac{\partial}{\partial y}\left(\frac{pq}{h}\right) = -\frac{n^2 \mathrm{pg}\sqrt{P^2+q^2}}{h^2} - gh\frac{\partial \zeta}{\partial x} + pf + \frac{\partial}{\rho \partial x}(h\tau_{xx}) + \frac{\partial}{\rho \partial y}(h\tau_{xy}) \qquad 3$$

$$\frac{\partial q}{\partial t}+\frac{\partial}{\partial y}\left(\frac{q^2}{h}\right)+\frac{\partial}{\partial y}\left(\frac{pq}{h}\right)=-\frac{n^2 qg\sqrt{P^2+q^2}}{h^2}-gh\frac{\partial \zeta}{\partial y}+qf+\frac{\partial}{\rho\partial y}(h\tau_{yy})+\frac{\partial}{\rho\partial y}(h\tau_{xy}) \quad (4)$$

where h is the water depth (m), p and q are the specific flow in the x and y direction ($m^2 s^{-1}$), ζ is the surface elevation (m), g is the acceleration due to gravity ($m s^{-2}$), n is the Manning resistance, ρ is the water density ($kg m^{-3}$), τ_{xx}, τ_{yy} and τ_{xy} are the components of the effective shear stress and f is the Coriolis (S^{-1}) (Gary Brunner, 2016) (Quirogaa et al., 2016) (Patel et al., 2017)

The stepwise procedure of LULC generation and methods are described in the next section. After importing the LULC map, it needs to allocate the values of manning regions of each class. In this case, the LULC map is categorized into cropland, barren land, water body, built-up, and forest. Each category of this map has been allotted the manning value per the DRIP chart. After allocating the manning values and importing the LULC map, the model needs to set the geometry in the window. For selecting a 2D flow area, some references are required to delineate the boundary. In this regard, the result of a 1D model is remarkable for creating a 2D flow area. The total region covered by the 2D flow area is 870.11 km^2. The mesh computation of a 2D flow area is an essential step for 2D simulations because the 2D model works with each cell generated in this mesh, as shown in Fig. 17; however, the better achievement of model stability, the trial-and-error method induced for the maximum to minimum size of mesh grid. After the mesh computation, the geometry windows allow the allocation of boundary conditions. As stated earlier, the basin is data-scarce because tidal data is available. The model necessarily simulates the normal depth condition. For the validation of a 2D model, the limited data set is available for comparison at four places; koylana, sharama, bagasara ghed and kadachh. The key places are extracted based on nearby areas of village built-up wheraes the ground observations are possible and the locations are easily accessible.

Here is the list of key places considered for analyzing various hazardous maps like water depth, percent time inundation map and velocity map. These key places have also been observed for the flood early warning system for a specific time range.

Sr no.	Name of place
1.	Osa
2.	Fulrama
3.	Bhathrot

4.	Ghodadar
5.	Ghed Bagasara
6.	Amipur
7.	Sandha
8.	Samarda
9.	Sarma
10.	Kadachh
11.	Mander
12.	Down stream area of Amipur dam
13.	Area between kadachh and Bagasra

Table 4.2 List of Key places where the result of a 2D model analysis of various hazard maps

The analysis of these places is essential for hydrodynamic aspects and other unsteady flow parameters. Initially, in the development stage of the 2D model, the cell size and time step are considered in large sizes like 100 m and 6 hr, respectively. Several simulations are made, and finally, the 30m cell size and 1hr time step are achieved by reducing the errors and other modifications in model development. In Fig. 17, the screenshot of the geometry window depicts the mesh of a 2D model with boundary conditions. On the upstream side, the shapur weir is considered for the u/s boundary here; the inflow hydrograph is inputted in the model. In the downstream boundary, two places are considered, because the Ozat River splits above delta region and meets the Arabian sea near two places Navi Bandar and pata village. As stated earlier, the d/s boundary condition is considered as normal depth. However, HEC-RAS allows selecting the d/s BC as tidal wave condition for more precise modeling, but the water surface elevation data is unavailable at the river mouth.

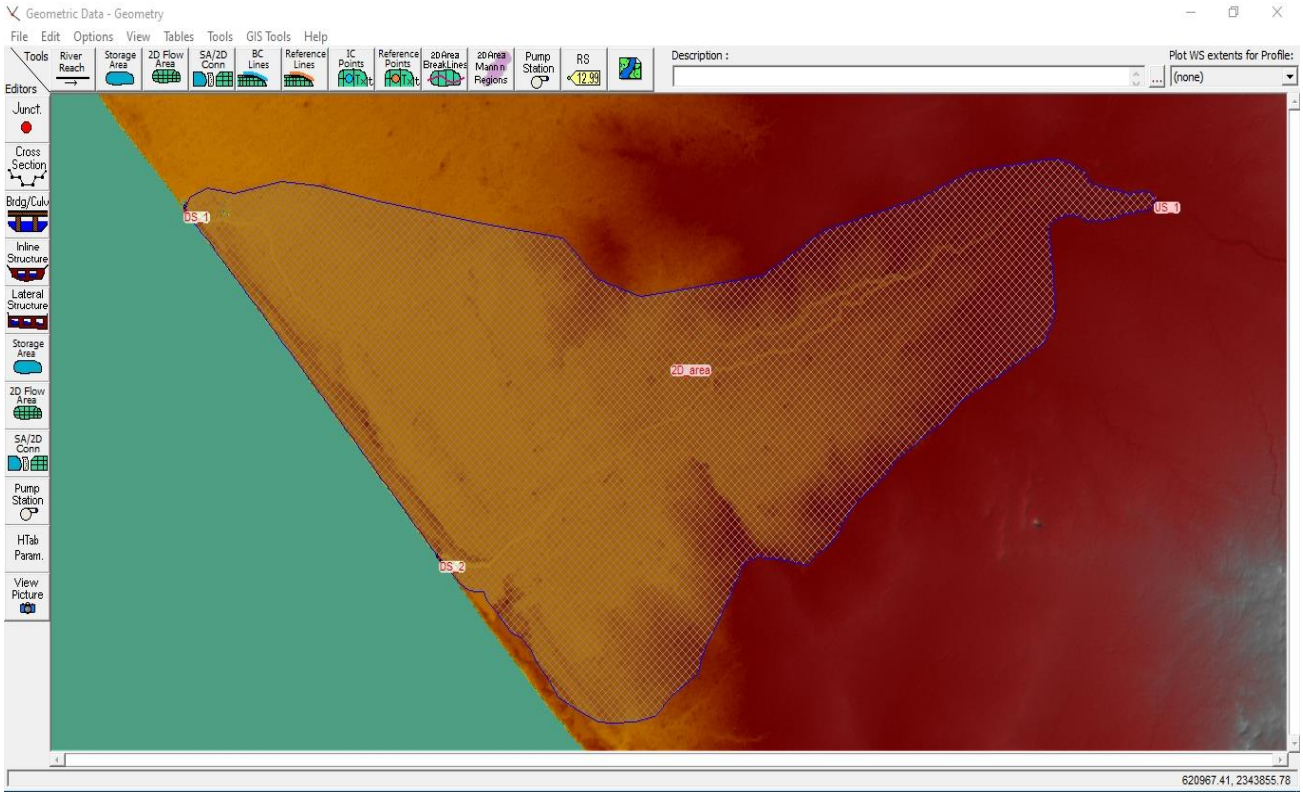

Figure 4.7 Geometry window for the 2D model development

The time step is essential for optimizing water flow, especially in open channels.

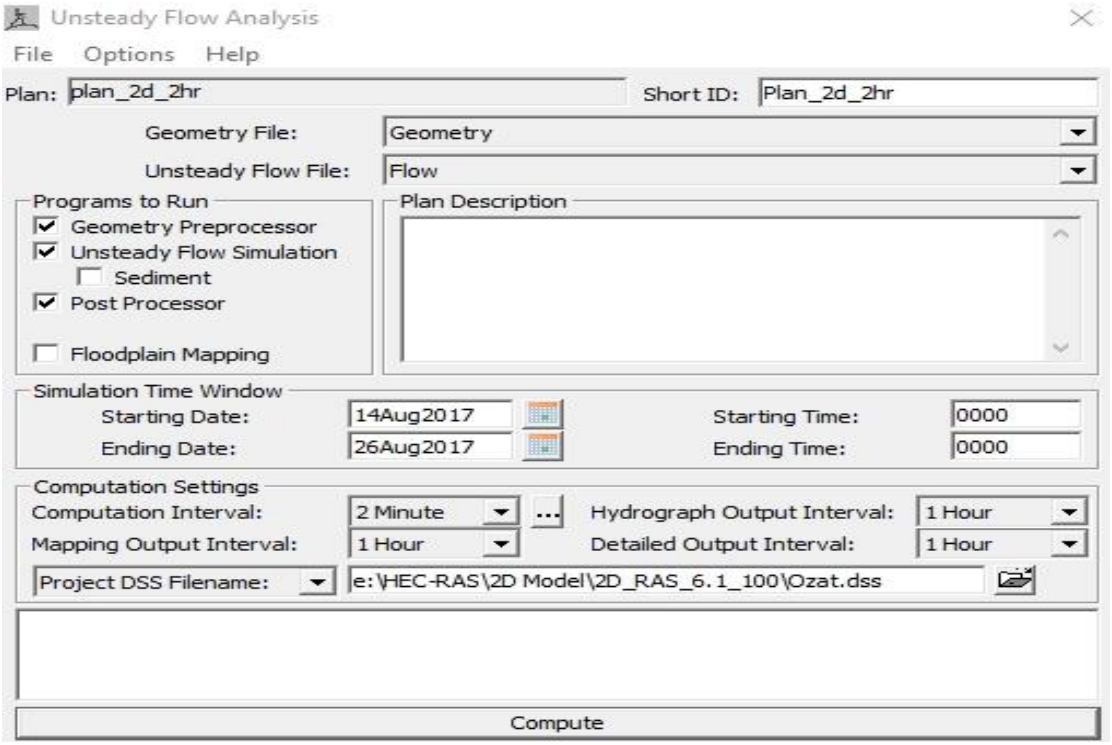

Figure 4.8 Timestep selection for a 2D model

For stability of the model, better optimization is needed with a minimum size of a cell and small-time steps. The HEC-RAS uses the courant – Friedrichs–Lewy optimization theory as per equations 5 and 6.

$$c = \frac{v\Delta T}{\Delta x} \leq 1.0 \qquad \text{With minimum C = 3.0} \qquad 5$$

$$\Delta T \leq \frac{\Delta x}{v} \qquad \text{With c = 1.0} \qquad 6$$

The above equations are helpful for model stability analysis and optimization. The HEC-RAS software manual depicts the smaller courant number that needs to be achieved as less than 3. The courant number (c) indicates that the particular water drop consumes time to travel within cells between cell faces. If the cell size is larger than ideal, the model runs faster; if the cell size is smaller than ideal, the model is unstable, and the travel time of water shows the incorrect values. Three types of times need to incorporate in the Fig. 18; computation interval, hydrograph output interval, mapping output interval, and detailed output interval; these are 2 minutes, 1 hr, 1 hr, and 1 hr, respectively.

4.2.1 Land use land cover (LULC) map generation

The land use land cover map is essential to check the effect of post-flood scenes on various classes of LULC maps. This research categorizes the LULC map into five land classes; water, built-up, cropland, forest, and barren land. Many techniques are available nowadays. However, an accurate method needs to be employed for precision analysis.

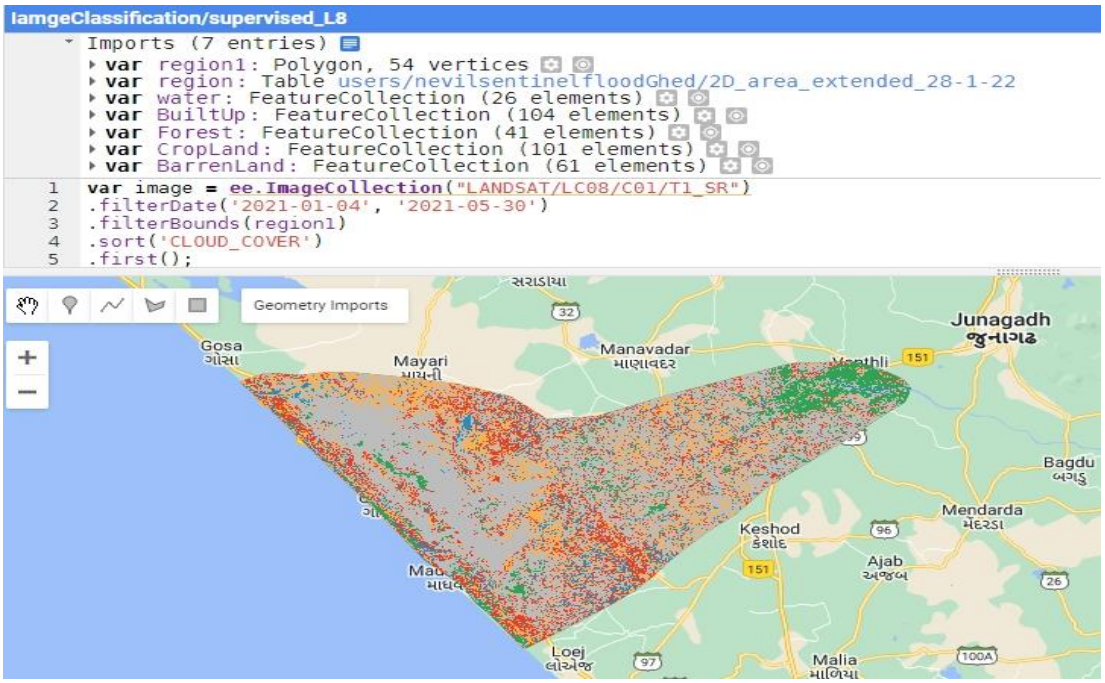

Figure 4.9 Screenshot of google earth engine code editor with result visualization

In the Fig. 19, the study area is divided into five classes, as stated earlier. Most of the land cover falls under the cropland category, while the flood inundation adversely affected other classes. In the Fig. 19, the google earth engine platform works with the machine learning algorithm with Javascript object notation (JASON). In this case, the input data needs to map in the imports window from the search box. The Landsat 8 OLI image is considered for this analysis. Many kinds of literature depict the superiority of Landsat images over other satellites because of their instruments. The selected image should be traced from the dry span of the year for cloud cover elimination. The latest available image is considered for LULC for current changes and activities on the ground. Many techniques are possible in the GEE platform for image classification. However, in this case, the classification and regression tree (CART) method has been employed for Ozat River basin study area; the CART method is part of the supervised classification system.

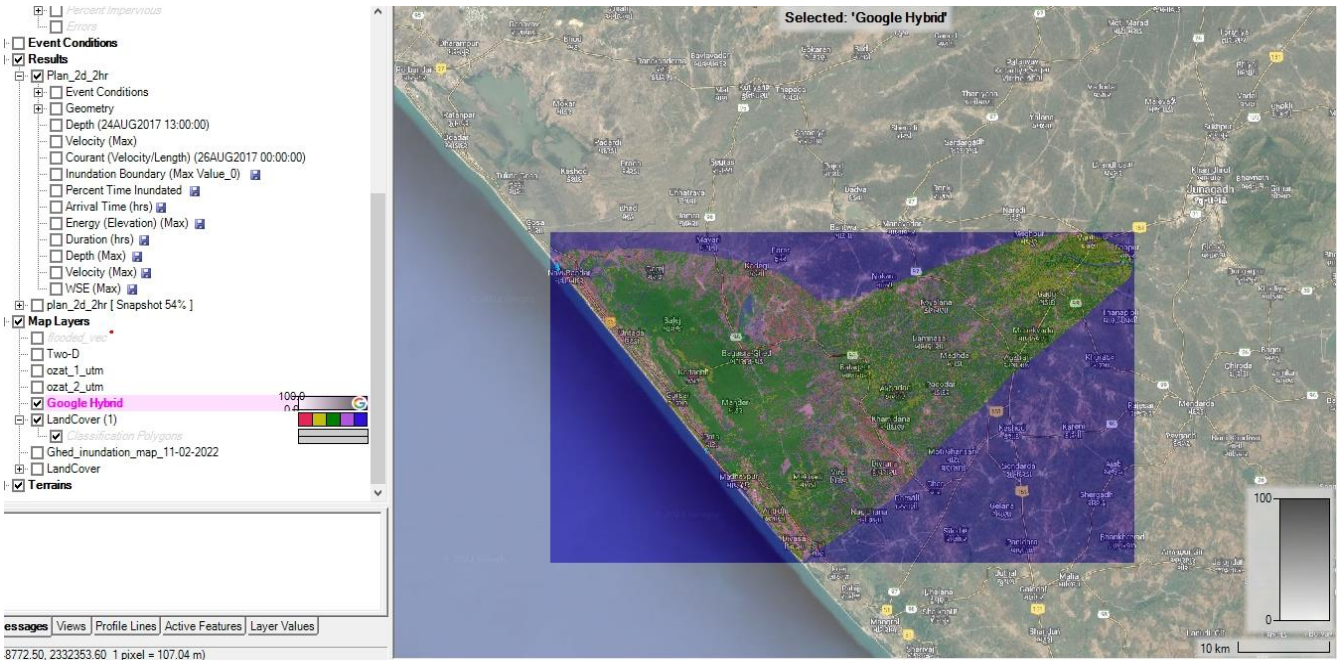

Figure 4.10 Imported LULC map in RAS mapper

In the development stage of the LULC map, the training samples are selected by loading the base map in the background layer. The maximum training samples are selected for better assessment and improvement in the accuracy of the map. In this context, the 26, 104, 41, 101, and 61 samples were selected from the land cover class of water, built-up, forest, cropland, and barren land area, respectively.

In the Fig. 20, the view of the RAS mapper depicts the imported LULC map with a background google hybrid layer. In this map, the new HEC-RAS v6 allows modifying and editing the land cover class and adding more classes with drawing tools. The various manning values are

allotted in this window for land classes per the DRIP chart discussed in the study area chapter. For this development, another layer must be overlayed as a river valley region for separate manning value allotment. Although, the land cover class is now five. This land cover of the river valley area needs to be separately allotted for precision modeling because, in the 1D model, the manning values of all reaches are calibrated and validated. The Table 9 shows the area of various land classes in square kilometers.

Sr No.	Land class	The total area of a particular class	Total area in percentage
1	Cropland	502.02	57.70
2	Barren land	139.16	15.99
3	Built-up	103.89	11.94
4	Forest	75.01	8.63
5	Waterbody	50.03	5.74
Total Area		870.11	

Table 4.3 LULC map classes with total area and area of each class

The Table 9 shows that most area lies under the cropland category and needs to evaluate the flood scenario in this class for better agricultural management.

4.3 Development of flood mapping algorithm in GEE

The Google earth engine is the platform which serves the interpretation of satellite images via machine learning. This technique is widely utilised because of quick results and no need to download any software. There are many tasks that are possible in research, like rainfall deviation, NDVI maps, NDWI maps, LULC, flood mapping, bathymetry analysis, drought management and watershed planning via time series analysis. In this regard, the downstream area of the Ozat River basin frequently experiences water inundation in the depression region. It is necessary to examine the ground condition with pre and post-flood scenarios for five years. In this context, the sentinel-1c band SAR data is used for this analysis; the data is available as cloud storage of GEE from 2016. Here, the Fig. 21 depicts the process algorithm for flood mapping via the google earth engine.

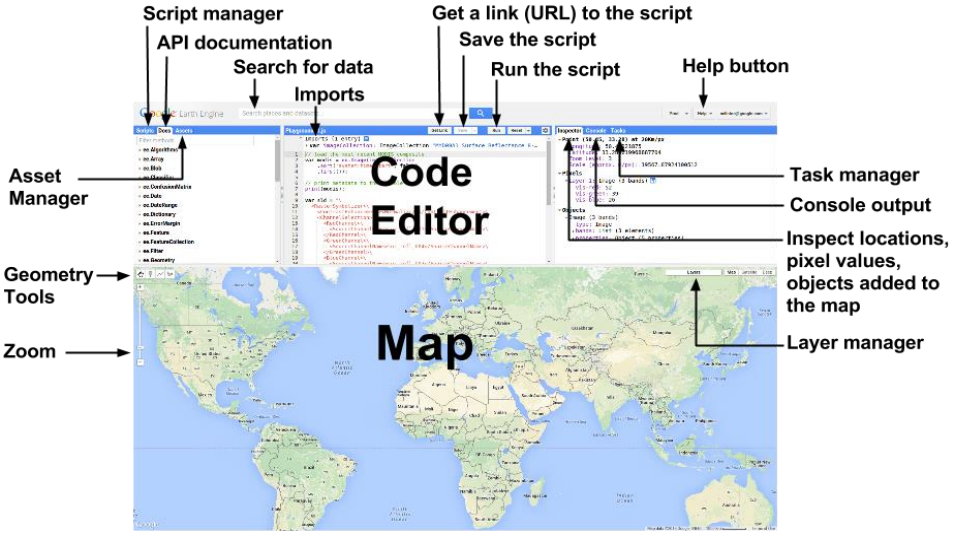

Figure 4.11 Google earth engine overview and useful pans

In the beginning, the users must know about the overview and basics of the google earth engine. In this regard, Fig. 21 Reveals all the things users keep in mind for using the GEE platform. The code editor is where users can write the code as per the requirements, and API documentation also helps the users to write the specific code and all other samples of function and strings. Another important feature is asset manager; this function allows users to store the vector and raster files for various projects and share the outside projects via copied links. The geometry tool is useful for drawing the geometry in various shapes like rectangles, circles and free-hand polygons to work with specific regions globally. The essential feature is the search toolbox; this place is vital for tracing the cloud data from the earth engine storage, and users can directly import through special links and assets of the earth engine. Top of the code editor, users can view the import entries and show the project necessity; at this place, users can also view the geometry created in the project. The top right corner shows the inspector button; at this place, users can inspect the layers via a single click, check the pixel values and inspect the area/regions. Right of this button, users can find the console tab; this tab helps users identify the results like charts, diagraphs, result values as tables and other direct result values as written in the code editor pan. Finally, the users can download the data via the task; this place helps the users to download the data in a prerequisite format in google drive. Earth engine can't allow the users to download in offline mode. Users should write the folder name which already exists on google drive.

In Fig. 22 , the stepwise procedure reveals the acquisition of data via Javascript object notation (JASON); JASON is the latest available technique that works with machine learning and cloud

computing without downloading any software. In this research, the analysis is made like a comparison of pre and post-flood analysis. The comparative analysis is made between the year 2016 to 2021 for five years. The sentinel-1C can interpret the non-seasonal water and detect the flood scene with the total area.

Initially, the satellite selection needs to enter into the code editor. In this case, it is, “ee.ImageCollection("COPERNICUS/S1_GRD")”. After this, the two kinds of dates need to be considered for pre and post-scene analysis. Generally, in India, especially in the western part of Gujarat, the monsoon activity starts in June and ends in October. For this, the latest dry season image was selected from the end of May, and the flood date was selected from the rainfall data acquired from the irrigation department. The flood date varies yearly and is considered the end of a big event. Furthermore, the geometry selection needs to be imported as a shape file prepared in GIS. The open source DEM needs to be utilised via a cloud platform; for this, the Hydroshed DEM is used with 30m spatial resolution.

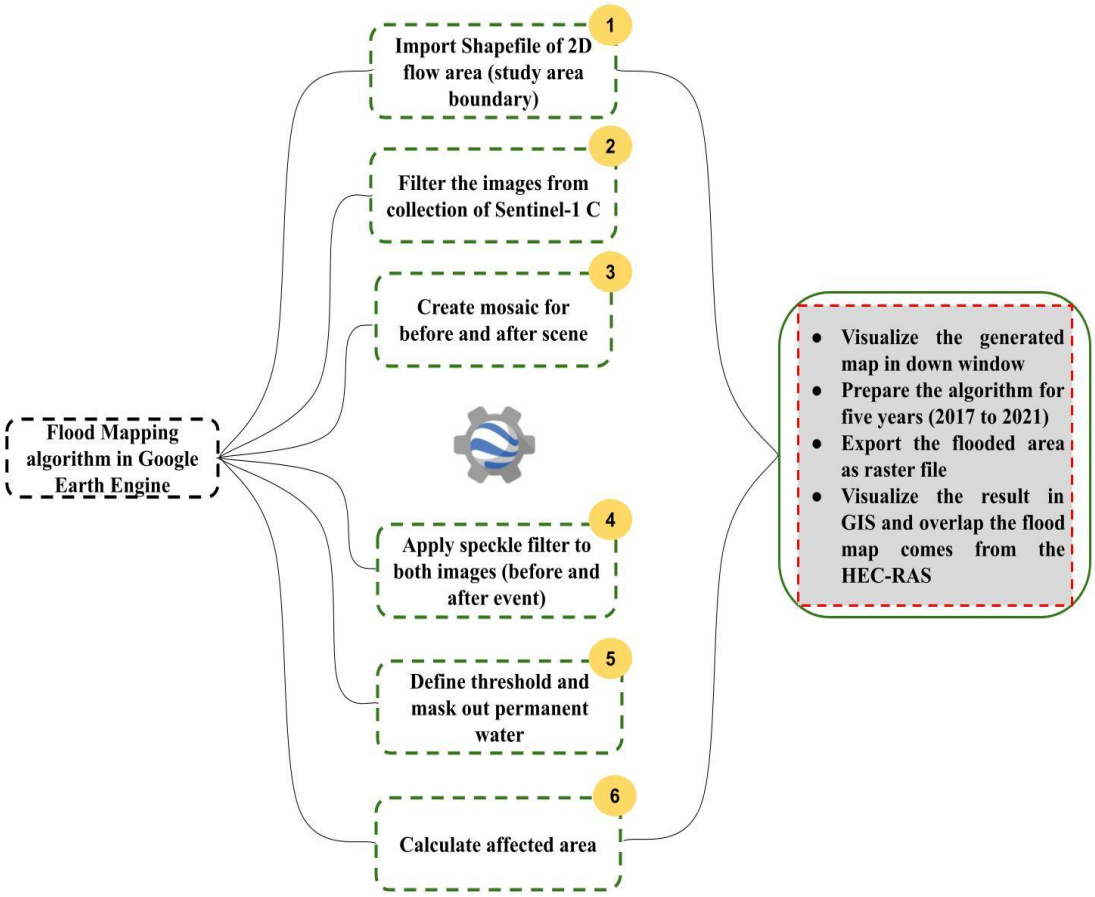

Figure 4.12 Process algorithm of the google earth engine for flood mapping analysis

Other necessary data are the slope of DEM, cloud sorting, application of color codes, and excluding permanent water. The outcomes from this analysis will be discussed in upcoming sections.

Chapter 5. Results

5.1 General

The results come from the hydrodynamic models, and the machine learning algorithm plays a vital role in assisting the local authority and people of the surrounding region. The outcomes are categorized in three ways; 1D model, 2D model, and google earth engine. The research of inundation mapping of ghed region is complex regarding data availability, human resource, and budget. However, authors try to overcome these contingencies to reach the best results. The study mainly focuses on hydraulic modeling; however, the end part of this research also exhibits machine learning in the google earth engine. The actual scenario has been evaluated for five years of analysis with this.

5.2 1D hydrodynamic model

The purpose of a 1D hydrodynamic model is to calibrate the manning roughness value, and river stage analysis along the river reaches. The geometry condition, data used, 1D model development, selection of parameters, and optimization of time steps are discussed in the study area, data used, and model development chapters. The 1D hydrodynamic model is vital regarding river stage analysis and model consistency for overbank discharge along reaches. In this part of the analysis, another purpose of the 1D model is to check the consistency of open-source DEM. In this context, the two DEMs, SRTM and ALOS, have been compared for reliability analysis. For this comparative analysis, the two criteria were emphasized; water surface elevation study (WSE changes) and cross-section inundation comparison. Better DEM is utilized with the 2D hydrodynamic modeling for detailed analysis. For all hydraulic simulations, many options are available for software consideration; HEC-RAS, MIKE, TUFLOW, and WMS. Out of all these, the past study reveals that HEC-RAS is best suited for hydrodynamic research and capable of sediment and water quality analysis.

The 1D model 3D perspective view enhanced the visualization capability of researchers. After the model simulations, one also can animate the result with this window. Many animated windows are available in HEC-RAS; view water-filled cross-sections, view profiles, and stage and flow hydrographs. Visualizing after the simulation is vital for measuring model accuracy and data validation. Fig. 23 shows the 3D perspective view of all three reaches; Ozat-1 Reach-1, Ozat-1 Reach-2, Ozat-2 Reach-1.

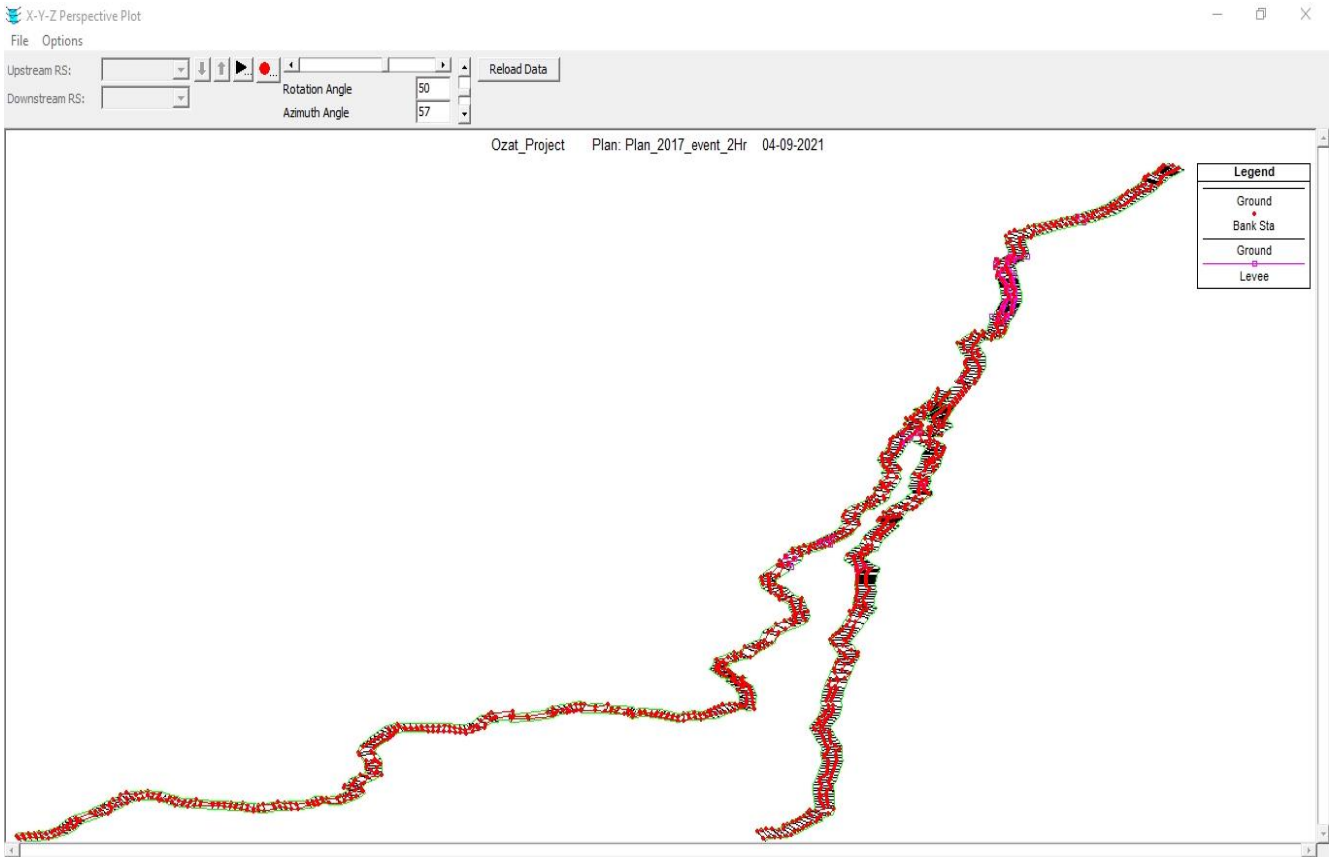

Figure 5.1 3D perspective view of Ozat River reaches

In the opinion of unsteady flow parameters, results from the 1D model depict the moves towards the downstream part, especially near the delta region, which exhibits the overbank discharge at every cross-section. The cross-section placement discussed in the study area and data used indicates the cross-section spacing is 200m and the cross-section width is 700m. The river bank lines and bank points are traced at every cross-section individually. The initial; portion of the model inflow point till the bifurcation point has sufficient width and depth; the model shows no overbank discharge, and flow goes smooth in-between banks. Fig. 24 shows the water surface level position in this section. Before the bifurcation point, all major and minor hydraulic structures are constructed like; gravity dams, major weirs, check dams and stop logs. However, the two reaches formed until the river's mouth after the bifurcation. Many villages are located asides from the river valley, which is a devasting thing in seasonal flow conditions. Fig. 24 depicts the water level condition after the bifurcation that a major portion of stretches indicate the overbank discharge, and it seems like the entire width of the cross-section has been inundated.

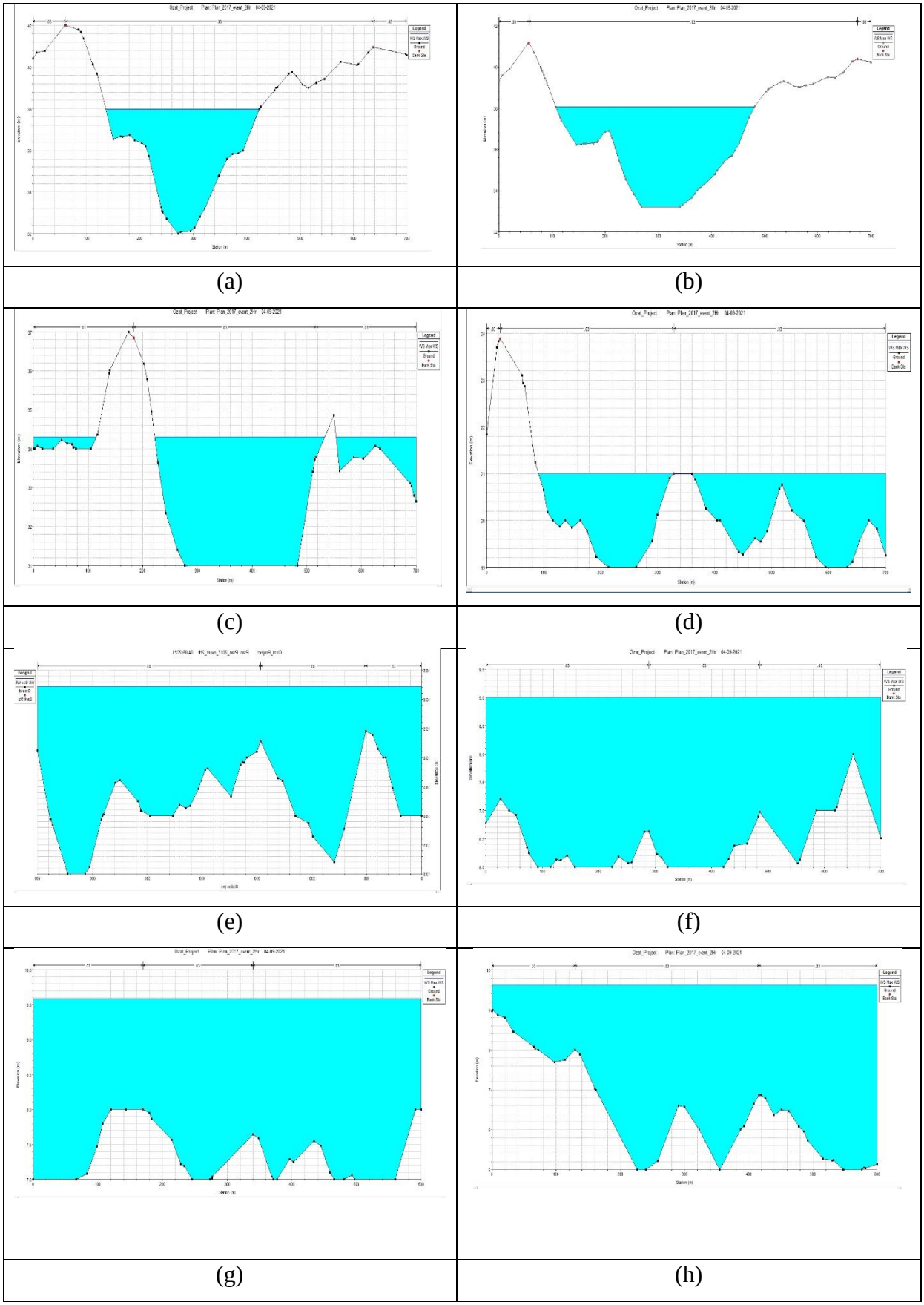

Figure 5.2 Water surface levels before and after bifurcation point of tikar village

This scenario shows that the major cross-section has been inundated after the bifurcated place, which needs to evaluate other conditions with the help of a 2D model for the water scattering area. Many villages are located on sides of the river valley and cross sections near this area show inundation on both banks. This situation becomes more hazardous day by day. The water scattering area measurement is not possible in the 1D model; this modeling needs to be enhanced with a 2D tool of HEC-RAS. However, before we go on to the 2D modeling result, the result of a 1D model necessarily calibrates and validates with the observed data.

5.3 1D model calibration

The result of a 1D model has been calibrated for 2015 and validated with the data of 2017. As stated earlier, the data and modeling have been performed for 14 days for both years. The observed data availability is for a limited period. The Ozat River basin is data-scarce regarding data availability of discharge, water surface level, and tidal wave elevations. The downstream boundary of a 1D model is considered normal depth rather than a tidal wave. Many past studies depict that the tidal wave downstream boundary condition is more accurate for flood modeling than normal depth. The water surface elevation data is available at three places in the study region near the valley area. However, other locations are also observed for WSE changes on the ground, but these places are far from the river valley area. These places are considered for the 2D model validation. Three observed locations near the valley area are vanthli bridge site, balagam ghed village, and indrana village. Out of these locations, the vanthli bridge site is considered for the WSE changes regarding manning roughness coefficient calibration and validation. In this context, for 2015, the model is performed between 27th July to 9th August 2015. These 14 days are selected because of limited data available for this span. Other two locations, balagam ghed village, and indarana village, are considered for the DEM comparison study.

For the model calibration, Fig. 25 shows the comparative chart of water surface elevation from the mean sea level for 2015.

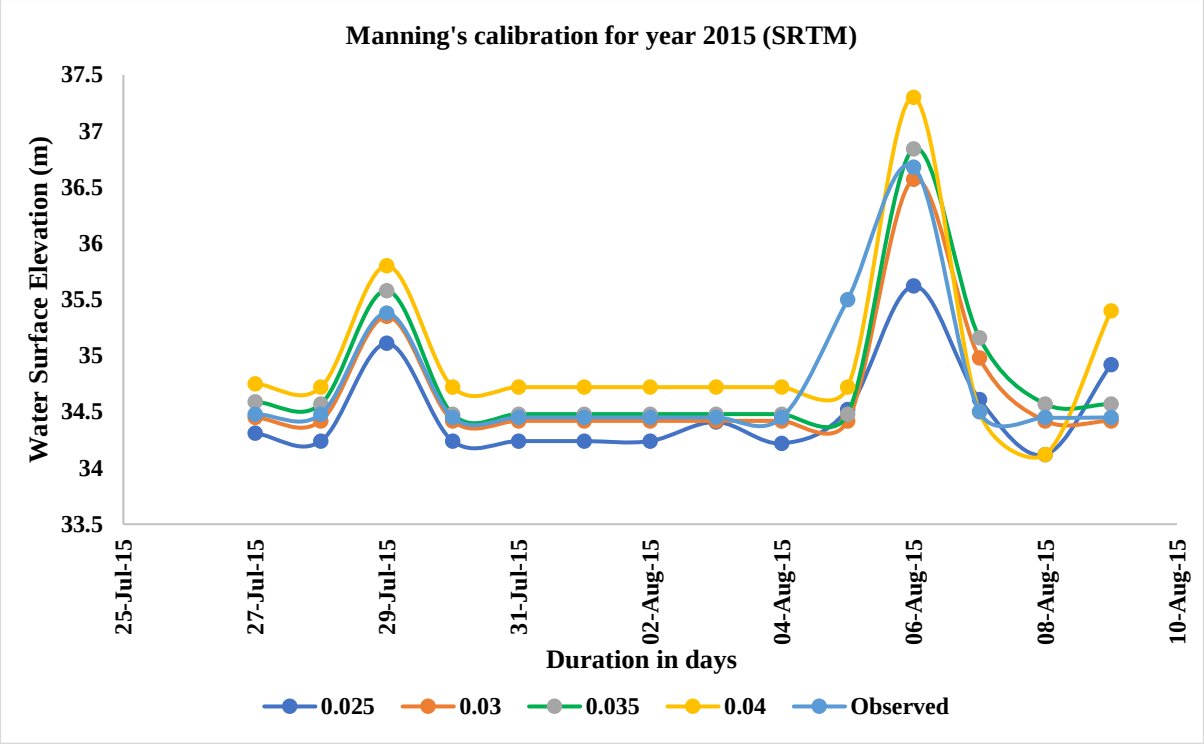

(a) Water surface elevation changes for year 2015 (SRTM)

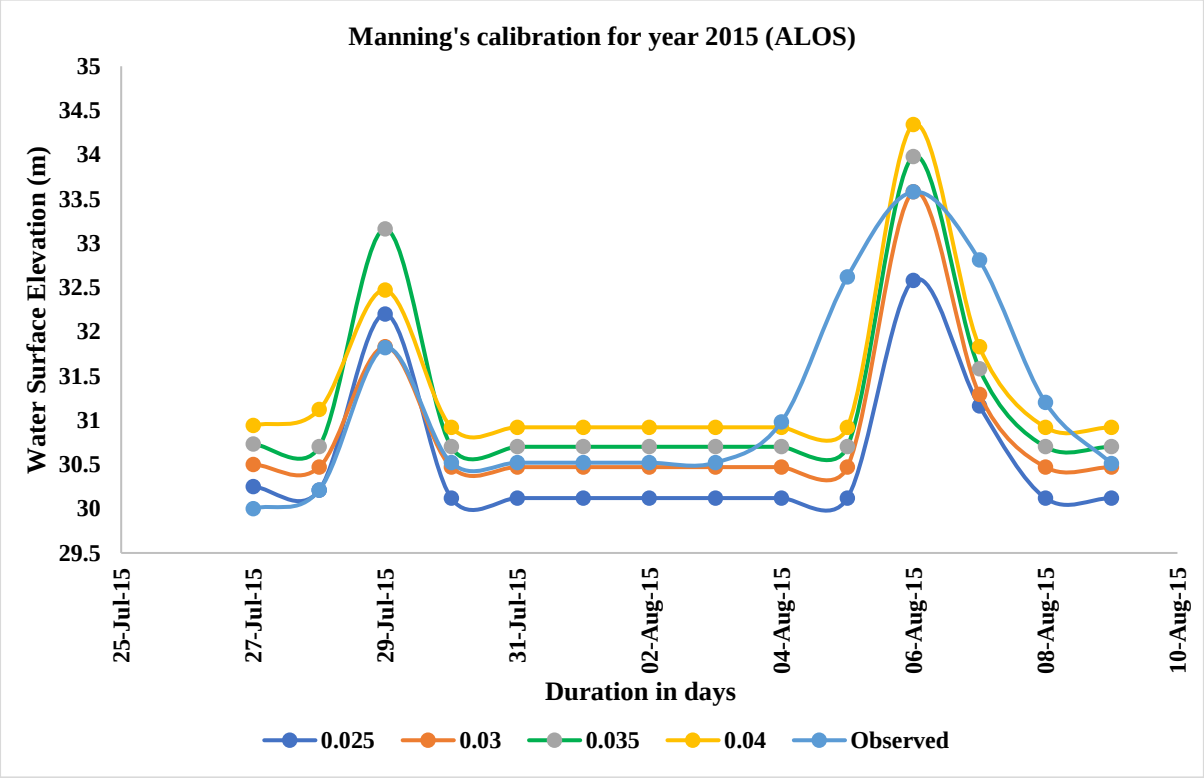

(b) Water surface elevation changes for the year 2015 (ALOS)

Figure 5.3 water surface comparison at vanthli bridge site for the calibration period on SRTM and ALOS

The model calibration is performed for both DEMs, ALOS and SRTM. These DEMs are frequently used in water resource studies, especially flood mapping. The range of manning roughness values is considered between 0.025n to 0.04. This range is selected based on past research performed for semiarid regions.

Fig. 26 indicated the scattered chart for calibration of the model using regression analysis. In the regression analysis, the coefficient of determination (R^2) has been determined with the observed and simulated water surface elevation. In this context, the coefficient of determination is evaluated for WSE changes comparison.

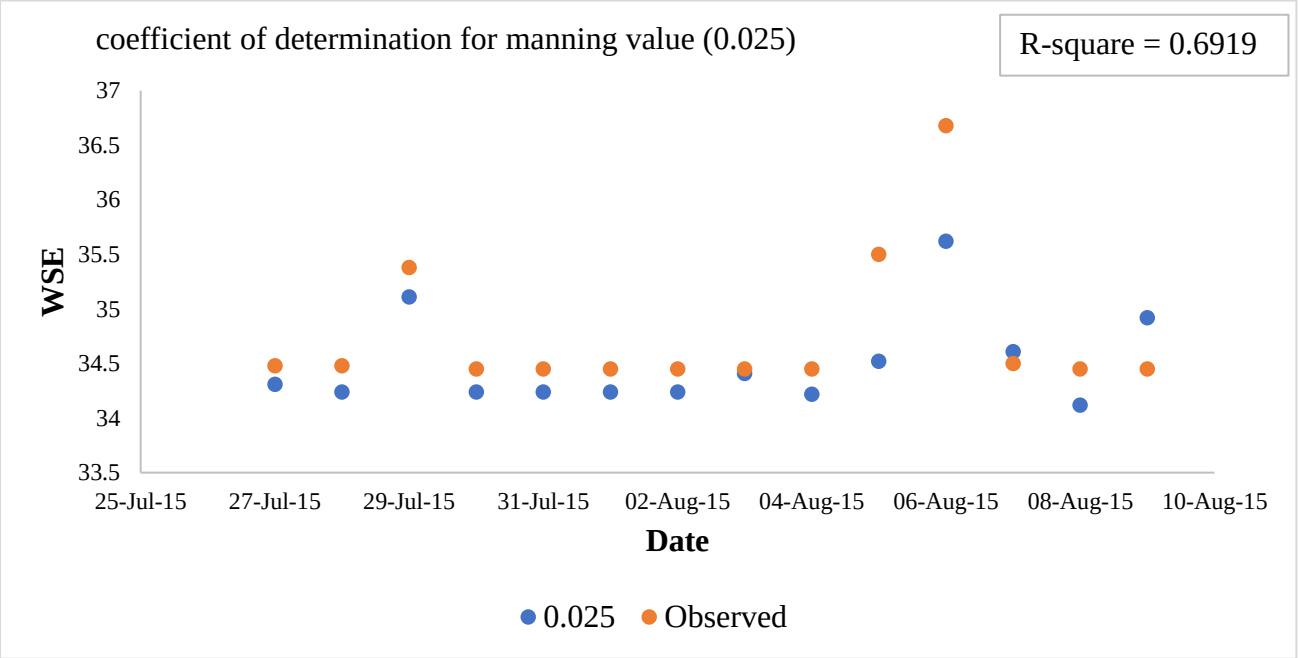

(a) R^2 determination for manning value 0.025 SRTM

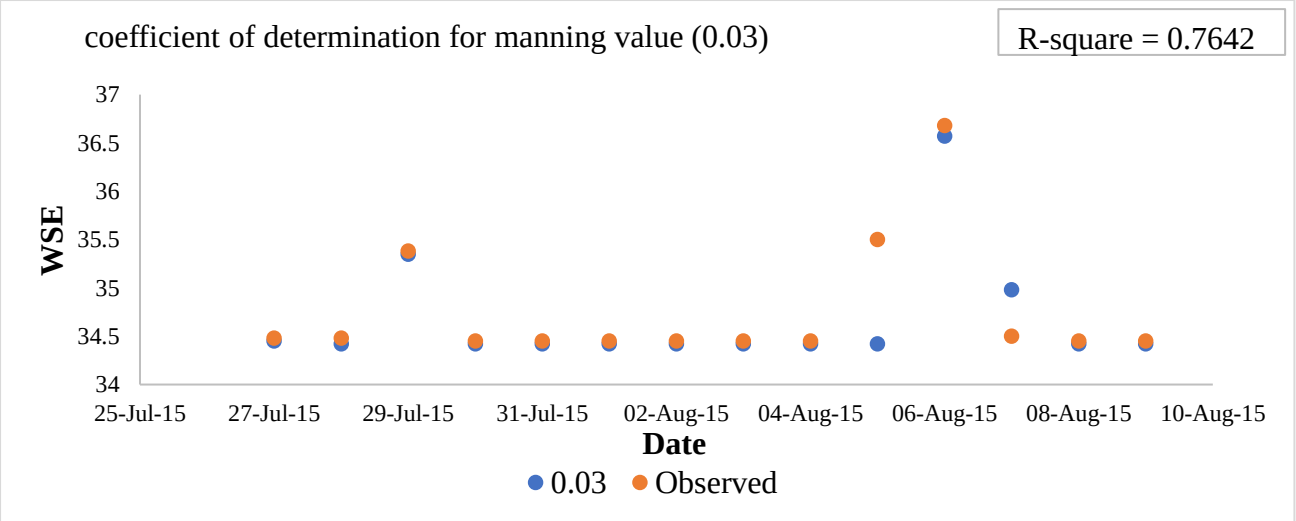

(b) R^2 determination for manning value 0.03 SRTM

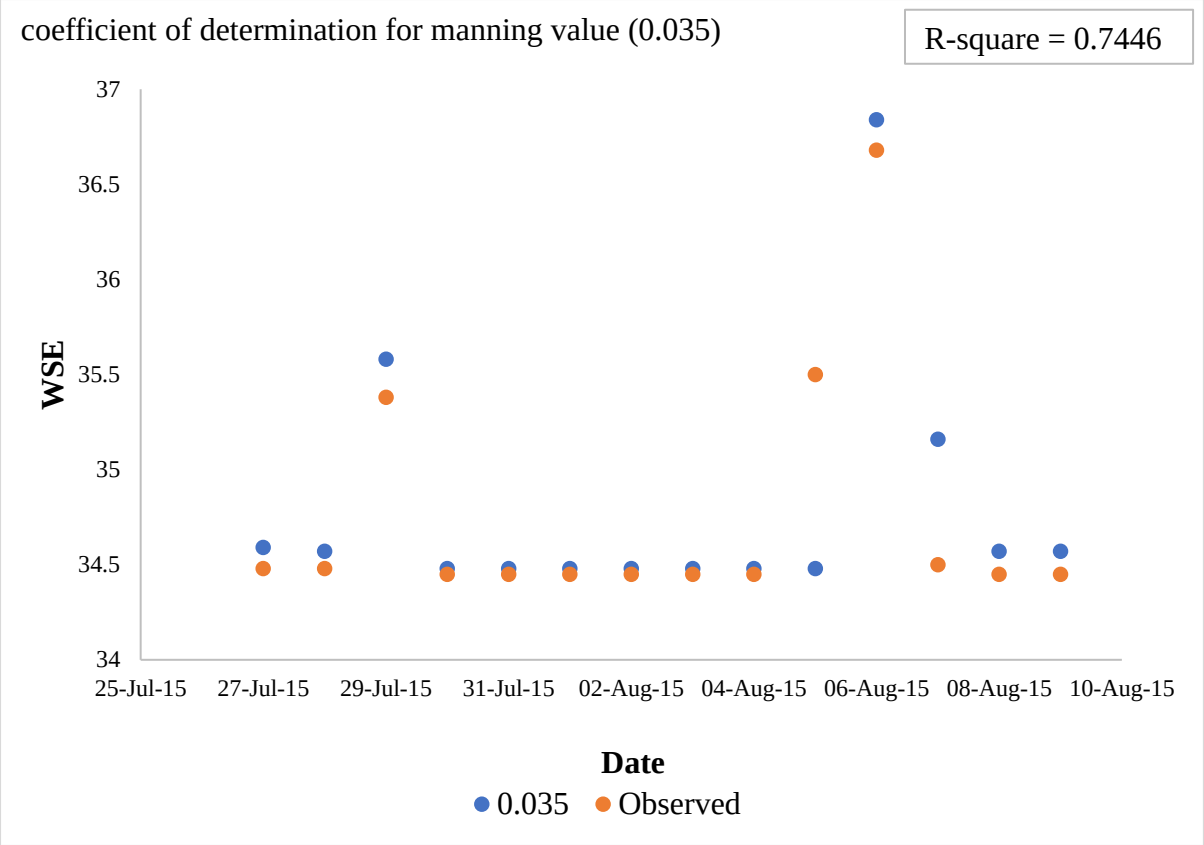

(c) R^2 determination for manning value 0.035 SRTM

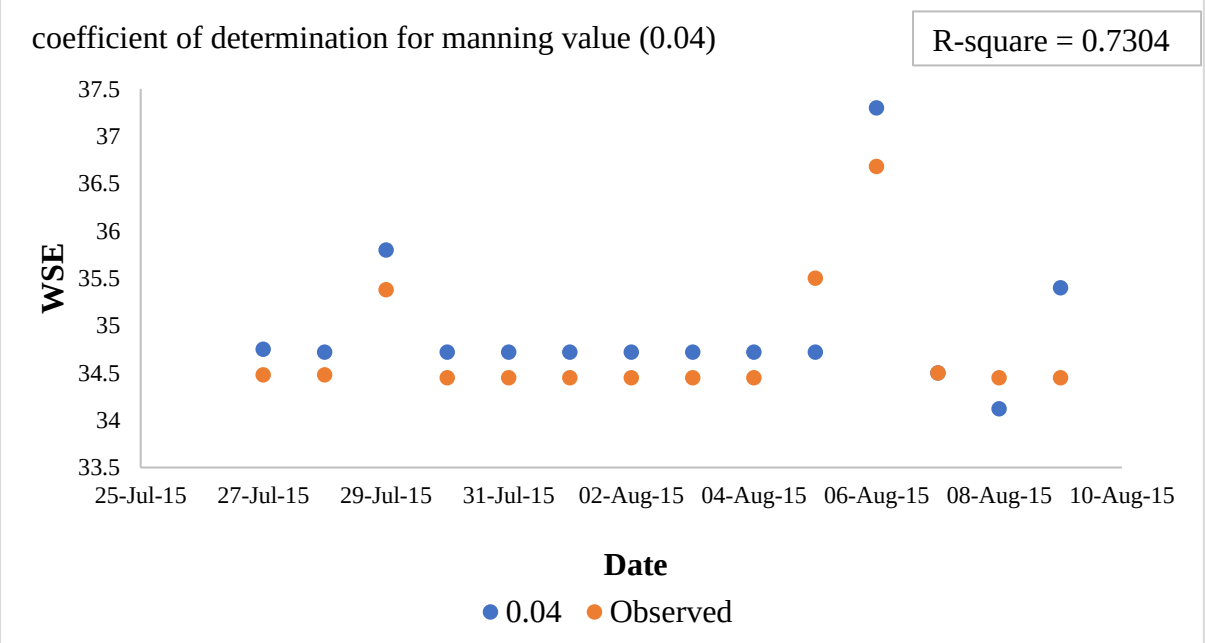

(d) R^2 determination for manning value 0.04 SRTM

Figure 5.4 Scattered chart of manning roughness values for SRTM 2015

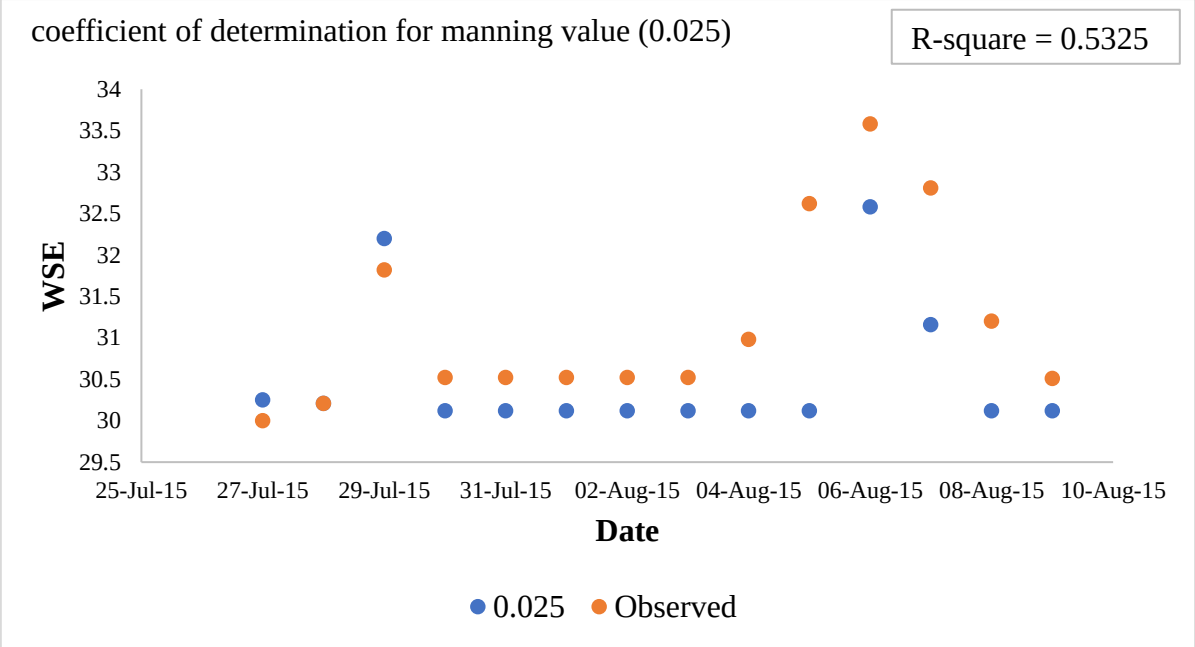

(a) R^2 determination for manning value 0.025 ALOS

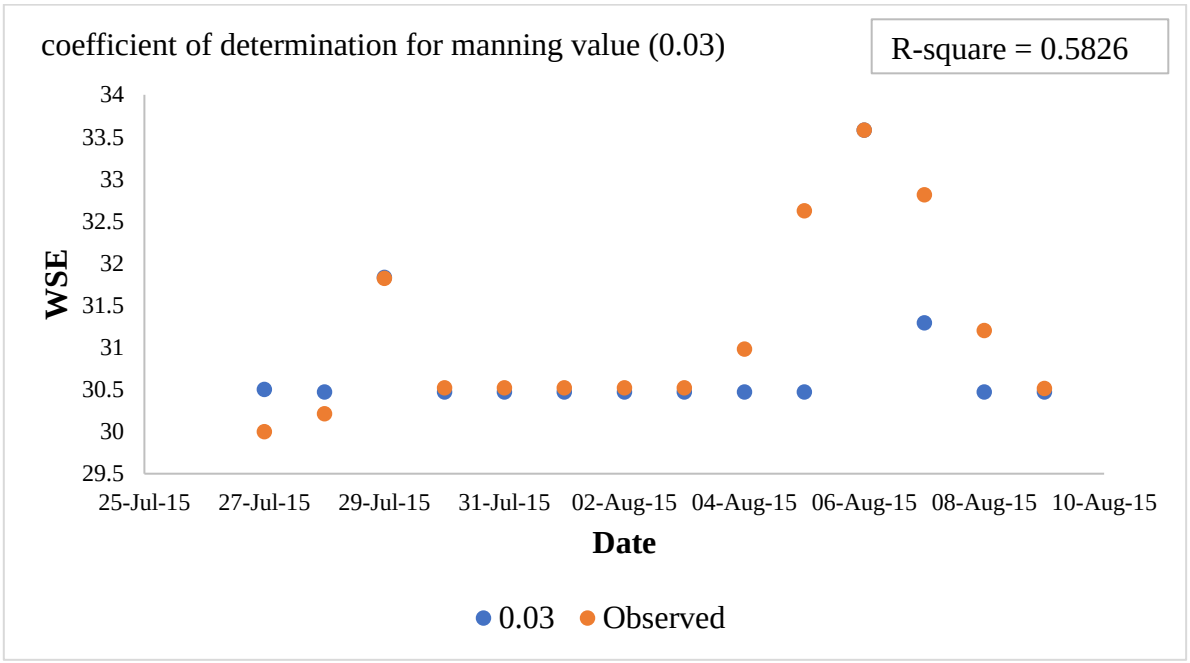

(b) R^2 determination for manning value 0.03 ALOS

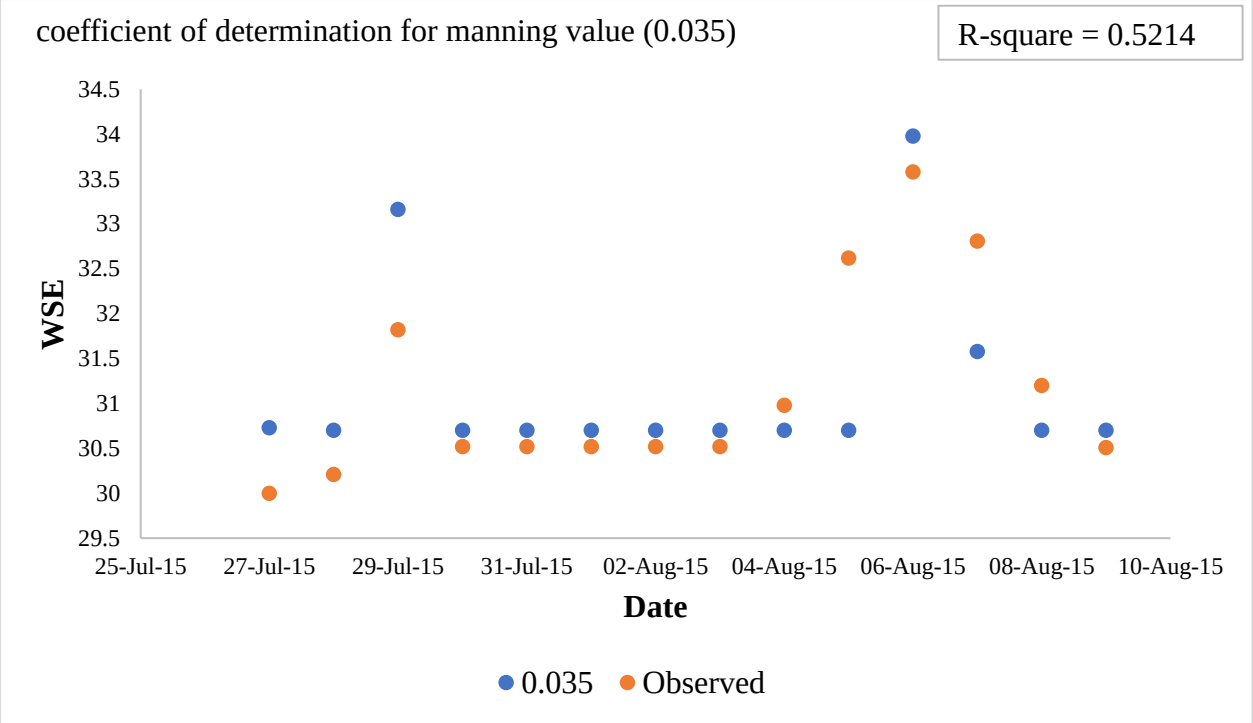

(c) R^2 determination for manning value 0.035 ALOS

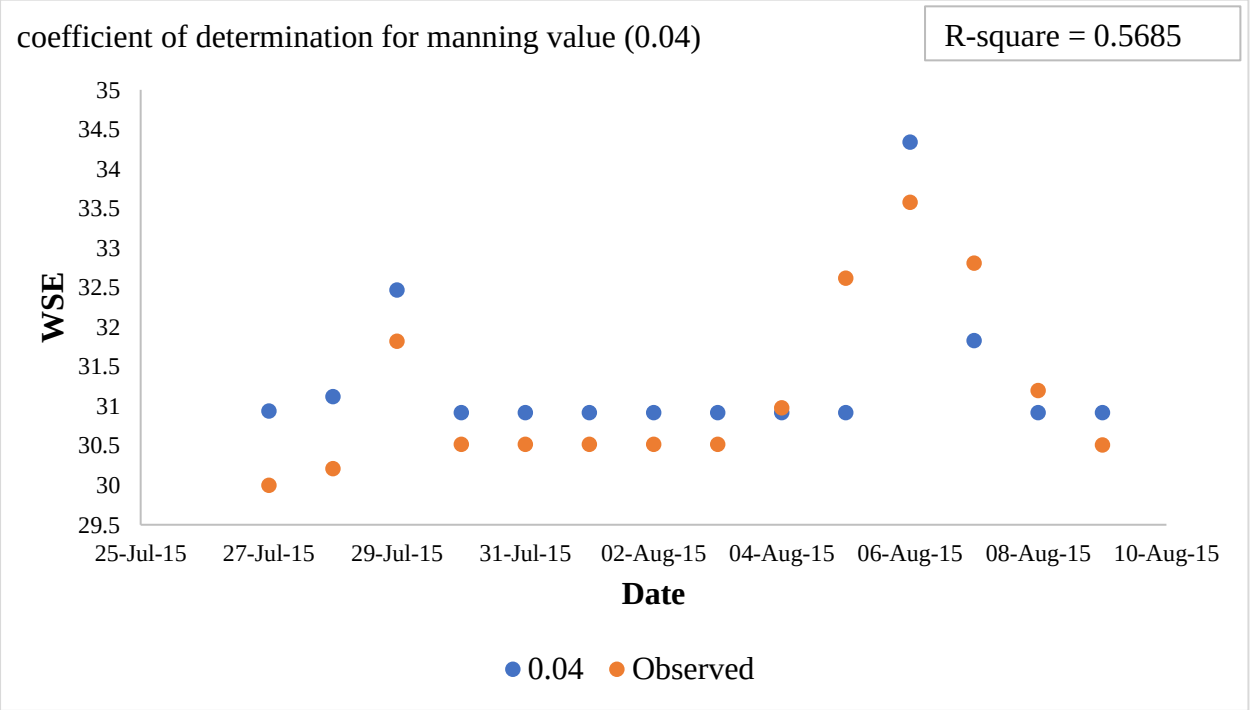

(d) R^2 determination for manning value 0.04 ALOS

Figure 5.5 Scattered chart of manning roughness values for ALOS 2015

The scattered diagrams help to identify the comparative study with mathematical expressions. In this view, the SRTM comes with a better DEM than ALOS. The summarized values of R^2

are indicated in the Table 10, which reveals that the SRTM reflects a better DEM and higher R^2 value.

Manning value	SRTM (R^2)	ALOS (R^2)	RMSE	NSE
0.025	0.691	0.532	0.44	0.86
0.030	**0.764**	**0.582**	**0.31**	**0.98**
0.035	0.744	0.521	0.33	0.92
0.040	0.730	0.568	0.44	0.89

Table 5.1 Coefficient of determination (R^2) for SRTM and ALOS for all manning values

5.4 1D model validation

The validation period of a 1D model is considered between 14th August to 27th August 2017. This span is also 14 days, like the calibration period of 2015. As per the result from the calibration period, the manning roughness value of 0.03 comes with the best fitment with observed data. In this context, the validation of the manning value for 2017 is directly used as 0.03 to check the consistency of the model.

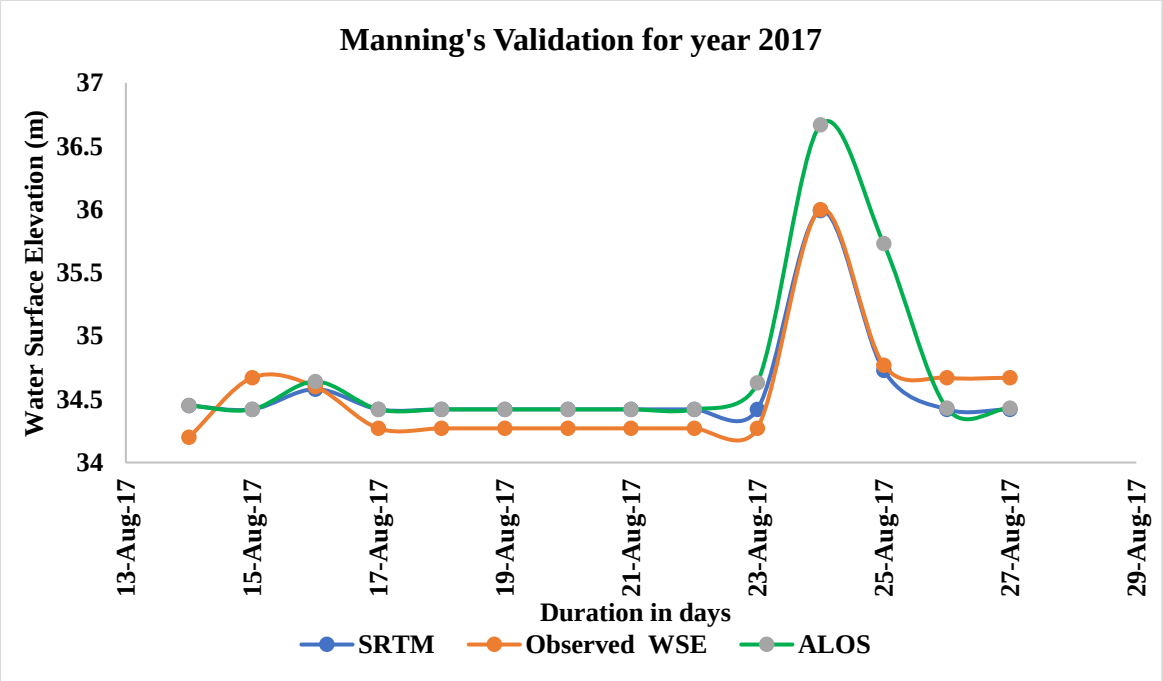

Figure 5.6 Comparison of WSE for ALOS and SRTM in validation period 2017

Fig. 28 depicts the close agreement of the manning value as 0.03 with ground data. The calibration result from the regression analysis is directly utilized in the validation span of 2017.

In this view, the discharge data is validated with the manning value of 0.03 and the coefficient of determination. The R^2 values of 0.8641 and 0.7759 have been evaluated for SRTM and ALOS, respectively. In all aspects, the SRTM is a better DEM, and further flood inundation mapping with SRTM DEM is acceptable, especially in the open-source option.

5.5 DEM comparison

Comparison of digital elevation models; SRTM and ALOS are performed not only for manning calibration but also executed for bifurcated reaches. In forming a comparative statement on bifurcated reaches, two criteria are emphasized for analysis: water surface elevation (WSE) and cross-section inundation studies. Usually, the open-source DEM is the only option for most researchers, especially researchers working with flood mapping; the DEM plays a vital role in analyzing and accurately assessing hydrodynamic results. In this context, as past studies elaborate, many ways are available for DEM comparison. Although, in this research, the comparative study of DEM has been performed with the specific cross-section inundation and WSE variation studies. The study area and data collection chapter use DEMs, SRTM, and ALOS with 30m spatial resolution. The criteria considered for this comparison are appropriate, especially for flood mapping.

5.5.1 Water surface elevation changes

In the Ozat River flood inundation mapping research, the available observed data is for a limited period, which is the major constraint for the researcher and local authority. The model inflow point is selected near the shapur weir; this consideration is due to the elimination of hydraulic structure input in hydrodynamic modeling because major structures are located upstream of this weir. After this location, three places are available where the water surface elevation data is available for a limited time extent; vanthli bridge site, Balagam ghed, and Indrana village. Out of these, the vanthli bridge site is selected for the manning roughness coefficient calibration and validation using two years, 2015 for calibration and 2017 validation. Fig. 29 (a) and (b) indicate the water surface elevation changes from mean sea level with the data of ground recorded and simulated in hydrodynamic models using SRTM and ALOS DEMs.

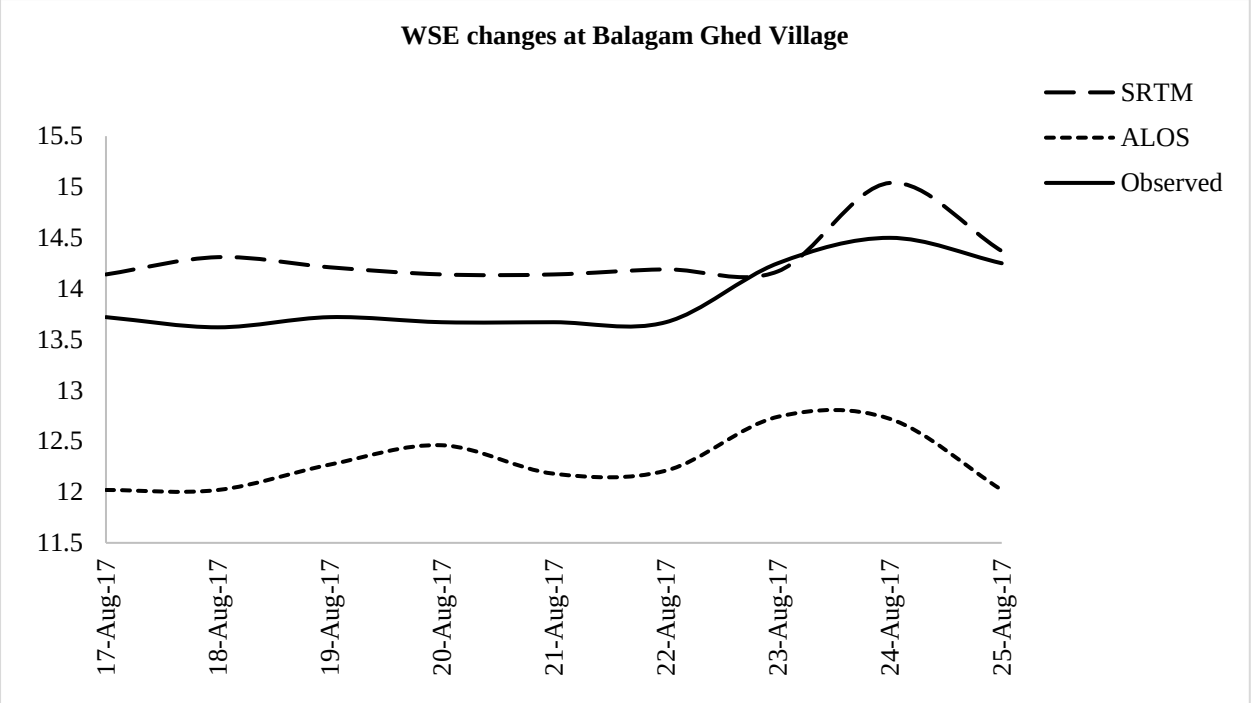

(a) WSE changes at Balagam ghed village with observed and simulated data

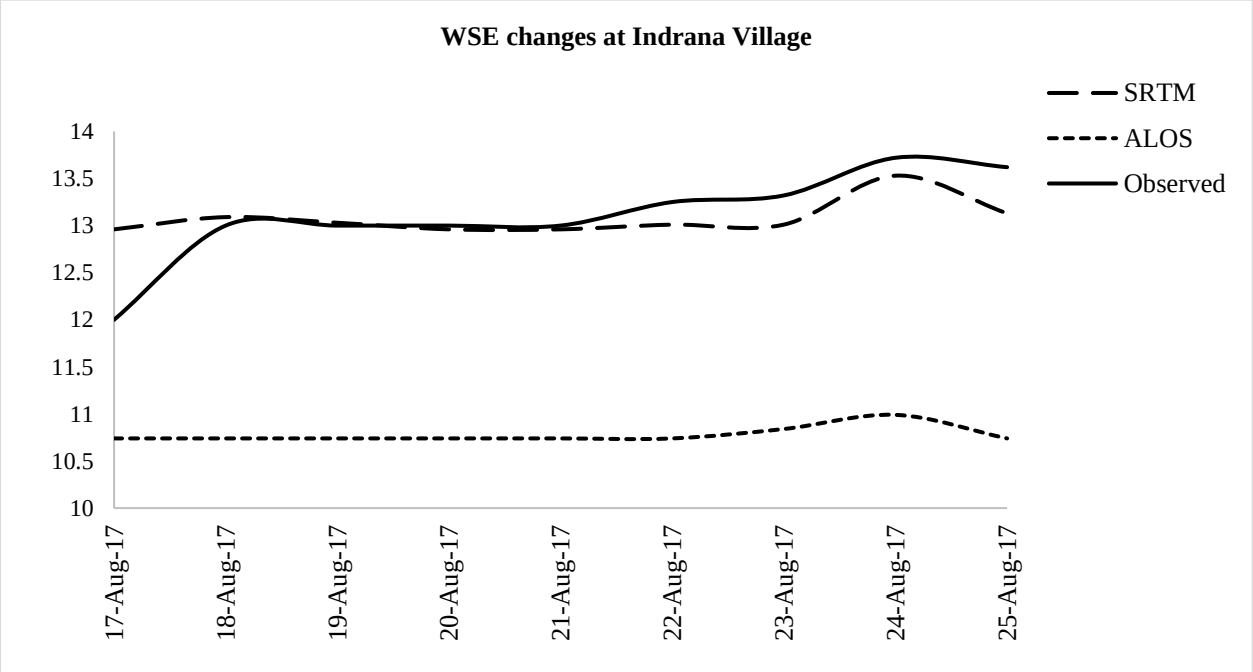

(b) WSE changes at Indrana village with observed and simulated data

Figure 5.7 WSE changes comparison on both DEMs

The water surface elevation changes on the bifurcated reaches reveal that SRTM comes with better agreement than ALOS. For numerical regression analysis, the root mean square error has

been calculated for better comparison and an accurate result of this study. In this concept, the table 11 (a) to (d) indicates the in-depth calculation of RMSE.

(a) Balagam ghed village for SRTM

Dates	Simulated	Observed	Error	Absolute value of error	square of error	Absolute value of error divided by actual value
17-Aug-17	14.14	13.72	-0.42	0.42	0.1764	0.030612
18-Aug-17	14.31	13.62	-0.69	0.69	0.4761	0.050661
19-Aug-17	14.21	13.72	-0.49	0.49	0.2401	0.035714
20-Aug-17	14.14	13.67	-0.47	0.47	0.2209	0.034382
21-Aug-17	14.14	13.67	-0.47	0.47	0.2209	0.034382
22-Aug-17	14.19	13.67	-0.52	0.52	0.2704	0.03804
23-Aug-17	14.17	14.25	0.08	0.08	0.0064	0.005614
24-Aug-17	15.04	14.5	-0.54	0.54	0.2916	0.037241
25-Aug-17	14.37	14.25	-0.12	0.12	0.0144	0.008421
	SUM		**-3.64**	**3.8**	**1.9172**	**0.27507**

(b) Balagam ghed village for ALOS

Dates	Simulated	Observed	Error	Absolute value of error	square of error	Absolute value of error divided by actual value
17-Aug-17	12.02	12	-0.02	0.02	0.0004	0.001667
18-Aug-17	12.02	13	0.98	0.98	0.9604	0.075385
19-Aug-17	12.27	13	0.73	0.73	0.5329	0.056154
20-Aug-17	12.46	13	0.54	0.54	0.2916	0.041538
21-Aug-17	12.18	13	0.82	0.82	0.6724	0.063077
22-Aug-17	12.21	13.25	1.04	1.04	1.0816	0.078491
23-Aug-17	12.74	13.32	0.58	0.58	0.3364	0.043544
24-Aug-17	12.72	13.72	1	1	1	0.072886
25-Aug-17	12.02	13.62	1.6	1.6	2.56	0.117474
	SUM		**7.27**	**7.31**	**7.4357**	**0.55022**

(c) Indrana village for SRTM

Dates	Simulated	Observed	Error	Absolute value of error	square of error	Absolute value of error divided by actual value
17-Aug-17	12.96	12	-0.96	0.96	0.9216	0.08
18-Aug-17	13.09	13	-0.09	0.09	0.0081	0.006923
19-Aug-17	13.03	13	-0.03	0.03	0.0009	0.002308
20-Aug-17	12.96	13	0.04	0.04	0.0016	0.003077
21-Aug-17	12.96	13	0.04	0.04	0.0016	0.003077
22-Aug-17	13.01	13.25	0.24	0.24	0.0576	0.018113
23-Aug-17	13.01	13.32	0.31	0.31	0.0961	0.023273
24-Aug-17	13.53	13.72	0.19	0.19	0.0361	0.013848
25-Aug-17	13.13	13.62	0.49	0.49	0.2401	0.035977
	SUM		**0.23**	**2.39**	**1.3637**	**0.1866**

(d) Indrana village for ALOS

Dates	Simulated	Observed	Error	Absolute value of error	square of error	Absolute value of error divided by actual value
17-Aug-17	10.74	12	1.26	1.26	1.5876	0.105
18-Aug-17	10.74	13	2.26	2.26	5.1076	0.173846
19-Aug-17	10.74	13	2.26	2.26	5.1076	0.173846
20-Aug-17	10.74	13	2.26	2.26	5.1076	0.173846
21-Aug-17	10.74	13	2.26	2.26	5.1076	0.173846
22-Aug-17	10.74	13.25	2.51	2.51	6.3001	0.189434
23-Aug-17	10.84	13.32	2.48	2.48	6.1504	0.186186
24-Aug-17	10.99	13.72	2.73	2.73	7.4529	0.19898
25-Aug-17	10.74	13.62	2.88	2.88	8.2944	0.211454
	SUM		**20.9**	**20.9**	**50.2158**	**1.58644**

Table 5.2 (a),(b),(c) and (d) RMSE calculates for water surface elevation changes on bifurcated reaches

The above tables are better for understanding the calculations regarding RMSE achievement. For this analysis, the summarized results are mentioned in the table 12. This result depicts that the lower the value of RMSE better the comparison with ground data.

Sr No.	Location & DEM	N (number of events)	MAD (mean absolute deviation)	MSE (mean squared error)	RMSE (Root Mean Squared Error)
1	Balagam Ghed (SRTM)	9	0.422	0.213	0.461
2	Balagam Ghed (ALOS)	9	0.81	0.82	0.90
3	Indrana (SRTM)	9	0.265	0.151	0.389
4	Indrana (ALOS)	9	2.322	5.579	2.362

Table 5.3 Summarized result of RMSE for WSE changes

The table 12 indicates the lower the value of SRTM than ALOS for both balagam ghed and Indrana village cases. For further analysis, the below section illustrates the comparison of both DEMs for the cross-section inundation study.

5.5.2 Cross section inundation study

A cross-section inundation study is an essential comparison of this research. In this context, the many sections along the reaches show the overbank discharge, which needs to validate whether a specific place is overbanked in a particular event. This comparison shows that some cross-sections show different results in DEMs, SRTM, and ALOS. The ground elevations on both DEMs are varied throughout the study area. After numerous simulations from the many cross-sections, the bifurcated reaches show significant overbank discharge. In this regard, It needs to validate that a major discharge happened on the ground for a particular location. In this research, for a 1D hydrodynamic model, the width of a cross-section is considered 700m. however, the model results reveal that this width is inundated by a river stretch of 40km from navi bandar river mouth. The scenario of this inundation of cross-section arises because of cup shape geometry. In addition to this, the comparison of DEM is illustrated by each cross-section, and ground data is collected from field visits. Fig. 30 indicates the comparative bar chart formed via data from modeling and observation.

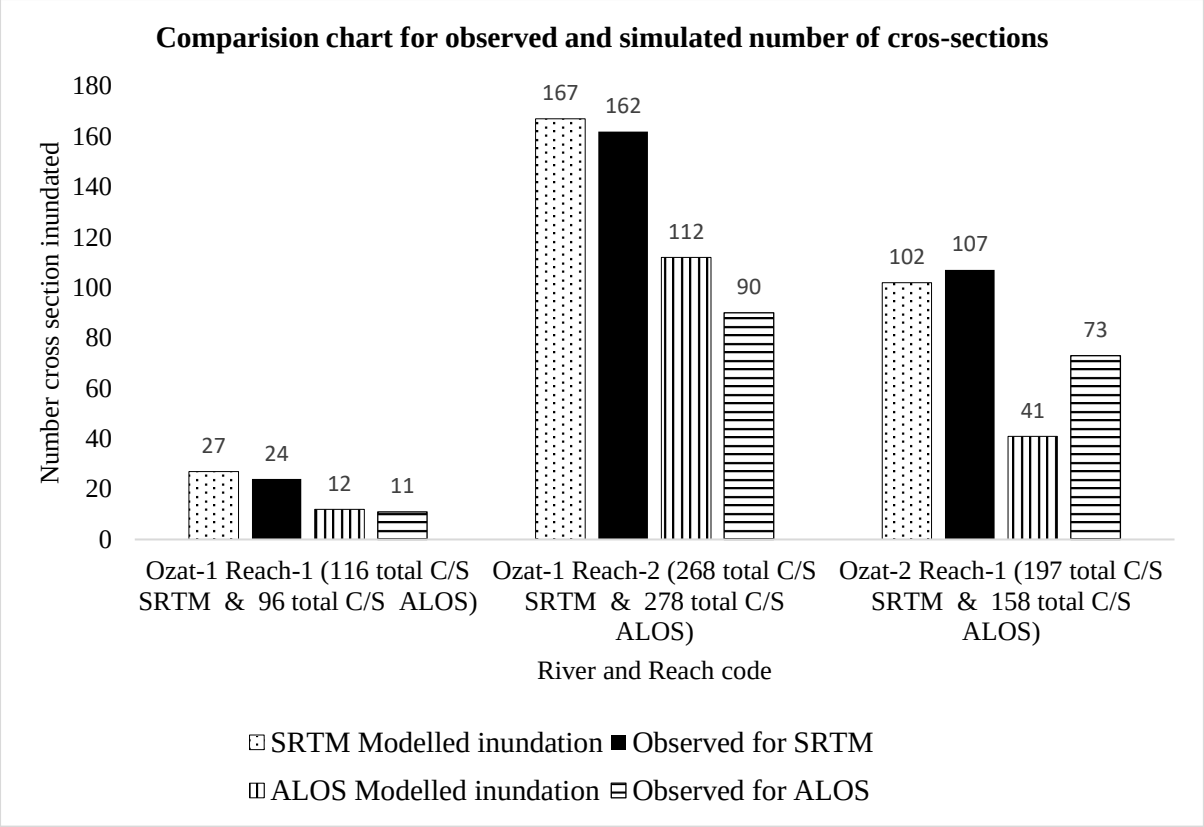

Figure 5.8 Bar chart for a number of cross-sections inundated and actual inundation in observed data

The Fig. 30 indicates the total cross-sections places and inundated on various three reaches; one before bifurcation and two after bifurcation.

Sr No.	Reach name	Total CS	DEM	Inundated CS (Model)	Inundated CS (Observed)	R^2
1.	Ozat-1 Reach-1	116	SRTM	27	24	0.859
2.	Ozat-1 Reach-1	96	ALOS	12	11	0.727
3.	Ozat-1 Reach-2	268	SRTM	167	162	0.835
4.	Ozat-1 Reach-2	278	ALOS	112	90	0.657
5.	Ozat-2 Reach-1	197	SRTM	102	107	0.719

6.	Ozat-2 Reach-1	158	ALOS	41	73	0.371

Table 5.4 Summarized data of cross-section model and observed inundation along reaches

The table 13 indicate cross-section inundation of summarized data along the all three reaches. In this context, in the same river reach code depict that total number of cross-sections have been placed with different number for both DEMs; because after the simulations specific places needs to be interpolate and as a result of this total number may be vary for same places. For the result of this, the SRTM comes with better DEM for cross-section inundation study, higher the value of R^2 better the DEM agreement.

5.6 2D hydrodynamic model

The result comes from the 1D hydrodynamic model assists the development of a 2D model. The 2D model is vital for inundation boundary mapping and other hydraulic aspects in this context. The 1D model generates the inundation at only cross-section areas, whereas a 2D model gives the water scattering area covered by the 2D flow area boundary. A 2D model needs to assess the hydraulic parameters of the unsteady flow of the Ozat River basin. As stated earlier, the Ozat River splits from the tikar village; this place is 82.4 km from the river origin point and 19.5 km away from the model inflow point. From this point, the Ozat River formed two separate tributaries; one ran straight towards the sea and met the Arabian sea near pata village, and another one ran towards the Ghed region (delta region of Ozat River) and scattered the water in sizeable depressed area before meeting the sea near Navi Bandar. The actual scene is that this depressed Ghed region frequently inundated more than 180 km^2. This research aims to assess the ground condition for inundation, time to fill this area from pre-decided benchmarks and generate an early warning system for the local community. In addition, the authors have also taken remedial measures to overcome this situation. As a result of the 2D model, various hazardous maps are generated to assist decision-makers. The various hazard maps are depth, velocity, per cent time inundation, and arrival time maps.

5.7 Simulation visualization

The simulation window of a 2D model depicts the water flow in the Ozat River basin to visualize how the water makes its path to river mouths. In this context, the total simulation time of the model is 224 hrs, and in between this river, water makes the path, bifurcation, scattering, filling water on the Ghed region and meeting the Arabian sea at two river mouths, everything can be visualized in the Fig. 31.

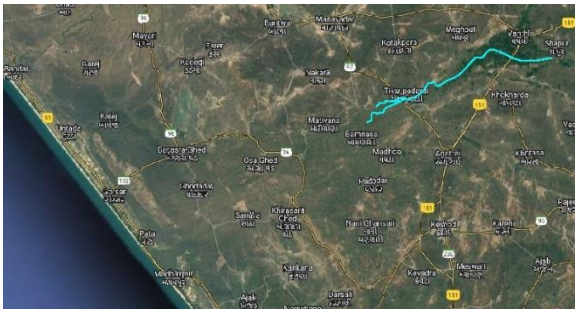

(a) Bifurcation

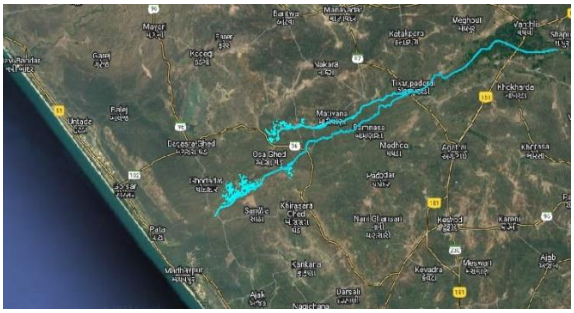

(b) started scattering

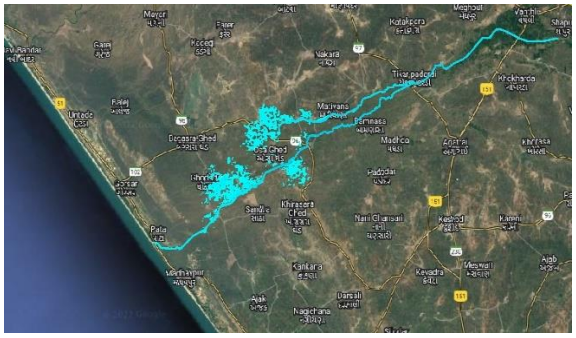

(c) O-2 R-1 reached at river mouth before O-1 R-2

(d) Filling depressed area

(e) O-1 R-2 reached the river mouth

(f) Maximum inundation map

Figure 5.9 chronology of flood simulations, screenshots indicate the incremental visualization

5.8 Validation of a 2D model

For model consistency, it is challenging to validate the scattered water on a large area. In this research, the large pond of ghed region filled with water and depressed land gets inundated for many days even after the monsoon season. The validation of water scattered region needs to be compared with observed data; it has already been mentioned in the title of this research that the Ozat River basin is data-scarce. Only a few places are available to validate the approach in this context. These places are located after the bifurcation, which is a pro thing for researchers. These places are koylana, Sharama, Bagasara ghed, and kadachh villages. The actual condition of reaches near these villages is narrow and deficit depth; it's a primary reason behind water scattering. The water depth near these villages was observed during the simulation period and

compared with modeled data. The figure depicts the locations of limited observation points considered for this analysis.

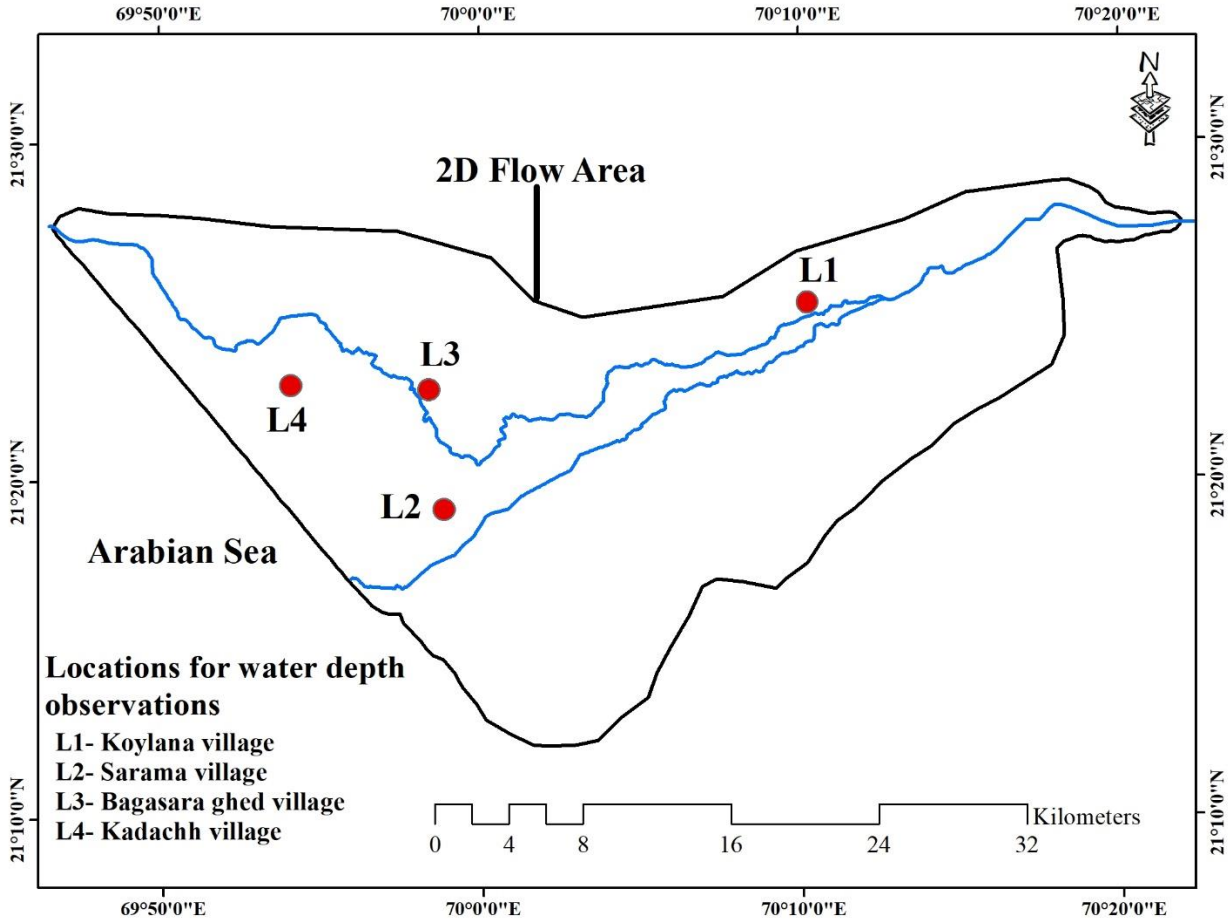

Figure 5.10 Location sketch of water depth observation points during the simulation period

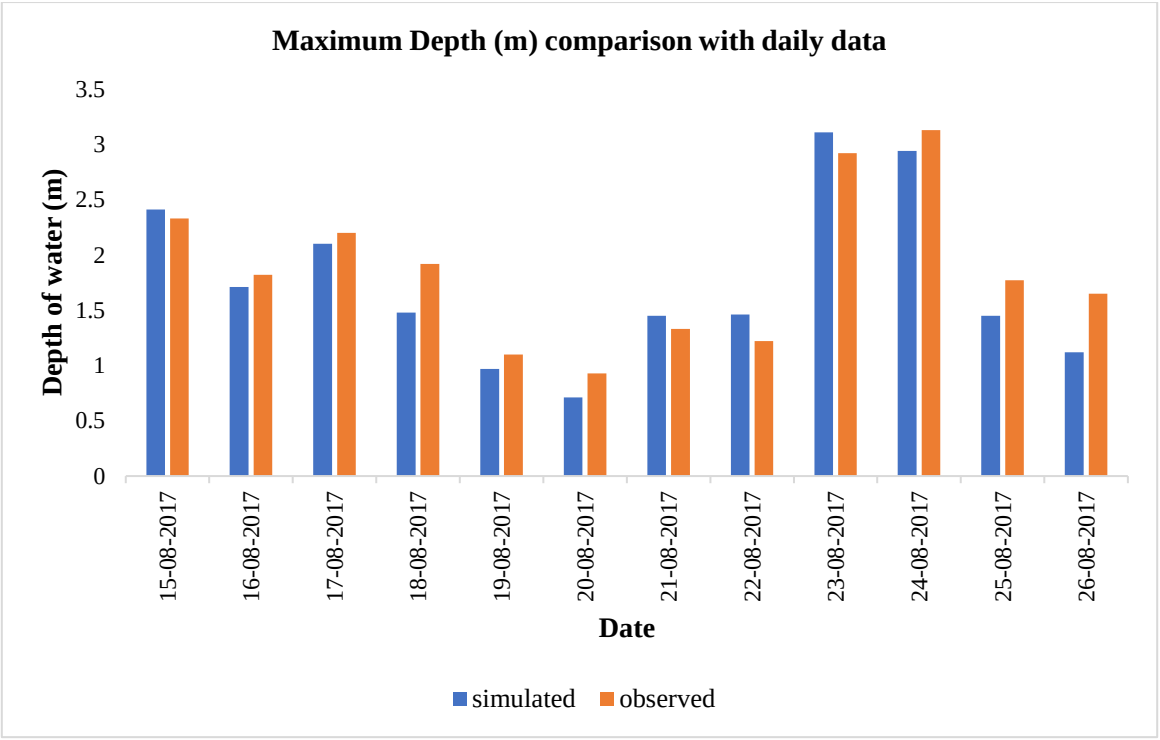
Maximum Depth (m) comparison with daily data
Depth of water (m)
3.5
3
2.5
2
1.5
1
0.5
0
15-08-2017
16-08-2017
17-08-2017
18-08-2017
19-08-2017
20-08-2017
21-08-2017
22-08-2017
23-08-2017
24-08-2017
25-08-2017
26-08-2017
Date
simulated
observed

(a)

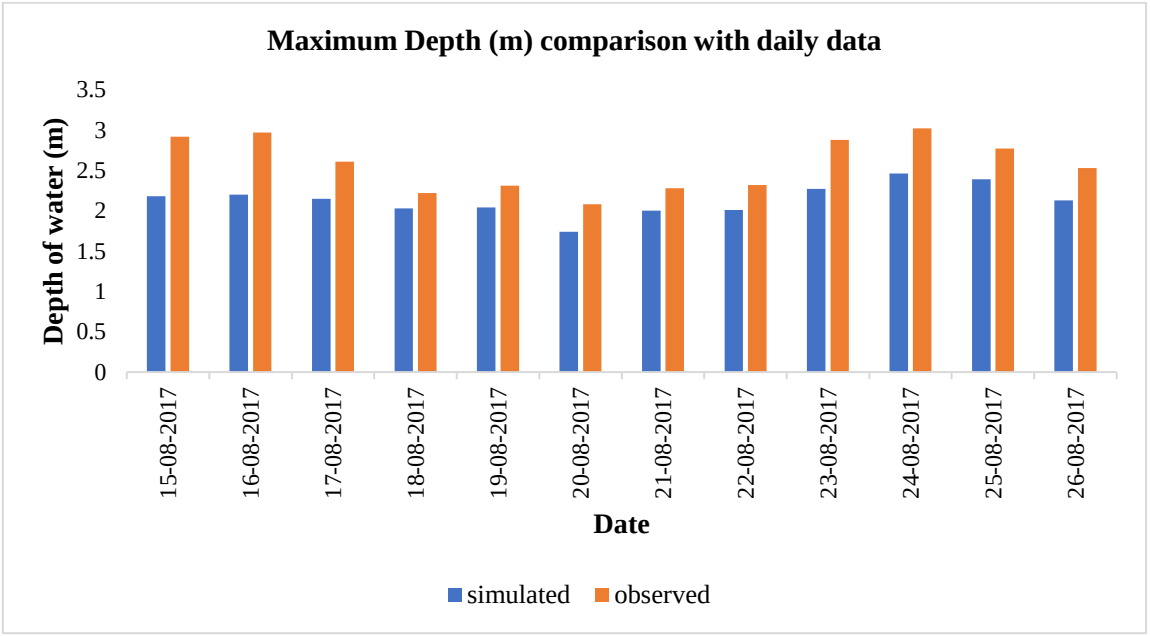
Maximum Depth (m) comparison with daily data
Depth of water (m)
3.5
3
2.5
2
1.5
1
0.5
0
15-08-2017
16-08-2017
17-08-2017
18-08-2017
19-08-2017
20-08-2017
21-08-2017
22-08-2017
23-08-2017
24-08-2017
25-08-2017
26-08-2017
Date
simulated
observed

(b)

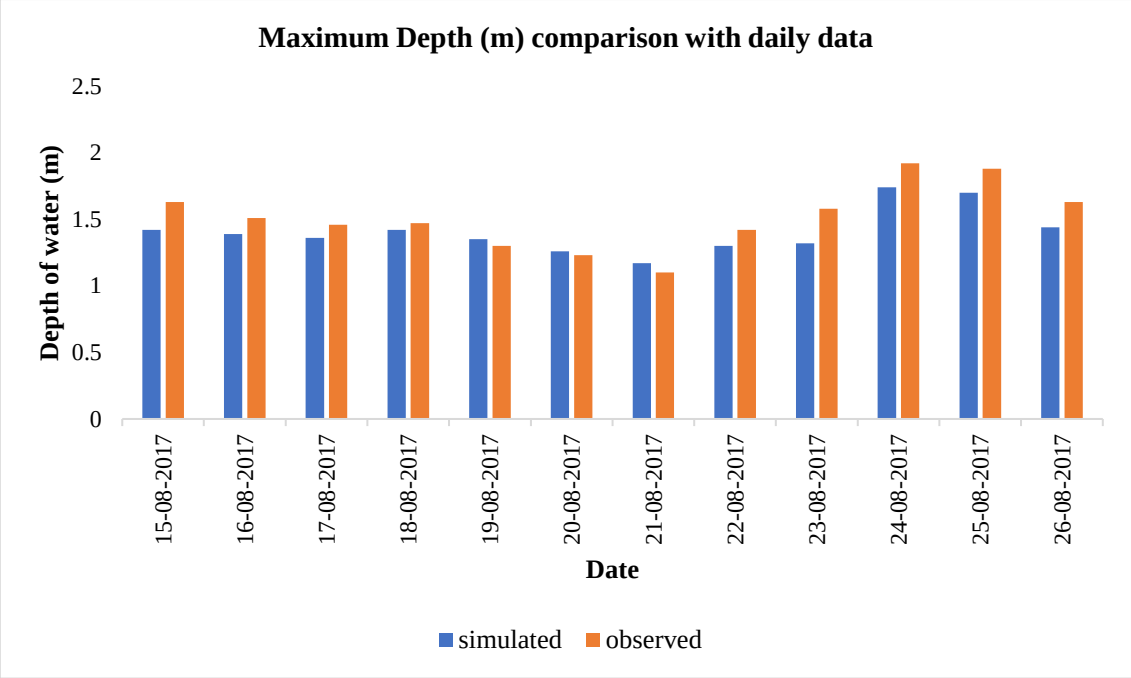

(c)

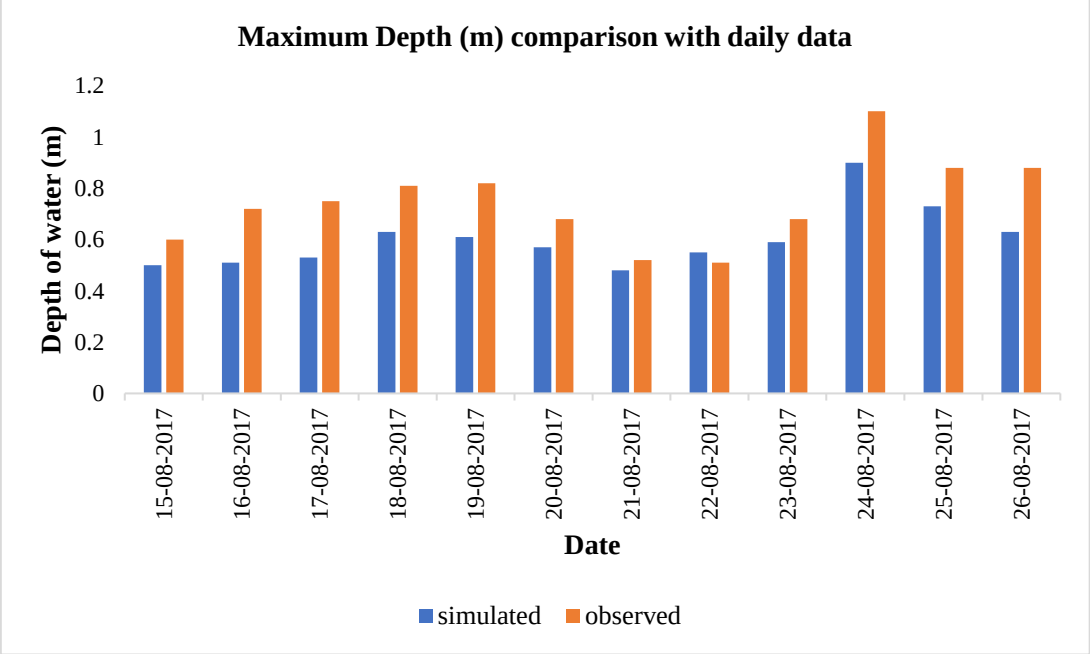

(d)

Figure 5.11 water surface comparison with observed and modeled water depth

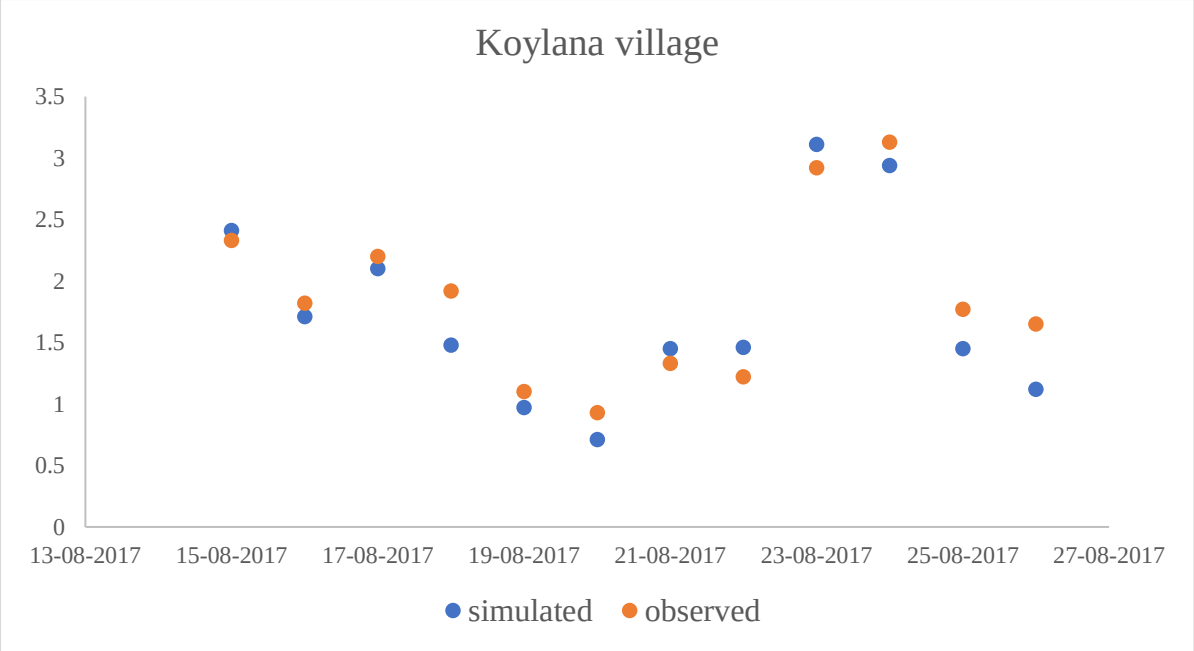
Koylana village
3.5
3
2.5
2
1.5
1
0.5
0
13-08-2017
15-08-2017
17-08-2017
19-08-2017
21-08-2017
23-08-2017
25-08-2017
27-08-2017
simulated
observed

(a)

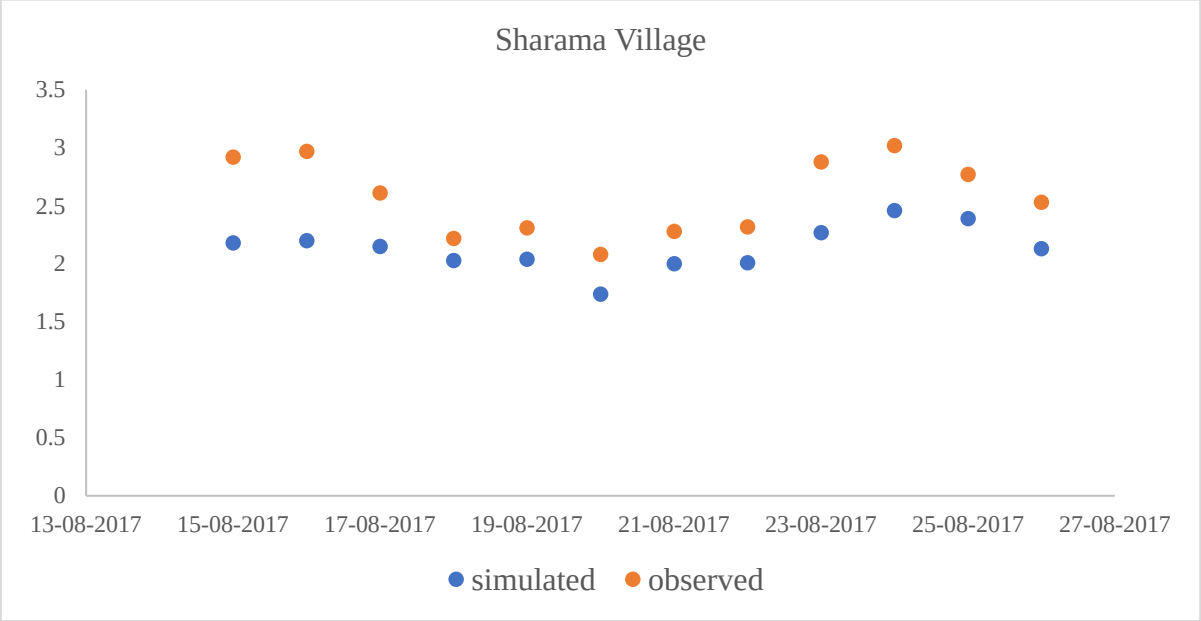
Sharama Village
3.5
3
2.5
2
1.5
1
0.5
0
13-08-2017
15-08-2017
17-08-2017
19-08-2017
21-08-2017
23-08-2017
25-08-2017
27-08-2017
simulated
observed

(b)

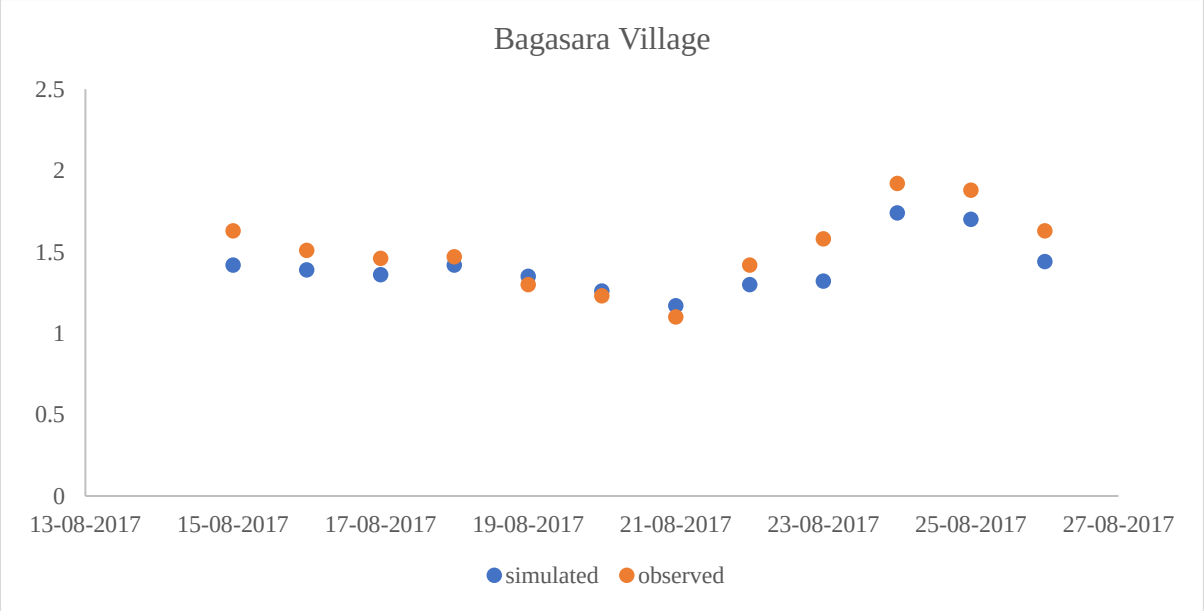

(c)

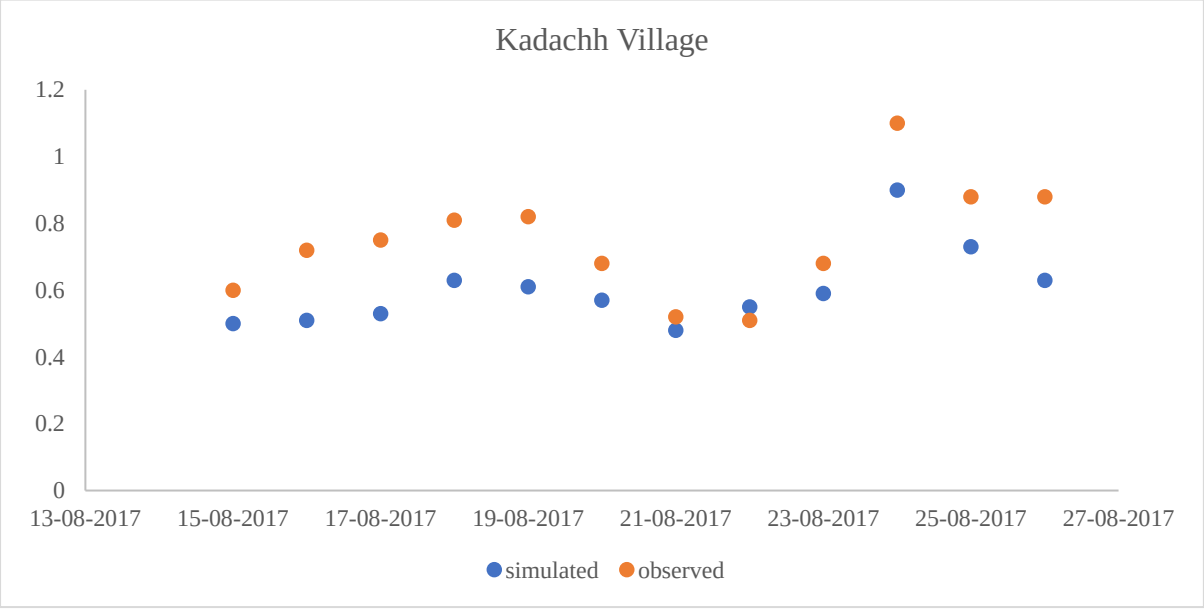

(d)

Figure 5.12 Scattered chart of water depth study at four specific places

	Koylana	**Sharama**	**Balagam**	**Kadachh**
R^2	0.8969	0.7576	0.8551	0.7704
RMSE	0.2605	0.4779	0.1478	0.1651
NSE	0.9998	0.9997	0.9999	0.9995

Table 5.5 R^2 values of water depth comparison near desired four villages

The table 14 indicates the values of R^2 at four places near the village area. Out of these places, the kadachh village is located periphery of the depressed ghed region whereas the water is observed like fill up the pond, at these places no tributary located but the specific boundary of low lied ghed is observed for water depth changes. The highest value achieved of R^2 at koylana village is 0.8969. Balagam, Kadachh, and Sharama villages came in at 0.8551, 0.7704, and 0.7576, respectively.

5.9 Hazard maps

The hazard maps are vital for framing the pre-flood preparations' decision-making system. In the case of the Ozat River basin, the hydraulic parameters of unsteady flow have been evaluated, and various flood maps are generated in the RAS mapper. The hazard maps are essential for predicting future events, establishing new hydraulic structures, and flood early warning systems. The Ozat River basin has fan shape catchment, which depicts the peak flow in a season as per the characteristics of the fan shape catchment. The downstream area of the basin after bifurcation shows significant inundation due to low laying area and higher elevated coastal line. In this context, the maximum depth map, velocity map, time to get inundation of ghed region, and water arrival time map are vital for decision making for local administration.

5.9.1 Depth map

The depth map is essential to check the model's consistency at various observed locations and validate the approach. Furthermore, the depth map helps the decision makers for terrain conditions at various locations along reaches and cup shape geometry where the depth of water has been analyzed. An inflow hydrograph is utilized to simulate the event of flood inundation. In this case, the inflow hydrograph, as shown in Fig. 14 reveals the number of six peaks. For these multiple peak conditions, the flood visualization result shows the multiple hazard events and variable depth of water. As stated earlier, the model has been simulated for 14 days; however, the first five peaks come from the first ten days, and the last remaining peak comes after that. The values of that peaks come from the days of 15th, 17th, 18th, 21st, 22nd, and 23rd Aug 2017 as 818, 662, 404, 416, 455, and 1275 cumecs, respectively. The prominent peak is 1275 cumecs from the mid night of 23rd Aug 2017. After the release from the shapur weir, the water runs through the Ozat River properly till tikar village. After that, the Ozat River leading reach bifurcates and separates into two different reaches, as discussed earlier. In this regard, one tributary runs straight, and another runs towards the area of interest (ghed region). After the release from the shapur weir (23rd Aug), the tributaries after the bifurcation shows significant overbank discharge. Fig. 35 indicates the depth map of the study area boundary at

the maximum condition of the event. In this case, the water gest filled in the depressed ghed region which the villages cover: amipur, balej, kadachh, sandha, osa, and bagasara villages. The major inundation and overbank discharge were carried out from the reach Ozat-1 Reach-2 after the significant release from the 23rd Aug at shapur weir. The water depth in this cup shape region is only 0.5 to 1.0m, but water stays here for more days even after the monsoon season. In this case, water depth is not a significant constraint, but water presence for more days, even after the event, creates contingencies for the local community. Fig. 35 depicts the visualization of the water depth map of the study region in maximum conditions.

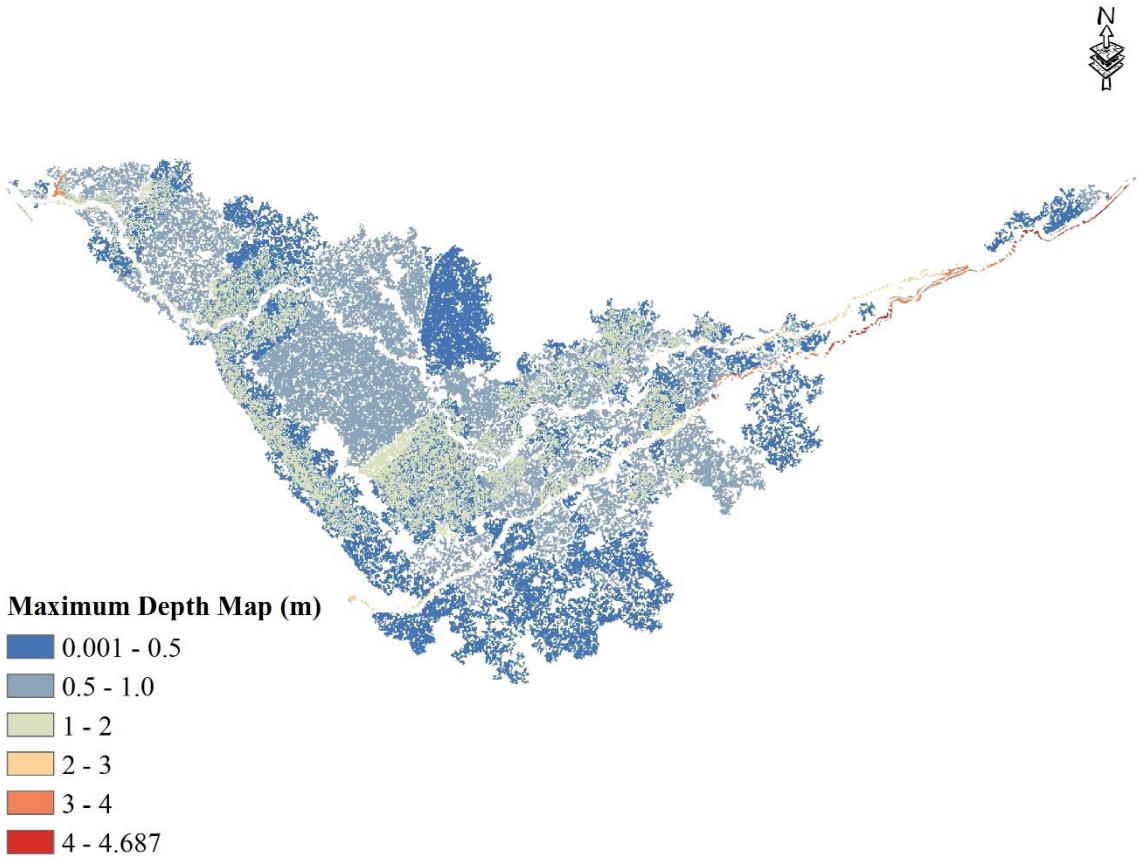

Figure 5.13 Maximum depth map

The Fig. 35 indicates that maximum water depth is 4 to 4.7m while it is achieved before bifurcation and this portion has sufficient width and depth compared to after bifurcation. The color code of ghed region indicates the water depth is barely between 0.5 to 1.0m. this portion is vital for research.

Sr no.	Date & time	Key places	Maximum depth of water (m)
1	24th Aug (3:26 am)	Osa	1.34
2	24th Aug (4:02 am)	Fulrama	1.06
3	24th Aug (6:24 am)	Bhathrot	1.38
4	24th Aug (9:06 am)	Ghodadar	1.51
5	24th Aug (11:12am)	Ghed Bagasara	1.68
6	24th Aug (02:23 pm)	Mander	1.02
7	24th Aug (08:34 pm)	Kadachh	0.87
8	24th Aug (10:23 pm)	Sarama	1.26
9	24th Aug (12:11 pm)	The area between kadachh and Bagasra	1.12
10	25th Aug (12:51 am)	Sandha	0.48
11	25th Aug (03:29 am)	D/S area of Amipur dam	0.75
12	25th Aug (10:54 am)	Samarda	0.45

Table 5.6 Depth of water at various key places of the study region

5.9.2 Velocity map

The velocity map is essential to check the surface velocity of flood water to analyze the area regarding the vulnerability of surface erosion and land degradation. In Fig. 36, The near areas of shapur weir, which is the inflow point of the model, depict substantial velocity values between 0.81 to 1.91 m/s. This portion of study region has natural and sufficient slope till bifurcation point near tikar village. The surface erosion is not happened in the study area because land quality is still maintained as per the farmer feedback. After the bifurcation, the natural slope of the river bed terrain becomes decreasing and the river width and depth also decreased till cup shape ghed region. Fig. 36 can visualize the velocity of water for entire study

region.

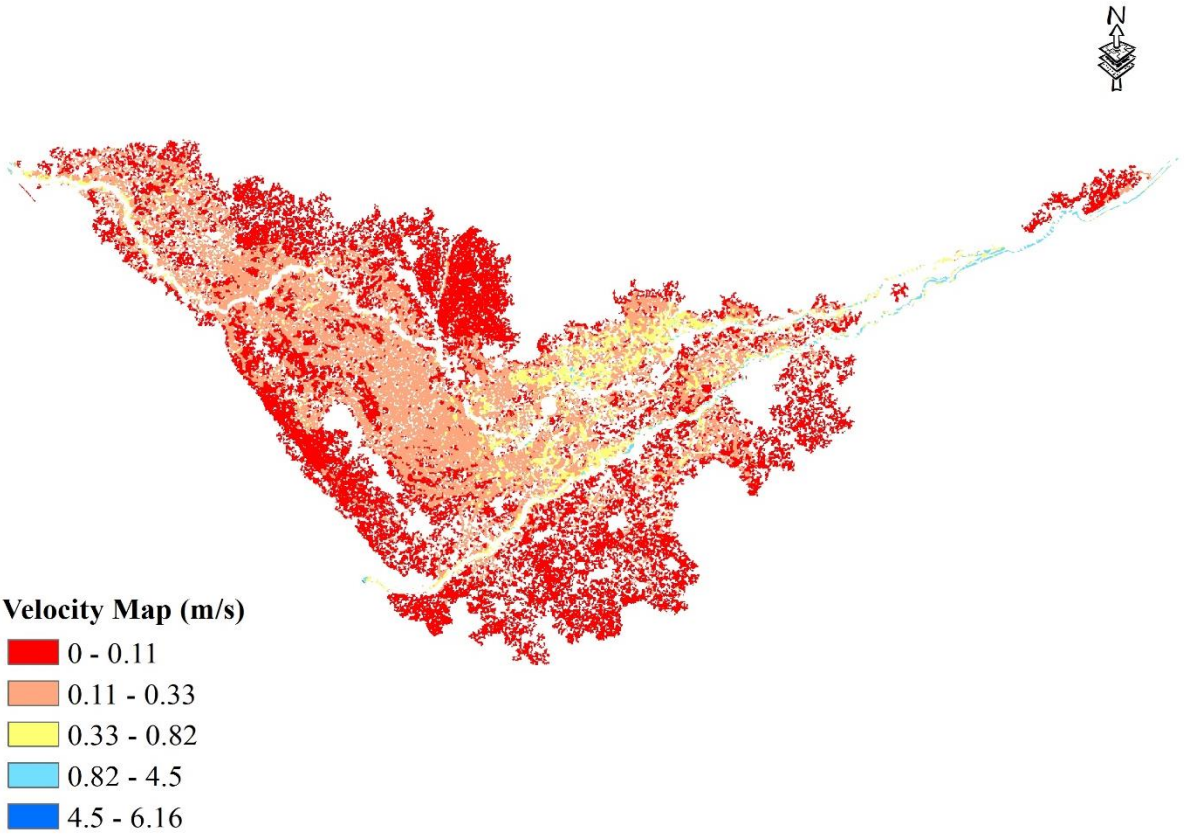

Figure 5.14 velocity map visualization of the study area

In Fig. 36, the higher velocity value is achieved near the model's inflow point (near shapur weir). After the bifurcation, the major areas are covered under the first and second categories as per the legend. The area of interest (ghed region) falls under this category of 0 to 0.33 m/s velocity. Although, the velocity is not a major constraint for the Ozat River basin.

5.9.3 Arrival time map

The arrival time map is important for framing the early warning system in which this map result reveals the time taken by water to reach various places of the study area. Decision-makers need an arrival time map (Fig. 37) to assess the early warning system. From the Tikar village, the Ozat River divides and travels through the Ghed region as a small valley. For this case study, the hydraulic model simulation took 288 hours. Following the Shapur Weir's water discharge, the simulation window shows that after 36 hours of simulations, water begins to emerge near Osa and Sandha and spread throughout the surrounding area. This section explains that the flooding period lasts between 55 and 90 hours.

As a result, 19 hours of leg time are available to alert people to this region. One segment of the reach (Ozat-2 Reach-1) takes 46 hours to travel to Pata village and 116 hours to traverse to the

Ghed region before arriving at the Arabian Sea. It takes longer to transport fresh water to the sea in Navi Bandar because of the higher seacoast. The water dispersed over the Ghed region takes only 55 to 90 hours, while the tributary to the Ghed region (Ozat-1 Reach-2) takes 116 hours to reach the estuary. As a result, flooding in the Ghed region occurs faster than water does when it reaches sea level. On average, the water covers 179 km^2 of the 870.11 km^2 total area under study, agriculture. Early warning to the local community enables people to leave their fields and arrive in the settlement area because most villages have a safe grade elevation. The timing of the water's arrival from the input point is shown in table 16 for villages and other important locations in the study region.

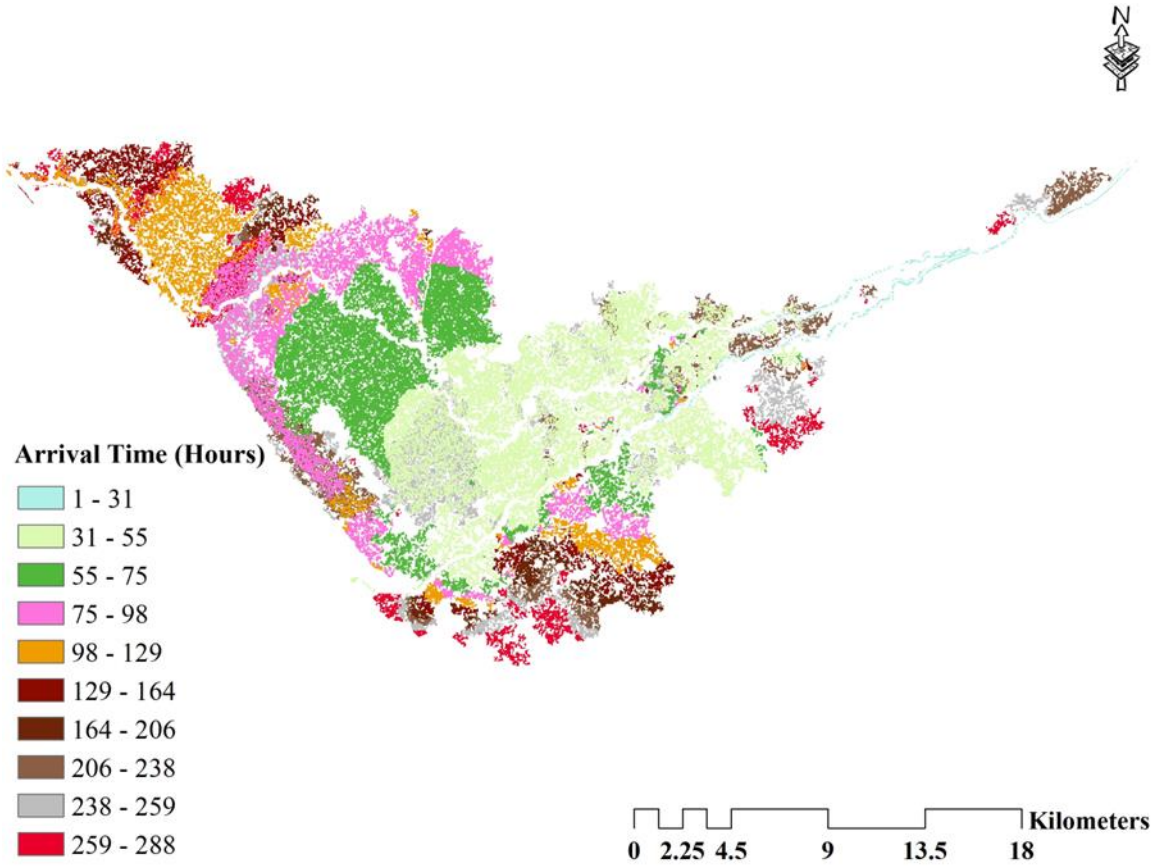

Figure 5.15 Arrival time map in hrs

Sr no.	villages and key places of the study area	Water arrival time from inflow place in hrs
1	Osa	44
2	Fulrama	47
3	Bhathrot	49

4	Ghodadar	45
5	Ghed Bagasara	53
6	Sandha	80
7	Samarda	59
8	Sarma	46
9	Kadachh	56
10	Mander	54
11	Downstream area of Amipur dam	73
12	Area between kadachh and Bagasra	55 to 90

Table 5.7 Arrival time (hrs) at various places along the study area

5.9.4 Percent time inundation map

A remarkable result map from the most current version of HEC-RAS, 6.1.0, is the percent time inundation (Fig. 38). This mapping result shows how much of the total simulation time is spent inundating a specific region. (in this case, simulation time is 14 days). According to the legend in Fig.38, the red color region falls between 81 and 100 percent; this area is flooded for 11 to 14 days. (80 to 100 percent of 14 days). The Ozat River valley area is submerged for the 14-day simulation period. The research area (Ghed region) stays wet for more than 80% of the time (for 12 days); satellite images show that this area still appears submerged in water even after the simulations are over. The green-colored region on Ozat-2 Reach-1's left side denotes a location where water lasts only 5 to 7 days before drying out. The water stays in this region for a while, so it isn't a major concern. Before the split, some areas are yellow. These places have overbanked water but only stay there for two to three days, so it is not a problem.

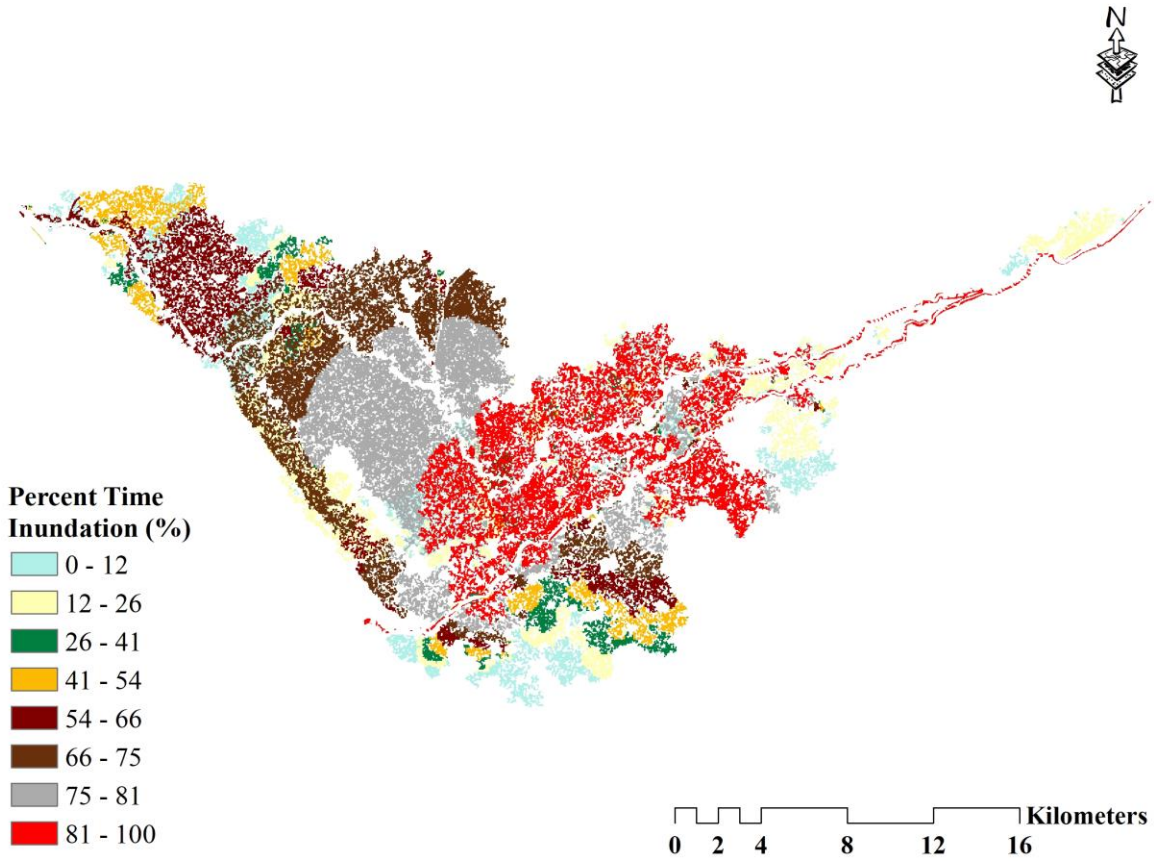

Figure 5.16 Visualization of percent time inundation map

Given that the majority of the red and green areas on the LULC map Fig. fall under the cropland class, and that this area is larger than 285 km^2, it is likely that the cropland has been under water for longer than the simulation period. More mapping was completed with the aid of Google Earth Engine cloud processing. The average proportion of the area that was flooded during the 14-day simulation is shown in table 17 below. Osa Village is located in a region with an 85.15 percent indicator, meaning it was flooded for 12 of the 14 days (85.15 percent of 14 days).

Sr No.	Key places of the study area	Percent time inundation (total simulation time 14 days) in percentage
1	Osa	85.15
2	Fulrama	83.39
3	Bhathrot	82.70
4	Ghodadar	84.43

5	Ghed Bagasara	81.31
6	Sandha	72.32
7	Samarda	79.24
8	Sarma	85.12
9	Kadachh	78.89
10	Mander	80.97
11	Downstream area of Amipur dam	74.39
12	Area between kadachh and Bagasra	79.24

Table 5.8 Percentage of inundation time near villages and key places

5.9.5 Flood Effect on Landcover Classes

In this case study, the flood effect has been simulated for 2017. However, this scenario has been frequent for many years. For this, the inundation boundary map has been overlapped on LULC to check the flood effect of each land cover class. Most cropland is situated in this study area, and a depressed portion is utilized. The table indicates that barrenland naturally gains water on 33.28 km^2 which needs to deepen for storing the water before reaching to Ghed region. The other affected land class has a less influencing area and is mostly safe against peak flow. The table shows the effect of flood on each land cover area out of the total area.

Sr No.	Land class	The total area of a particular class	Inundated part
1	Cropland	502.02	179.27
2	Barren land	139.16	33.28
3	Built-up	103.89	16.96
4	Forest	75.01	12.50
5	Waterbody	50.03	14.26
Total Area		870.11	256.27

Table 5.9 Flood effect on each land cover class

5.10 Flood mapping algorithm in google earth engine

The flood mapping algorithm has been generated using the google earth engine cloud platform. The process diagram is shown in Fig. 22 for google earth engine cloud computing. In this case, the sentinel images are used for the satellite image analysis for flood scene extraction. This kind of analysis was made for five years, from 2017 to 2021. The time series map is shown in Fig. 40.

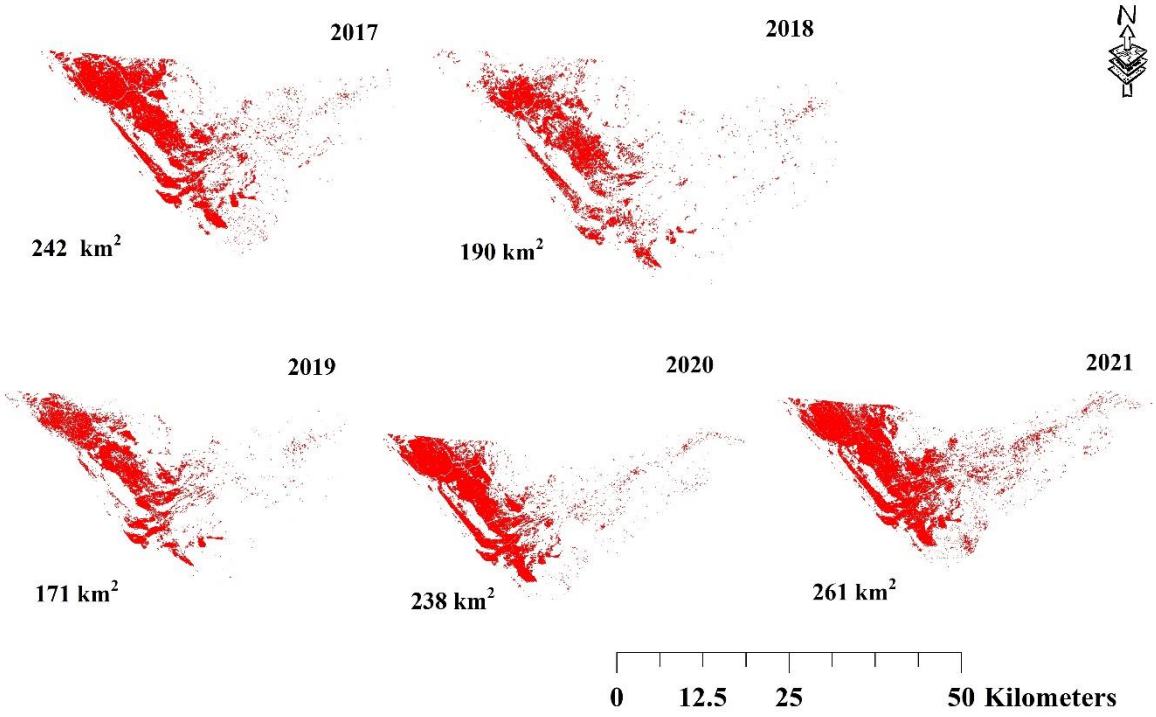

Figure 5.17 Time series flood map analysis for five years with the consideration of peak moments

The time series analysis depicts the more than 170 km^2 area frequently inundated. This kind of effect occurred in ghed region for many years. As a result, the frequently inundated portion becomes vulnerable because surface water is matched with salted groundwater.

Further, this research emphasizes the new approach of flood validation using satellite images for inundation boundary maps. For this analysis, the post-flood image has been validated with the actual scene extracted from a satellite image. Fig. 41 depicts the agreement between these scenes to compare the inundation boundary map. In this case, the model simulated between 14th Aug to 27th Aug 2017 and the GEE flood map with the sentinel image illustrated between 1st Sep to 15th Sep 2017 (post flood image). GEE analysis depicts 242 $km^{2,}$ whereas the HEC-

RAS inundation boundary depicts 256.27 km^2.

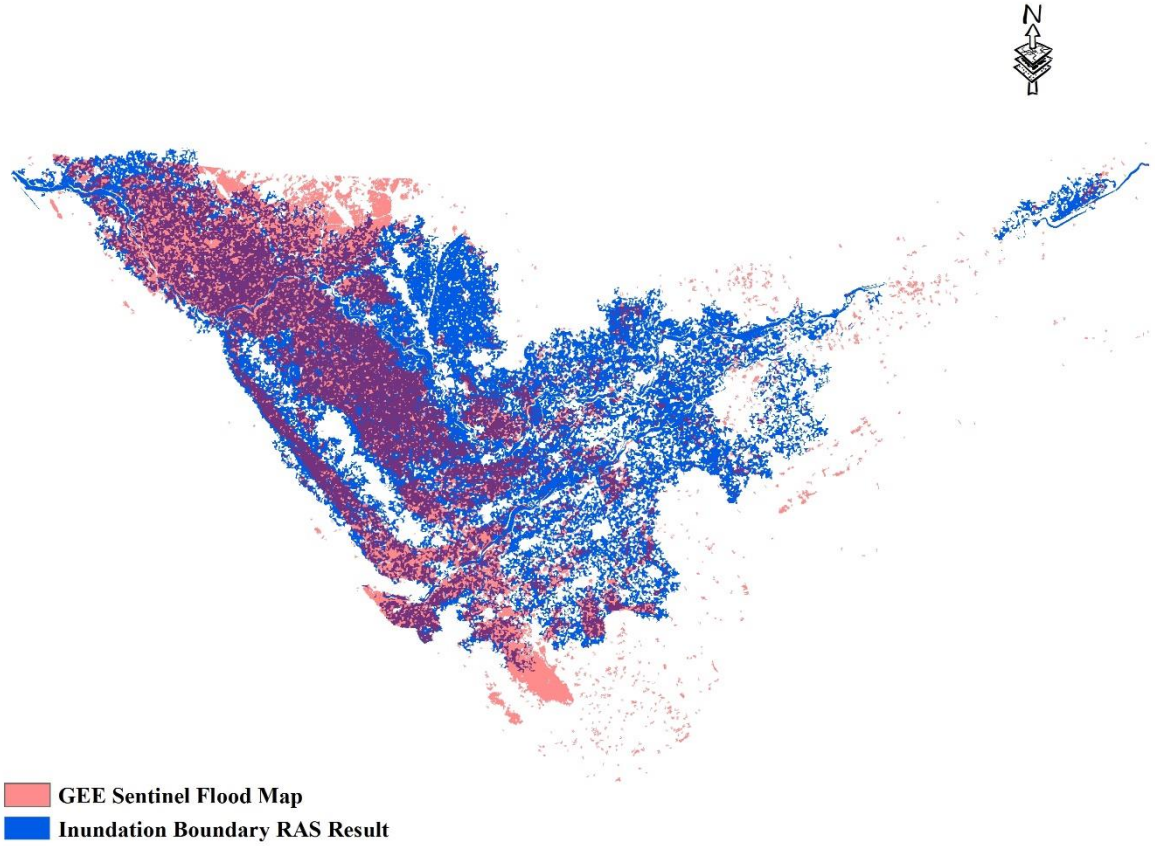

Figure 5.18 An overlapped image of the HEC-RAS inundation boundary and post-flood scene from google earth engine

The comparison indicates major similarity, and the difference is simply due to the date specific of both platforms.

Chapter 6. Discussion

As already mentioned, the lack of data in the Ozat River basin makes it challenging to evaluate actual ground conditions for flood inundation mapping in the Ghed region. In this case study, the HEC-RAS was employed for small scale basin that has 870.11 km^2 in which the result can be validated precisely by time step optimization. On the ground, data is only temporarily available in a few places and only for a short period. The current work is an example of flood inundation mapping and early warning systems in this dearth of data, which is a restriction of the researchers in this field. Here are a few limitations that were discussed during the simulation and analysis.

- DEM resolution plays a crucial role in mapping floods and accurately assessing the impact of flooding on various land cover classes. This study makes use of the SRTM DEM with a 30 m resolution. For accurate hazard maps, producing a high-resolution DEM from an unmanned aerial vehicle (UAV) with a horizontal resolution of fewer than 1 meter is desirable.
- Only two DEMs have been used for 1D hydrodynamic analysis; however, this research emphasizes dealing with open-source data and centric flood mapping. Many open-source DEMs, like GDEM, hydroShed, ASTER, and Bhuvan, are available for terrain file generation. SRTM is used in this research because many pieces of the literature reveal that SRTM makes a better agreement with ground data.
- The latest version of HEC-RAS, 6.1.0, introduces numerous new hydraulic simulation features. In the 2D flow area mesh for the Ozat River basin case study, there are 970480 cells, each with a 30 m grid size. The HEC-RAS documentation recommends 48 cores and a 16 GB RAM machine for simulations due to a large number of cells and thorough area analysis. The simulation in this scenario uses an AMD RYZEN 3 CPU, a Hexa core, 8 GB of RAM, and a 64-bit OS. Numerous simulations using Intel and Ryzen processors have demonstrated that Ryzen offers greater time savings than Intel.
- By generating the DEM, the 1D model performs 200 m cross-section spacing with a 700 m width for each section. The field-surveyed cross-section is advised, especially for cropland away from the river reach. All three reaches require a total of 581 cross-sections to be surveyed for elevation data, and the model must simulate using this data chart.
- The Ozat River is a non-perennial river, and numerous check dams have been built to use water from the river's source to its mouth during the dry season. However, these

structures are not measured for the hydrodynamic flow study due to a lack of field survey funding and staff. It suggests measuring and importing the geometry data of small structures for HEC-RAS hydraulic simulations.

- The Ozat River basin's natural stream tries to meander at each portion of the trail, but after bifurcation, it emerges at fourteen locations, one of which is particularly near to the area of interest (Ghed region). Reach's meandering S-section is encroached upon by inhabitants of the nearby valley, who straighten it out and fill it with earthwork for farming reasons. During the following flood season, the river tries to meander itself again, and people try the river straight after the season. Due to this activity, artificially cultivated land is frequently drained from surface water by velocity. These illicit activities have detrimental effects on crops, such as deteriorated land quality, lack of cultivable surface, and nutrient deficit on the topsoil.
- Future rainfall and runoff correlations must be predicted using hydrometeorological parameters. Most large dams in the Ozat River watershed are built before the model's inflow point; therefore, simulations and validation directly use the hydrograph at hand. It suggests creating a rainfall-runoff model to evaluate discharge data for forecasting future flood events.
- After the model inflow point, many nearby lower-order tributaries emerged. There is no measurement of the discharge from these remote places. Additionally, the hydraulic model does not consider direct rainfall in the Ghed area. These two points, release from minor reaches and direct rain in the study zone, are crucial in the hydrodynamic flow analysis of the Ozat River basin because a 2D flow area of 870.11 km^2 demands an exact flood inundation estimate.
- Due to the geometry of the cup and the water's prolonged stay, there has been a significant inundation between Kadachh and Ghed Bagasra Village. From the agricultural perspective, farmers usually follow the same crop pattern, eliminating the need for land management. Due to inaccessible agriculture fields with reliable water, this technique has developed. This growing crop has altered the topsoil's nutrition and the land's condition. However, the crop pattern, surface soil analysis, and subsurface groundwater location must be examined in this area. From an agricultural perspective, this research supports farmers' crop selection and land quality perceptions.

Chapter 7. Conclusion

Flood assessment is crucial for underdeveloped nations, where farming is the main source of income. Despite the cup-shaped geometry of the Ozat River delta, where velocity is not a major issue, water must pass through this region to reach the river mouth. As a result, water spreads across a considerable portion of the Ghed region before reaching the Arabian Sea. To improve the community's ability to make decisions and to act as an early warning system; this study will examine flood inundation dangers in the data-scarce Ghed, particularly in light of 1D and 2D hydraulic modelling for 2017.

- The Manning roughness coefficient of 0.030 has been satisfactorily calibrated for all three river reaches using the 1D hydrodynamic model. This outcome helps construct a 2D model; when assigning Manning region values, the river reach is given a Manning value of 0.030 individually, and the values for the other land cover classes are established following the DRIP chart. For semi-arid climate conditions, the outcome regarding the attained human resources value range is acceptable.
- The Kadachh and Mander villages are at significant risk, according to the depth map produced by a 2D model. Since the land around these settlements is less elevated, the water stays constant there for a very long time. Providing a higher elevated road link to these settlements is important because the coastal highway is only a 5-kilometer drive away.
- The inundation boundary map shows that cropland receives the most water effect, followed by arid land. In 2017, however, natural terrain supplied water to a bare land area of 33.28 km^2 out of 139.16 km^2 (Table 8). Before the water reaches the Ghed region, the earth should be dug deeper to boost this area's capacity for water storage. Additionally, washed-out land should benefit from the improved fertility provided by the gathered soil.
- The bifurcation tributaries' 2D model values for overbank discharge are considerable. From the communities of Osa and Sandha, water radiated outward until it reached Ozat-1 Reach-2 and Ozat-2 Reach-1, respectively. Water travels 36 hours to reach these towns from the inflow source. After that, spreading across the 170 km2 Ghed region requires 19 hours. Scattered water will take longer to reach the Arabian because of the estuary's higher elevation. While river water flows through these towns, decision-makers can alert the neighborhood to provide an early warning system.

- In the worst scenario, most villages are protected from flooding due to their sufficient elevation. However, because many of these locations will likely become isolated during peak flow events, they must be protected from future disasters. Levee construction is required close to the village built-up area at Kadachh, Mander, Ghodadar, Sarama, Osa, Padardi, and the right side of the riverbed between Ambaliya and Matiyana to protect against overbank discharge. As the tributary (Ozat-1 Reach-2) flows through the cup-shaped Ghed region, it is suggested to deepen the river stretch (Ozat-2 Reach-1) between Tikar village and the river mouth close to Pata village to carry excess water.

Chapter 8. Recommendations

The result comes from the hydrodynamic models, and GEE revealed some recommendations to eliminate the adverse conditions formed on the ground. The formation of these statements is majorly on a technical basis, results of modeling; some suggestions are also based on the field visit to overcome complications.

i. The 1D model reveals that the reach Ozat-2 Reach-1 passes through the slopped terrain, and the natural slope is 1:2614. Although, the authors suggested that this reach is considered for constructing a lined canal from the bifurcation point to the river mouth near Pata village. However, the other purpose is to divert the access water of the reach Ozat-1 Reach-1, which passes through the cup shape Ghed region.

ii. The hydrodynamic modeling starts from the shapur weir, field study, and geometry analysis, as well as a result from the 1D model, depicts that the river has significant width from model start point till the bifurcation point, although the over bank discharge does not appear in this section of the river reach. However, the tributary of Uben river tries to meet the Ozat River near vanthli village. But in the peak flow condition, the water level of the Ozat River is higher than Uben, which will not meet this point and find a new way to meet. In this context, Uben River formed another way to meet the Ozat River, and again tried to meet at Pipalana village on the downstream side, but the same scenario arose, and Uben River did not get to meet the Ozat River. From the Pipalana village, the water of Uben spreads through the open area and submerges the surrounding. After the Pipalana, on a downstream side of just 1.29 km, Ozat River tries to bifurcate and creates another path to tikar village on the right bank side; this portion needs to construct a flood wall on the right bank of the river and stop to bifurcate the reach. At the tikar village, the surrounding region's remote reaches meet and form a large lake near the existing stop log. This open area needs to confine to a flood wall, and logged water should be met into the proposed line canal section (Ozat-2 Reach-1). The authors suggested the two head regulators near vanthli village and one near pipalana village to stop the water scattering in ghed region.

iii. The LULC map depicts the total barren land of the study area as 139.16 km^2, out of the entire study area of 870.11 km2. The result of a 2D model indicates that water naturally runs over 33.28 km^2 of barren land. Authors suggest deepening this bare land area and storing maximum water to retain and serve the inundation in the downstream part of Ghed region. Storing water on barren land will help to consume the water in the dry

season and recharge groundwater. However, the area in the upstream phase of the Ghed region suffered from the freshwater except during the monsoon season; this practice will boost the freshwater source for irrigation and improve the groundwater quality.

iv. As per the 2D hydrodynamic simulations, the portion of reach Ozat-2 Reach-1 between balagam ghed and sharama village is much vulnerable to overbank discharge right over bank. The water from this over bank scattered into cup shape ghed region. However, it needs to be confined to flood protection walls on both river banks. Many minor reaches after the bifurcation are spread and connected to the large pond of the Ghed region; it needs to be confined with concrete work, and a meeting point of reaches should be constructed at the bed and banks. This mitigation practice helps to eliminate the water spread from the small tributaries. However, these reaches in the study area show the over bank discharge; excavating the river bed and confining the bank till the Ghed region is preferable. However, the lined work of these reaches is challenging to maintain because of the significant length; it enhances the storage capacity and reduces soil erosion.

v. After the bifurcation point, the two reaches of Ozat River (Ozat -1 Reach-2 and Ozat-2 Reach-1) show the deficit width and depth till river mouths, as discussed in the study area section. However, these reaches try to meander at 14 locations in the cropland area. People of surrounding places made these sections straight for farming activity and encroached on the natural hydrology. In the next monsoon season, these sections along reach again try to meander and wash out the surface land, resulting in a large amount of land erosion. After the monsoon, the local community has made it straight; this repeated encroachment action results in adverse conditions on cropland. Authors suggest informing the local community about the formation process of river meandering and immediate stop to straighten the sections. This activity will enhance the land quality and better farming results in upcoming years.

vi. Many villages are located on the periphery of the polygon formed by the cup shape Ghed region. However, out of all these villages, Kadachh and Mander are situated just in the polygon. In this condition, the surrounding area of these two villages is lower elevated except built-up area. Although, in the peak flow condition, water gets stayed in this periphery and remains present for many days, even in the dry season. Thus, the interconnectivity of these two and other villages gets overwhelmed. The road connectivity between villages of the Ghed regions must be higher than the current. The road line between kadachh to the coastal highway, kadachh to mander village, and

mander to the coastal highway needs to construct at higher elevations than the current situation.

vii. As stated previously, the hydrodynamic modeling starts from the shapur weir as an inflow point of the model; at this place, the width of the Ozat River is nearly 230 m, and the upstream side of this place has sufficient width till the river origin place. After 20 km from the shapur weir, the river reaches, and depth gradually appears in decreasing mode till the river mouth. The author recommends constructing a large storage area before shapur weir to store the maximum amount of water. These areas should be built like gravity flow of the river would be reaching at these places to eliminate the pumping stations.

viii. A railway bridge has been located near the inflow place (Shapur weir), just 210 m downstream. The Madhuvanti River flows parallel to the left side of the Ozat River, and the distance is nearly 2.23 km from the railway bridge. The authors recommend to built a lined canal or pipe to transfer the excess water to Madhuvanti River. The interlink path is 2.23 km; the elevation difference between these places is just 0.832 m, sufficient to transfer surplus water to Madhuvanti River. It has been observed that peak flow appeared in the Ozat River, while discharge in Madhuvanti River is not in peak condition. This situation happened because of fan shape catchment of the Ozat River basin, whereas Madhuvanti River basin has a fern shape catchment that doesn't show the peak flow in ordinary conditions.

ix. As mentioned in the research title, the Ozat River basin is data-scarce. For the model input parameter, the inflow hydrograph plays a vital role in hydraulic simulations and water surface elevation changes till the river mouth. In the catchment area of the Ozat River basin, the only stream gauge available near Khambhaliya village is located near the river origin point. After this place, many hydraulic structures are available in the downstream area. The authors recommend establishing another river gauge 4 km upstream of the pipalana village. This location is suitable for stream gauge placement because, after this location, no major hydraulic structure is located, and only small check dams are constructed, which is ideal for hydrodynamic modeling for future events.

8.1 Flood mitigation plan

The flood mitigation plan has been developed from the study region's hydrodynamic modelling and field analysis. In this regard, multi-level remedy measures are suggested per the previous

discussion. The flood mitigation plan (FMP) is prepared with an integrated and separate view to understand remedial measures better.

In Fig. 40, the integrated flood mitigation plan shows that the mitigation plan is divided into four parts per the measure taken and site location. In this view, the “A” location denotes the board view in the upper right corner, which depicts the small tributary trying to join the main reach of the ozat river at “X” location, but the in the peak flow condition, the water level of the mainstream is higher than small reach. In this case, the small reach finds another way and again tries to meet the main reach at “Y” location. For this scenario, the path between X and Y must be confined with a lined canal, and both locations are suggested for head regulators.

In Fig. 42, the middle right view “B” elaborates on the interlink path between ozat and the parallel passage of madhuvanti river. This remedy measure is highly suggested for the long-term inter-basin transfer solution. The bottom right corner, “D” depicts balagam ghed village view located on the split reach that travels straight towards the pata village. This is the only location constructed close to the river valley area for this reach. However, the reach that travels to the ghed region (area of interest) has few structures besides the valley area, but this is the most devasting reach because of the depressed region.

Fig. 42 shows the “C” window near the top left, which depicts the encroachment of natural hydrology. In this context, the people living near the valley region frequently try encroaching on the river, meandering to straighten the sinuous portion.

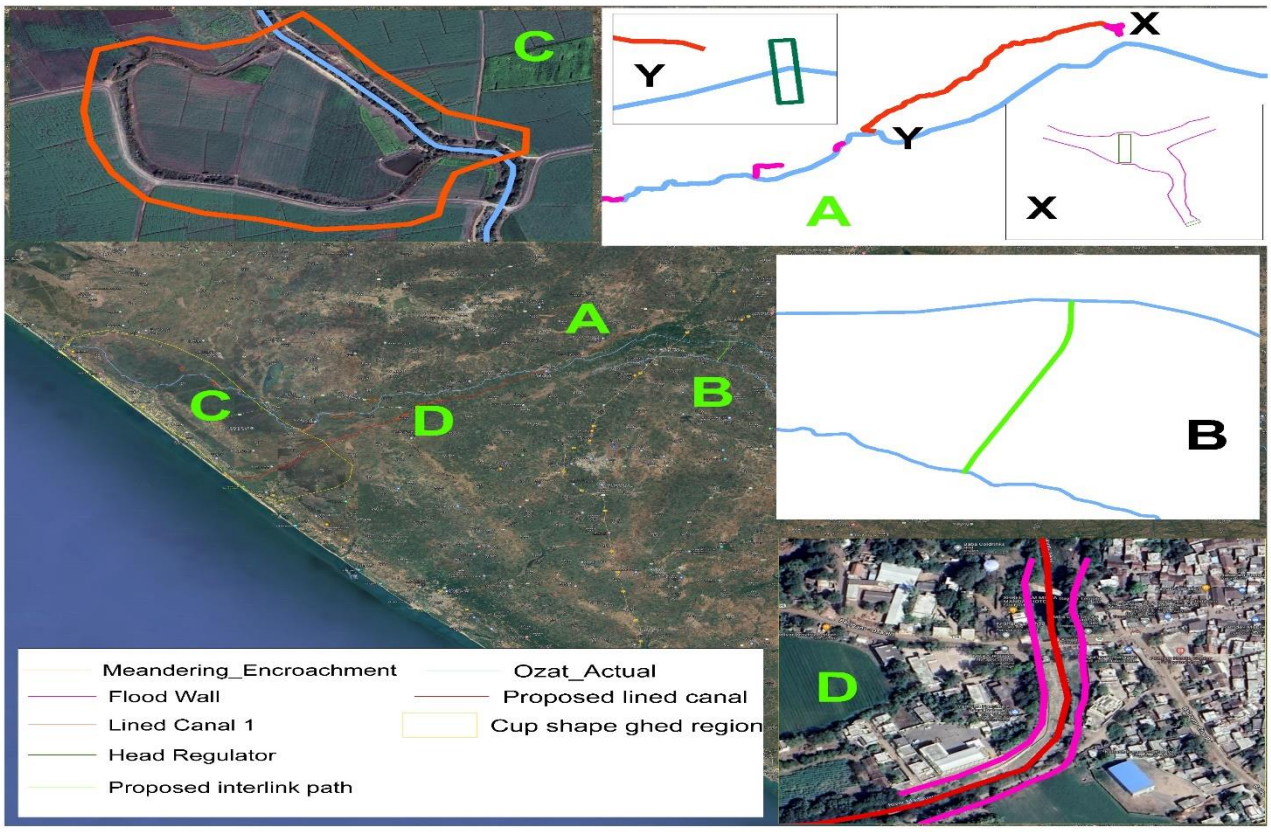

Figure 8.1 Integrated flood mitigation plan

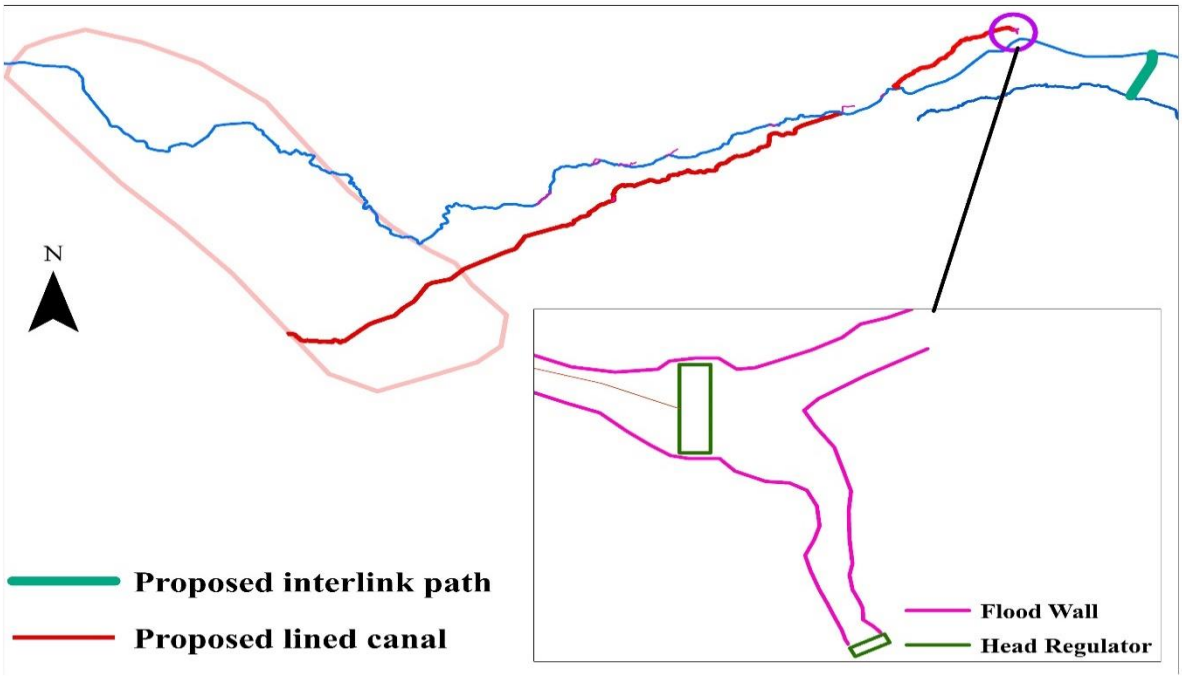

Figure 8.2 Proposed lined canal at two locations and Suggested interlinking path

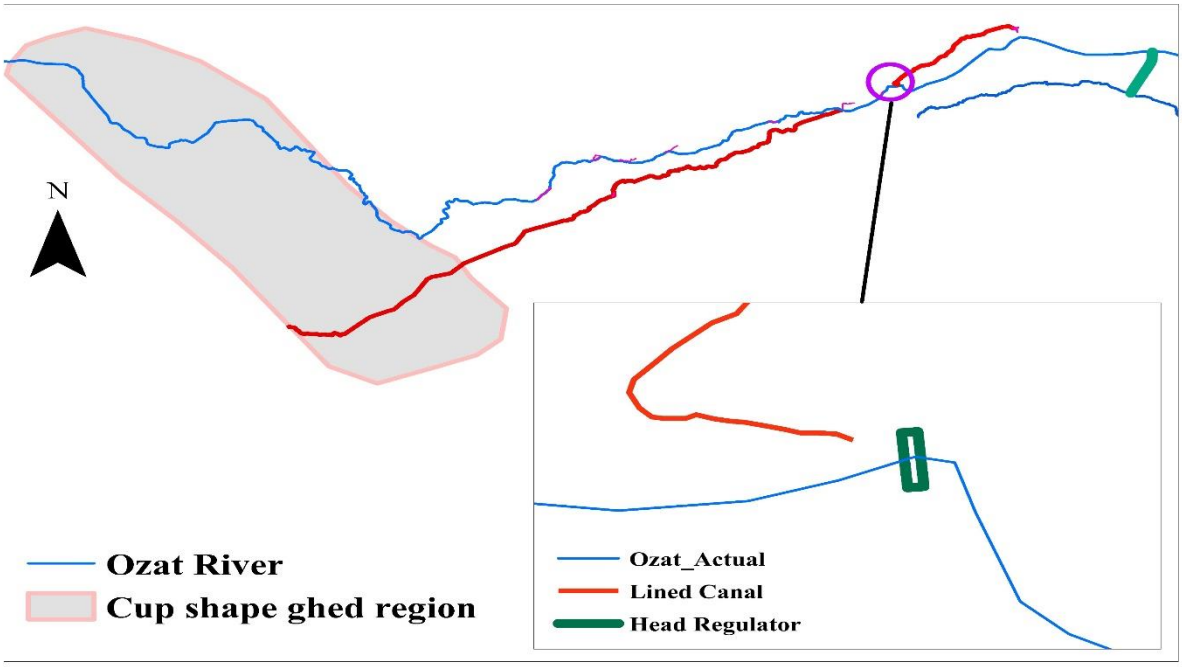

Figure 8.3 Suggested head regulator near pipalana village

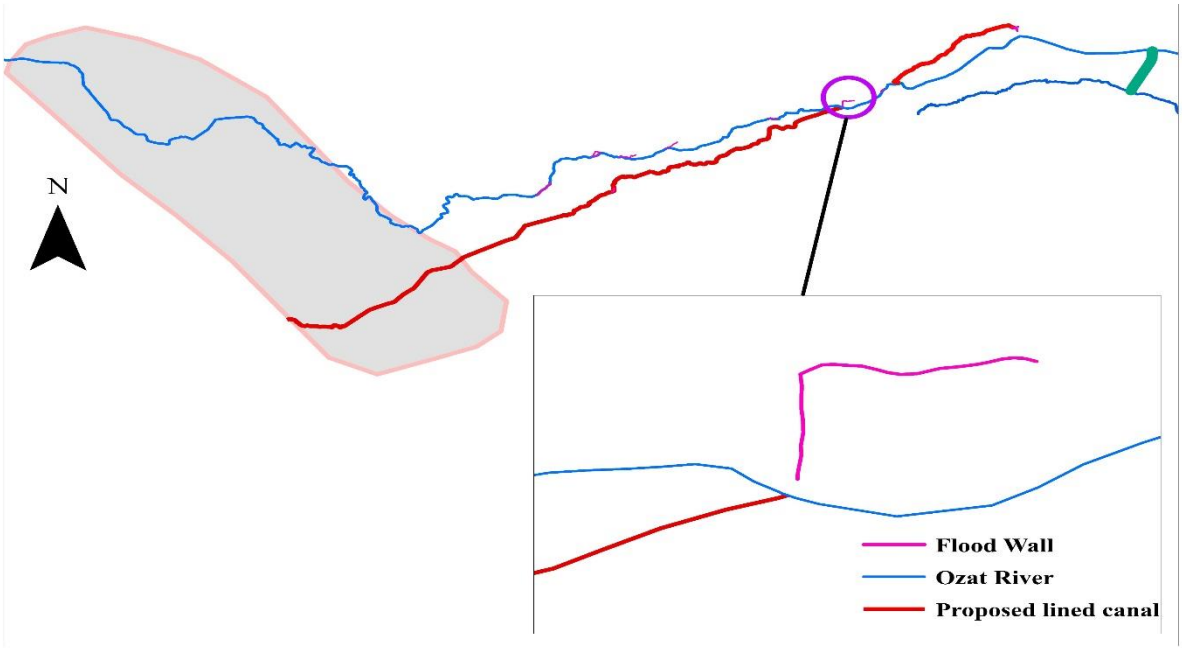

Figure 8.4 Concrete bucket suggested near bifurcation point

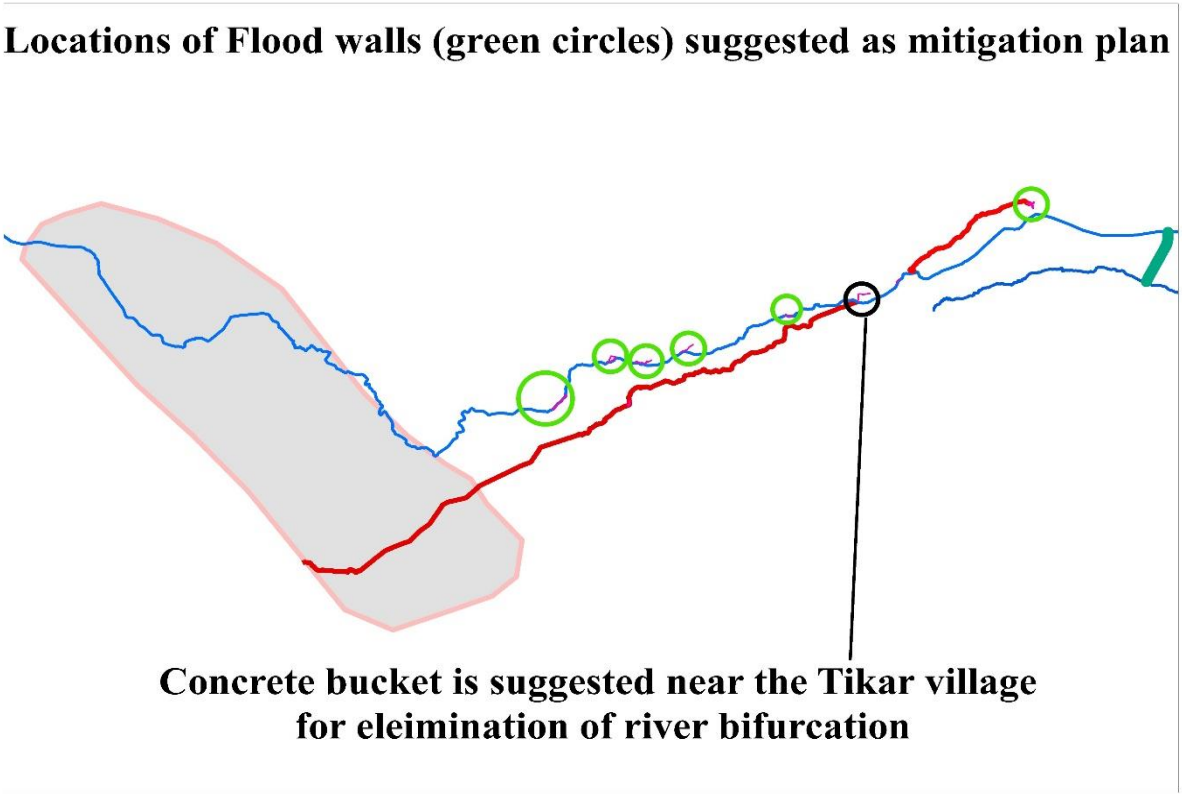

Figure 8.5 Green circles depict the flood wall that needs to be constructed for the elimination of water scattering

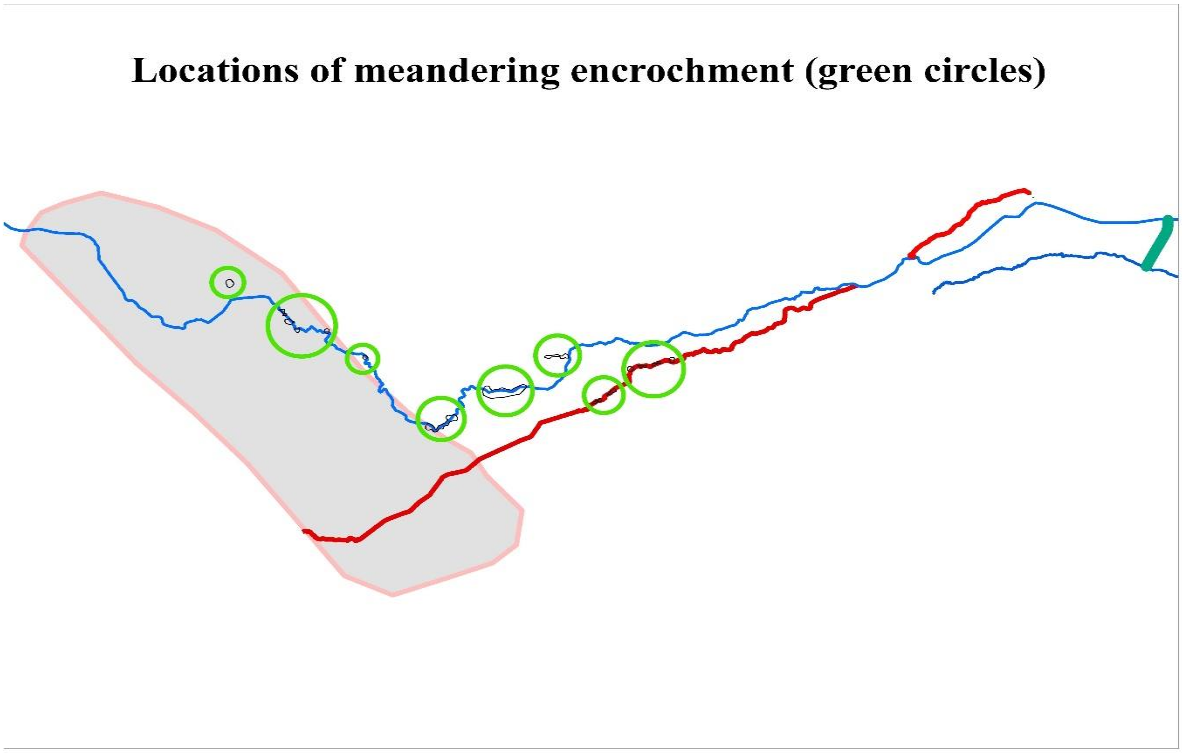

Figure 8.6 Green circles indicating the area needs to protect against the encroachment of natural hydrology from the local community

References

Amorati, R., Alberoni, P. P., Levizzani, V., & Nanni, S. (2000). IR-based satellite and radar rainfall estimates of convective storms over northern Italy. *Meteorological Applications, 7*(1), 1–18. https://doi.org/10.1017/S1350482700001328

Arash, A. M., & Yasi, M. (2023). The assessment for selection and correction of RS-based DEMs and 1D and 2D HEC-RAS models for flood mapping in different river types. Journal of Flood Risk Management, 16(1), 1–15. https://doi.org/10.1111/jfr3.12871

Asitatikie, A. N., Kifelew, M. S., & Shumey, E. E. (2022). Flood inundation modeling using HEC-RAS: the case of downstream Gumara river, Lake Tana sub basin, Ethiopia. Geocarto International, 37(25), 9625–9643. https://doi.org/10.1080/10106049.2021.2022014

Azouagh, A., El Bardai, R., Hilal, I., & Stitou el Messari, J. (2018). Integration of GIS and HEC-RAS in Floods Modeling of Martil River (Northern Morocco). *European Scientific Journal, ESJ, 14*(12), 130. https://doi.org/10.19044/esj.2018.v14n12p130

Boori, M. S., Choudhary, K., Kupriyanov, A. V., Sugimoto, A., & Paringer, R. (2016). Land use/cover change detection and vulnerability assessment in Indigirka River Basin, Eastern Siberia, Russia. *CEUR Workshop Proceedings, 1638,* 270–283. https://doi.org/10.18287/1613-0073-2016-1638-270-283

Chandra, R., Saha, U., & Mujumdar, P. P. (2015). Model and parameter uncertainty in IDF relationships under climate change. *Advances in Water Resources, 79,* 127–139. https://doi.org/10.1016/j.advwatres.2015.02.011

Chawla, I., Osuri, K. K., Mujumdar, P. P., & Niyogi, D. (2018). Assessment of the Weather Research and Forecasting (WRF) model for simulation of extreme rainfall events in the upper Ganga Basin. *Hydrology and Earth System Sciences, 22*(2), 1095–1117. https://doi.org/10.5194/hess-22-1095-2018

Chowdhury, A., Reshad, S., & Kumruzzaman, M. (2020). Hydrodynamic Flood Modelling for the Jamuna River using HEC-RAS & MIKE 11. *Proceedings of the 5th International Conference on Advances in Civil Engineering (ICACE-2020), Chattogram, Bangladesh, May*, 21–23.

Chung, H. W., Liu, C. C., Cheng, I. F., Lee, Y. R., & Shieh, M. C. (2015). Rapid response to a

typhoon-induced flood with an SAR-derived map of inundated areas: Case study and validation. *Remote Sensing*, *7*(9), 11954–11973. https://doi.org/10.3390/rs70911954

Devia, G. K., Ganasri, B. P., & Dwarakish, G. S. (2015). A Review on Hydrological Models. *Aquatic Procedia*, *4*(Icwrcoe), 1001–1007. https://doi.org/10.1016/j.aqpro.2015.02.126

DeVries, B., Huang, C., Armston, J., Huang, W., Jones, J. W., & Lang, M. W. (2020). Rapid and robust monitoring of flood events using Sentinel-1 and Landsat data on the Google Earth Engine. Remote Sensing of Environment, 240, 111664. https://doi.org/https://doi.org/10.1016/j.rse.2020.111664

Doherty, J., & Welter, D. (2010). A short exploration of structural noise. *Water Resources Research*, *46*(5), 1–14. https://doi.org/10.1029/2009WR008377

Dotto, C. B. S., Mannina, G., Kleidorfer, M., Vezzaro, L., Henrichs, M., McCarthy, D. T., Freni, G., Rauch, W., & Deletic, A. (2012). Comparison of different uncertainty techniques in urban stormwater quantity and quality modelling. *Water Research*, *46*(8), 2545–2558. https://doi.org/10.1016/j.watres.2012.02.009

Duan, W., He, B., Nover, D., Fan, J., Yang, G., Chen, W., Meng, H., & Liu, C. (2016). Floods and associated socioeconomic damages in China over the last century. *Natural Hazards*, *82*(1), 401–413. https://doi.org/10.1007/s11069-016-2207-2

Durga Rao, K. H. V., Rao, V. V., & Dadhwal, V. K. (2014). Improvement to the Thornthwaite Method to Study the Runoff at a Basin Scale Using Temporal Remote Sensing Data. *Water Resources Management*, *28*(6), 1567–1578. https://doi.org/10.1007/s11269-014-0564-8

Elhag, M., & Abdurahman, S. G. (2020). Advanced remote sensing techniques in flash flood delineation in Tabuk City, Saudi Arabia. *Natural Hazards*, *103*(3), 3401–3413. https://doi.org/10.1007/s11069-020-04135-0

Gabriel, G. V. M., Oliveira, L. C., Barros, D. J., Bento, M. S., Neu, V., Toppa, R. H., Carmo, J. B., & Navarrete, A. A. (2020). Methane emission suppression in flooded soil from Amazonia. *Chemosphere*, *250*. https://doi.org/10.1016/j.chemosphere.2020.126263

Ganguli, P., Nandamuri, Y. R., & Chatterjee, C. (2020). Analysis of persistence in the flood timing and the role of catchment wetness on flood generation in a large river basin in India. *Theoretical and Applied Climatology*, *139*(1–2), 373–388.

https://doi.org/10.1007/s00704-019-02964-z

Gary Brunner, C.-H. (2016). *HEC-RAS User's Manual, CPD-68* (Version 5.). US Army Corps of Engineers, Institute of Water Resources, Hydrologic Engineering Center.

Ghimire, E., Sharma, S., & Lamichhane, N. (2022). Evaluation of one-dimensional and two-dimensional HEC-RAS models to predict flood travel time and inundation area for flood warning system. *ISH Journal of Hydraulic Engineering*, *28*(1), 110–126. https://doi.org/10.1080/09715010.2020.1824621

Huffman, G. J. (1997). Estimates of root-mean-square random error for finite samples of estimated precipitation. *Journal of Applied Meteorology*, *36*(9), 1191–1201. https://doi.org/10.1175/1520-0450(1997)036<1191:EORMSR>2.0.CO;2

Huo, A. Di, Guan, W. K., Dang, J., Wu, T. Z., Shantai, H., Wang, W., & Liew, M. W. V. (2016). Submerged area of typical torrential flood and debris-flow disasters in Mengzong Gully, China. *Geomatics, Natural Hazards and Risk*, *7*(June), 18–24. https://doi.org/10.1080/19475705.2016.1181340

Hurkmans, R. T. W. L. (2009). *Effect of climate variability and land use change on the water budget of large river basins*. Wageningen University and Research.

Indu, J., & Nagesh Kumar, D. (2014). Evaluation of TRMM PR sampling error over a subtropical basin using bootstrap technique. *IEEE Transactions on Geoscience and Remote Sensing*, *52*(11), 6870–6881. https://doi.org/10.1109/TGRS.2014.2304466

Inman, V. L., & Lyons, M. B. (2020). Automated inundation mapping over large areas using landsat data and google earth engine. *Remote Sensing*, *12*(8), 1–12. https://doi.org/10.3390/RS12081348

Jena, P. P., Panigrahi, B., & Chatterjee, C. (2016). Assessment of Cartosat-1 DEM for Modeling Floods in Data Scarce Regions. *Water Resources Management*, *30*(3), 1293–1309. https://doi.org/10.1007/s11269-016-1226-9

Ji, Y., Zhou, G., Wang, S., & Wang, L. (2015). Increase in flood and drought disasters during 1500–2000 in Southwest China. *Natural Hazards*, *77*(3), 1853–1861. https://doi.org/10.1007/s11069-015-1679-9

Johnston, R., & Smakhtin, V. (2014). Hydrological Modeling of Large river Basins: How Much is Enough? *Water Resources Management*, *28*(10), 2695–2730.

https://doi.org/10.1007/s11269-014-0637-8

Khattak, M. S., Anwar, F., Saeed, T. U., Sharif, M., Sheraz, K., & Ahmed, A. (2016). Floodplain Mapping Using HEC-RAS and ArcGIS: A Case Study of Kabul River. *Arabian Journal for Science and Engineering*, *41*(4), 1375–1390. https://doi.org/10.1007/s13369-015-1915-3

Kumar, S., Jaswal, A., Pandey, A., & Sharma, N. (2017). Literature Review of Dam Break Studies and Inundation Mapping Using Hydraulic Models and GIS. *International Research Journal of Engineering and Technology*, *4*(4), 2395–56. https://www.irjet.net/archives/V4/i5/IRJET-V4I511.pdf

Masood, M., & Takeuchi, K. (2012). Assessment of flood hazard, vulnerability and risk of mid-eastern Dhaka using DEM and 1D hydrodynamic model. *Natural Hazards*, *61*(2), 757–770. https://doi.org/10.1007/s11069-011-0060-x

Mitchell, S., Beven, K., & Freer, J. (2009). Multiple sources of predictive uncertainty in modeled estimates of net ecosystem CO2 exchange. *Ecological Modelling*, *220*(23), 3259–3270. https://doi.org/10.1016/j.ecolmodel.2009.08.021

Mondal, A., & Mujumdar, P. P. (2012). On the basin-scale detection and attribution of human-induced climate change in monsoon precipitation and streamflow. *Water Resources Research*, *48*(10), 1–18. https://doi.org/10.1029/2011WR011468

Mosavi, A., Ozturk, P., & Chau, K. W. (2018). Flood prediction using machine learning models: Literature review. *Water (Switzerland)*, *10*(11), 1–40. https://doi.org/10.3390/w10111536

Mudashiru, R. B., Sabtu, N., & Abustan, I. (2021). *Quantitative and semi-quantitative methods in flood hazard / susceptibility mapping : a review*.

Namara, W. G., Damisse, T. A., & Tufa, F. G. (2021). Application of HEC-RAS and HEC-GeoRAS model for Flood Inundation Mapping, the case of Awash Bello Flood Plain, Upper Awash River Basin, Oromiya Regional State, Ethiopia. *Modeling Earth Systems and Environment*, *2015*. https://doi.org/10.1007/s40808-021-01166-9

Nandalal, K. D. W. (2009). Use of a hydrodynamic model to forecast floods of Kalu River in Sri Lanka. *Journal of Flood Risk Management*, *2*(3), 151–158. https://doi.org/10.1111/j.1753-318X.2009.01032.x

Pandey, A. C., Kaushik, K., & Parida, B. R. (2022). Google Earth Engine for Large-Scale Flood Mapping Using SAR Data and Impact Assessment on Agriculture and Population of Ganga-Brahmaputra Basin. Sustainability (Switzerland), 14(7). https://doi.org/10.3390/su14074210

Parhi, P. K. (2013). HEC-RAS Model for Mannnig's Roughness: A Case Study. *Open Journal of Modern Hydrology*, *03*(03), 97–101. https://doi.org/10.4236/ojmh.2013.33013

Patel, D. P., Ramirez, J. A., Srivastava, P. K., Bray, M., & Han, D. (2017). Assessment of flood inundation mapping of Surat city by coupled 1D/2D hydrodynamic modeling: a case application of the new HEC-RAS 5. *Natural Hazards*, *89*(1), 93–130. https://doi.org/10.1007/s11069-017-2956-6

Pathan, A. I., Agnihotri, P. G., Patel, D., & Prieto, C. (2022). Mesh grid stability and its impact on flood inundation through (2D) hydrodynamic HEC-RAS model with special use of Big Data platform—a study on Purna River of Navsari city. Arabian Journal of Geosciences, 15(7), 659. https://doi.org/10.1007/s12517-022-09813-w

Petteri Alho, J. A. (2008). Comparing a 1D hydraulic model with a 2D hydraulic model for the simulation of extreme glacial outburst flood. *HYDROLOGICAL PROCESSES*, *22*(July 2007), 1537–1547. https://doi.org/10.1002/hyp

Pinos, J., & Timbe, L. (2019). Performance assessment of two-dimensional hydraulic models for generation of flood inundation maps in mountain river basins. *Water Science and Engineering*, *12*(1), 11–18. https://doi.org/10.1016/j.wse.2019.03.001

Quirogaa, V. M., Kurea, S., Udoa, K., & Manoa, A. (2016). Application of 2D numerical simulation for the analysis of the February 2014 Bolivian Amazonia flood: Application of the new HEC-RAS version 5. *Ribagua*, *3*(1), 25–33. https://doi.org/10.1016/j.riba.2015.12.001

Rangari, V. A., Umamahesh, N. V., & Bhatt, C. M. (2019). Assessment of inundation risk in urban floods using HEC RAS 2D. *Modeling Earth Systems and Environment*, *5*(4), 1839–1851. https://doi.org/10.1007/s40808-019-00641-8

Rind, M. A., Ansari, K., Saher, R., Shakya, S., & Ahmad, S. (2018). 2D Hydrodynamic Model for Flood Vulnerability Assessment of Lower Indus River Basin, Pakistan. *World Environmental and Water Resources Congress 2018: Watershed Management, Irrigation*

and Drainage, and Water Resources Planning and Management - Selected Papers from the World Environmental and Water Resources Congress 2018, *May*, 468–482. https://doi.org/10.1061/9780784481400.044

Saha, S., Banerjee, S., Burley, S. D., Ghosh, A., & Saraswati, P. K. (2010). The influence of flood basaltic source terrains on the efficiency of tectonic setting discrimination diagrams: An example from the Gulf of Khambhat, western India. *Sedimentary Geology*, *228*(1–2), 1–13. https://doi.org/10.1016/j.sedgeo.2010.03.009

Saidani, M., & Shibani, A. (2014). Use of Physical and Numerical Models in Engineering Design Education. *4th International Conference on Industrial Engineering and Operations Management*, 61–67. http://ieomsociety.org/ieom2014/authors2.html#S

Seal, V. (2012). A Simple Flood Forecasting Scheme Using Wireless Sensor Networks. *International Journal of Ad Hoc, Sensor & Ubiquitous Computing*, *3*(1), 45–60. https://doi.org/10.5121/ijasuc.2012.3105

Shah, H. L., & Mishra, V. (2016). Hydrologic changes in Indian subcontinental river basins (1901-2012). *Journal of Hydrometeorology*, *17*(10), 2667–2687. https://doi.org/10.1175/JHM-D-15-0231.1

Shekhar, S., Mawale, Y. K., Giri, P. M., Jaipurkar, R. S., & Singh, N. (2021). Remote Sensing and GIS Based Extensive Morphotectonic Analysis of Tapti River Basin, Peninsular India. *Journal of Scientific Research*, *65*(03), 23–30. https://doi.org/10.37398/jsr.2021.650304

Shustikova, I., Domeneghetti, A., Neal, J. C., Bates, P., & Castellarin, A. (2019). Comparing 2D capabilities of HEC-RAS and LISFLOOD-FP on complex topography. *Hydrological Sciences Journal*, *64*(14), 1769–1782. https://doi.org/10.1080/02626667.2019.1671982

Sinclair, S., & Pegram, G. (2005). Combining radar and rain gauge rainfall estimates using conditional merging. *Atmospheric Science Letters*, *6*(1), 19–22. https://doi.org/10.1002/asl.85

Singh, S., Dhote, P. R., Thakur, P. K., Chouksey, A., & Aggarwal, S. P. (2021). Identification of flash-floods-prone river reaches in Beas river basin using GIS-based multi-criteria technique: validation using field and satellite observations. *Natural Hazards*, *105*(3), 2431–2453. https://doi.org/10.1007/s11069-020-04406-w

Singha, M., Dong, J., Sarmah, S., You, N., Zhou, Y., Zhang, G., Doughty, R., & Xiao, X. (2020). Identifying floods and flood-affected paddy rice fields in Bangladesh based on Sentinel-1 imagery and Google Earth Engine. *ISPRS Journal of Photogrammetry and Remote Sensing*, *166*(June), 278–293. https://doi.org/10.1016/j.isprsjprs.2020.06.011

Siswanto, S. Y., & Francés, F. (2019). How land use/land cover changes can affect water, flooding and sedimentation in a tropical watershed: a case study using distributed modeling in the Upper Citarum watershed, Indonesia. *Environmental Earth Sciences*, *78*(17). https://doi.org/10.1007/s12665-019-8561-0

Soncini, E., Slatter, M. A., Jones, L. B. K. R., Hughes, S., Hodges, S., Flood, T. J., Barge, D., Spickett, G. P., Jackson, G. H., Collin, M. P., Abinun, M., Cant, A. J., & Gennery, A. R. (2009). Unrelated donor and HLA-identical sibling haematopoietic stem cell transplantation cure chronic granulomatous disease with good long-term outcome and growth. *British Journal of Haematology*, *145*(1), 73–83. https://doi.org/10.1111/j.1365-2141.2009.07614.x

Tamiminia, H., Salehi, B., Mahdianpari, M., Quackenbush, L., Adeli, S., & Brisco, B. (2020). Google Earth Engine for geo-big data applications: A meta-analysis and systematic review. *ISPRS Journal of Photogrammetry and Remote Sensing*, *164*(January), 152–170. https://doi.org/10.1016/j.isprsjprs.2020.04.001

Teng, J., Jakeman, A. J., Vaze, J., Croke, B. F. W., Dutta, D., & Kim, S. (2017). Flood inundation modelling: A review of methods, recent advances and uncertainty analysis. *Environmental Modelling and Software*, *90*, 201–216. https://doi.org/10.1016/j.envsoft.2017.01.006

Thameemul Hajaj, P. M., Yarrakula, K., Durga Rao, K. H. V., & Singh, A. (2019). A Semi-distributed Flood Forecasting Model for the Nagavali River Using Space Inputs. *Journal of the Indian Society of Remote Sensing*, *47*(10), 1683–1692. https://doi.org/10.1007/s12524-019-01019-0

Timbadiya, P. V., Patel, P. L., & Porey, P. D. (2011). Calibration of HEC-RAS Model on Prediction of Flood for Lower Tapi River, India. *Journal of Water Resource and Protection*, *03*(11), 805–811. https://doi.org/10.4236/jwarp.2011.311090

Walker, W. E., Harremoes, P., Rotmans, J., Van Der Sluijs, J. P., Van Asselt, M. B. A., Janssen, P., & Krayer Von Krauss, M. P. (2003). Defining Uncertainty. *Integrated Assessment*,

4(1), 5–17. https://www.narcis.nl/publication/RecordID/oai:tudelft.nl:uuid:fdc0105c-e601-402a-8f16-ca97e9963592

Warmink, J. J., van der Klis, H., Booij, M. J., & Hulscher, S. J. M. H. (2011). Identification and Quantification of Uncertainties in a Hydrodynamic River Model Using Expert Opinions. *Water Resources Management*, *25*(2), 601–622. https://doi.org/10.1007/s11269-010-9716-7

Wu, W., Emerton, R., Duan, Q., Wood, A. W., Wetterhall, F., & Robertson, D. E. (2020). Ensemble flood forecasting: Current status and future opportunities. In *Wiley Interdisciplinary Reviews: Water* (Vol. 7, Issue 3). https://doi.org/10.1002/WAT2.1432

Xie, P., Rudolf, B., Schneider, U., & Arkin, P. A. (1996). Gauge-based monthly analysis of global land precipitation from 1971 to 1994. *Journal of Geophysical Research Atmospheres*, *101*(14), 19023–19034. https://doi.org/10.1029/96jd01553

Yadavrao Nandurkar, R., Nandurkar, R., More, R., & Deshpande, S. (2017). *Urban Flash Flood Modelling Using Remotely Sensed Data And Hec-RAS: Pune Case Study Village level groundwater assessment using geospatial technique View project Urban Prediction Modelling View project URBAN FLASH FLOOD MODELLING USING REMOTELY SENSED DATA*. *October*. https://www.researchgate.net/publication/320843085

Yaduvanshi, A., Sharma, R. K., Kar, S. C., & Sinha, A. K. (2018). Rainfall–runoff simulations of extreme monsoon rainfall events in a tropical river basin of India. *Natural Hazards*, *90*(2), 843–861. https://doi.org/10.1007/s11069-017-3075-0

Zhao, Q., Yu, L., Li, X., Peng, D., Zhang, Y., & Gong, P. (2021). Progress and trends in the application of google earth and google earth engine. *Remote Sensing*, *13*(18), 1–21. https://doi.org/10.3390/rs13183778

List of Publications

1. Paper published on, Feasibility Study of Proposed Interlinking between Ozat and Mahuvanti Rivers: A Review Paper, The International journal of analytical and experimental modal analysis, volume XI, issue IX, September 2019, ISSN: (0886-9367) (UGC approved)
2. Paper published on, "Comparison of two open-source digital elevation models for 1D hydrodynamic flow analysis: a case of Ozat River basin, Gujarat, India". Model. Earth Syst. Environ. (2022). https://doi.org/10.1007/s40808-022-01426-2 , E-ISSN: 2363-6211,ISSN: 2363-6203 (Scopus Indexed)
3. Paper published on, "Development of a 2D hydrodynamic model for inundation assessment and flood early warning system: a case of depressed Ghed region, India", water practice and technology (accepted on 11th Sept.2023). https://doi.org/10.2166/wpt.2023.145, ISSN:1751-231X (Scopus Indexed)
4. Paper presented on "Flood mapping and Submergence analysis of Ozat River basin: A Review Paper", Recent Advances in Civil Engineering for Sustainable Development (RACESD- 2021), organized by MANIT Bhopal, 13-14 Fab 2021, International Conference